

EFFECT OF FEEDBACK-RESISTANT *aroG* OVEREXPRESSION ON L-
PHENYLALANINE PRODUCTION IN *Escherichia coli*



A Thesis Submitted in Partial Fulfillment of the Requirements
for the Degree of Master of Science in Biochemistry and Molecular Biology

Department of Biochemistry

Faculty of Science

Chulalongkorn University

Academic Year 2018

Copyright of Chulalongkorn University

ผลของการแสดงออกเกินปกติของ *aroG* ที่ด้านการควบคุมแบบย้อนกลับต่อการผลิตแอล-
ฟีนิลอะลานีนใน *Escherichia coli*



วิทยานิพนธ์นี้เป็นส่วนหนึ่งของการศึกษาตามหลักสูตรปริญญาวิทยาศาสตรมหาบัณฑิต
สาขาวิชาชีวเคมีและชีววิทยาโมเลกุล ภาควิชาชีวเคมี
คณะวิทยาศาสตร์ จุฬาลงกรณ์มหาวิทยาลัย
ปีการศึกษา 2561
ลิขสิทธิ์ของจุฬาลงกรณ์มหาวิทยาลัย

Thesis Title	EFFECT OF FEEDBACK- RESISTANT <i>aroG</i> OVEREXPRESSION ON L- PHENYLALANINE PRODUCTION IN <i>Escherichia coli</i>
By	Mrs. Maria Ulfah
Field of Study	Biochemistry and Molecular Biology
Thesis Advisor	Assistant Professor Kanoktip Packdibamrung

Accepted by the Faculty of Science, Chulalongkorn University in Partial
Fulfillment of the Requirement for the Master of Science

..... Dean of the Faculty of Science
(Professor POLKIT SANGVANICH)

THESIS COMMITTEE

..... Chairman
(Assistant Professor Rath Pichyangkura)

..... Thesis Advisor
(Assistant Professor Kanoktip Packdibamrung)

..... Examiner
(Assistant Professor Kunlaya Somboonwivat)

..... Examiner
(Associate Professor TEERAPONG BUABOOCHA)

..... External Examiner
(Assistant Professor Ratre Wongpanya)

มาเรีย อูลฟา : ผลของการแสดงออกเกินปกติของ *aroG* ที่ด้านการควบคุมแบบย้อนกลับต่อการผลิตแอล-ฟีนิลอะลานีนใน *Escherichia coli*. (EFFECT OF FEEDBACK-

RESISTANT *aroG* OVEREXPRESSION ON L-PHENYLALANINE PRODUCTION IN *Escherichia coli*)

อ.ที่ปรึกษาหลัก : กนกทิพย์ ภักดีบำรุง

แอล-ฟีนิลอะลานีน (L-Phe) เป็นกรดอะมิโนที่มีความสำคัญในอุตสาหกรรมอาหารและยาซึ่งถูกนำไปเป็นอาหารเสริมและสารตั้งต้นในการสังเคราะห์วัตถุเจือปนอาหารอย่างกว้างขวาง จากความต้องการแอสพาแตมซึ่งเป็นสารให้ความหวานแทนน้ำตาลที่เพิ่มมากขึ้นกระตุ้นให้ตลาดของ L-Phe ขยายมากขึ้นด้วย เอนไซม์สำคัญในวิถีการสังเคราะห์กรดอะมิโนชนิดอะโรมาติกใน *Escherichia coli* คือ 3-deoxy-D-arabino-heptulosonate-7-phosphate synthase (DAHP-synthase) ซึ่งเร่งปฏิกิริยาแรกของวิถีเอนไซม์นี้ประกอบด้วย 3 ไอโซฟอร์ม คือ AroG AroF และ AroH ซึ่งถูกควบคุมแบบย้อนกลับโดย L-Phe L-Tyr และ L-Trp ตามลำดับ AroG ซึ่งเข้ารหัสโดย *aroG* เป็นไอโซฟอร์มหลัก มีแอกทิวิตีคิดเป็น 80% ของแอกทิวิตีทั้งหมดของ DAHP เพื่อที่จะระบุบริเวณของการควบคุมแบบย้อนกลับของ AroG Leu175 ได้ถูกแทนที่โดย Asp (L175D) และ Gln151 ได้ถูกแทนที่โดย Ala (Q151A) Leu (Q151L) และ Asn (Q151N). ในการศึกษา *aroG* ที่ด้านทานการควบคุมแบบย้อนกลับแต่ละชนิดได้ถูกโคลนร่วมกับยีนที่สำคัญในวิถีการผลิต L-Phe (*aroB aroL phedh* และ *tktA*) ใน pRSFDuet-1 หลังจากนั้นทำการทรานส์ฟอร์มพลาสมิดลูกผสมที่ได้ (pBLPTG*) ร่วมกับ pBAD33 ที่มียีนที่เข้ารหัสโปรตีนที่นำกรดอะมิโนชนิดอะโรมาติกออกนอกเซลล์ (*gfp*) และยีนที่เข้ารหัสโปรตีนที่นำกรดอะมิโนชนิดอะโรมาติกออกนอกเซลล์ (*yddG*) (pYF) เข้าสู่ *E. coli* BL21(DE3) โคลนที่มีพลาสมิด pBLPTG*Q151L & pYF และ pBLPTG*Q151N & pYF ผลิต L-Phe ได้สูงสุด (1.8 g/L) เมื่อเลี้ยงในอาหารเลี้ยงเชื้อกลีเซอรอลเป็นเวลา 6 วัน คิดเป็น 7.7 เท่าของโคลนควบคุมที่มี *aroG* ไรต์ไทป์ (pBLPTG & pYF) ขณะที่โคลน pBLPTG*L175D & pYF และ pBLPTG*Q151A & pYF ให้ L-Phe เป็น 2.7 และ 2.5 เท่า ตามลำดับ ผลการทดลองที่ได้แสดงให้เห็นว่าการแทนที่ Gln151 ด้วย Leu และ Asn สามารถลดการควบคุมแบบย้อนกลับได้ จากนั้นโคลน pBLPTG*Q151L ได้ถูกคัดเลือกเพื่อใช้ในการหาส่วนประกอบของอาหารขั้นต่ำที่เหมาะสมด้วย response surface methodology (RSM) พบว่าผลิต L-Phe สูงสุด 2.03 กรัมต่อลิตร เมื่อเลี้ยงในอาหารที่มีกลีเซอรอล 60 กรัมต่อลิตรและแอมโมเนียมซัลเฟต 42.4 กรัมต่อลิตร ที่ 37 องศาเซลเซียสเป็นเวลา 6 วันหลังการเหนี่ยวนำด้วยอะราบิโนส 0.02 เปอร์เซ็นต์

สาขาวิชา ชีวเคมีและชีววิทยาโมเลกุล

ลายมือชื่อนิสิต

ปีการศึกษา 2561

ลายมือชื่อ อ.ที่ปรึกษาหลัก

5872022823 : MAJOR BIOCHEMISTRY AND MOLECULAR BIOLOGY

KEYWORD: aroG/ Feedback-resistant/ L-phenylalanine production

Maria Ulfah : EFFECT OF FEEDBACK-RESISTANT *aroG* OVEREXPRESSION ON L-PHENYLALANINE PRODUCTION IN *Escherichia coli*. Advisor: Asst. Prof. Kanoktip Packdibamrung

L-Phenylalanine (L-Phe) is one of the most important amino acids in food and pharmaceutical industries. It is widely used as a nutritional supplement and a precursor for the synthesis of food additives. The market of L-Phe has been stimulated by increasing demand for the low-calorie sweetener, aspartame. In *Escherichia coli*, the key enzyme which catalyzes the first committed step of aromatic amino acid biosynthesis pathway is 3-deoxy-D-arabino-heptulosonate-7-phosphate synthase (DAHP-synthase). The enzyme has 3 isoforms, AroG, AroF and AroH, which are feedback inhibited by L-Phe, L-Tyr and L-Trp, respectively. AroG, encoded by *aroG*, is the major isoform contributed about 80% of the total DAHP activity. To investigate the feedback inhibition site of AroG, Leu175 was replaced by Asp (L175D) and Gln151 was replaced by Ala (Q151A), Leu (Q151L) and Asn (Q151N). In this study, each feedback resistant *aroG* was cloned with other pivotal genes in L-Phe biosynthesis pathway (*aroB*, *aroL*, *phedh* and *tktA*) into pRSFDuet-1 vector. The recombinant plasmid (pBLPTG*) were then co-expressed with pBAD33 vector containing a glycerol uptake gene (*glpF*) and an aromatic amino acid exporter gene (*yddG*) (pYF) into *E. coli* BL21(DE3). The highest production of L-Phe at 1.8 g/L was obtained when both pBLPTG*Q151L & pYF and pBLPTG*Q151N & pYF clones were cultured in glycerol medium for 6 days. These L-Phe yields were 7.7 fold higher than obtained from the control with *aroG* wild-type (pBLPTG & pYF), while L-Phe yield from pBLPTG*L175D & pYF and pBLPTG*Q151A & pYF were 2.7 and 2.5 fold, respectively. The results revealed that substitution of Leu and Asn at Gln151 could well reduce the feedback inhibition. After that the recombinant clone of pBLPTG*Q151L & pYF was selected for optimization of medium components using response surface methodology (RSM). The maximum L-Phe production at 2.03 g/L was obtained when the pBLPTG*Q151L & pYF was cultured in minimum medium containing 60 g/L glycerol and 42.4 g/L (NH₄)₂SO₄ after induction with 0.02% arabinose at 37 °C for 6 days.

Field of Study: Biochemistry and Molecular Biology Student's Signature

Academic Year: 2018 Advisor's Signature

ACKNOWLEDGEMENTS

The biggest praise may address to Allah, God the Almighty who give me life, health, care and this great opportunity.

I would like to express my gratitude to my thesis advisor Assistant Professor Dr. Kanoktip Packdibamrung and her kind-hearted to accept me as her student with all my weaknesses. Teach me how to learn and to be patient to pass this amazing period of study. My heart-felt thanks to her for the priceless time that she spent to help me finishing this thesis including its content, approach, advice, and effective guidance throughout this project.

I would also like to send my grateful to members this thesis committee; Assistant Professor Dr. Rath Pichyangkura, Assistant Professor Dr. Kunlaya Somboonwiwat, Associate Professor Dr. Teerapong Buaboocha and Assistant Professor Dr. Ratre Wongpanya for their contributions on comments and recommendations to this thesis.

My grateful was also addressed for my Director in Center for Bioindustrial Technology, Agency for The assessment and Application of Technology, Indonesia who give me permission and chance to continue study and explore my knowledge. My senior staff and colleagues who always gave me support through this study.

For all friends and colleagues at Department of Biochemistry, Faculty of Science, Chulalongkorn University, especially in room numbers 707, I am pleased to express my thankful for their assistance, friendships, advice to improve my knowledge and skills. For my Indonesian friends that I cannot mention one by one, who always be there when I needed, thanks for being good friends, sister and even family for me.

Finally, my deepest gratitude was dedicated to my family, my husband Andri Noviandy, my children Ahza Rijal Aufa and Myesha Shakira Aufa who accompany me in this great journey. A million thanks for the good and the bad times, for tears and thousand smiles we have been through together. For my mother; Hj. Yusriah, my sisters and brother; Dewi Hairani, Teddy Asyikin, Nuraini, Diana Yusrini, thank you for the pray that never been absence to be sent in every single times, that really meant a lot. I

addressed my grateful for their understanding, helping and supporting to pass this chapter.

The last but not least, I address my grateful to the Office of the Higher Education Commission, Thailand, The Chulalongkorn University Graduate Scholarship to commemorate the 72nd anniversary of His Majesty King Bhumibol Adulyadej for supporting my study.

Maria Ulfah



TABLE OF CONTENTS

	Page
.....	iii
ABSTRACT (THAI).....	iii
.....	iv
ABSTRACT (ENGLISH).....	iv
ACKNOWLEDGEMENTS.....	v
TABLE OF CONTENTS.....	vii
LIST OF TABLES.....	xi
LIST OF FIGURES.....	xii
LIST OF ABBREVIATION.....	xiv
CHAPTER I INTRODUCTION.....	1
1.1 Amino acid.....	1
1.2 L-phenylalanine.....	3
1.3 L-phenylalanine production.....	4
1.4 L-phenylalanine biosynthesis pathway in <i>E. coli</i>	5
1.5 Metabolic engineering for biosynthesis of L-phenylalanine in <i>E. coli</i>	8
1.6 Two plasmid-mediated co-expression in <i>E. coli</i>	13
1.7 Using glycerol as a carbon source.....	15
1.8 Response surface methodology for optimization of L-Phe.....	18
1.9 Objective of the research.....	21
CHAPTER II MATERIALS AND METHODS.....	22
2.1 Equipments.....	22

2.2 Disposable materials.....	23
2.3 Markers	23
2.4 Kits.....	23
2.5 Chemicals.....	23
2.6 Enzymes and restriction enzymes.....	25
2.7 Bioinformatics tools	25
2.8 Bacterial strains and plasmids	25
2.9 Oligonucleotides.....	26
2.10 Amplification of <i>aroG</i> wild-type and <i>aroG</i> ^{fbr}	27
2.10.1 Plasmid extraction.....	27
2.10.2 Agarose gel electrophoresis.....	29
2.10.3 PCR amplification of <i>aroG</i> wild-type and <i>aroG</i> ^{fbr}	29
2.11 Construction of pBLPTG and pBLPTG*	30
2.11.1 Vector DNA preparation	30
2.11.2 Insert DNA preparation	31
2.11.3 Ligation of vector and insert DNA	31
2.11.4 Transformation of recombinant plasmid.....	33
2.11.4.1 Preparation of competent cell.....	33
2.11.4.2 Electroporation	33
2.11.5 Selection of recombinant clone.....	34
2.11.5.1 Rapid selection by colony PCR	34
2.11.5.2 Plasmid extraction and restriction enzyme digestion.....	35
2.11.6 Nucleotide sequencing.....	35
2.12 Co-transformation of pBLPTG or pBLPTG* and pYF into <i>E. coli</i> BL21(DE3)	35

2.12.1 Electroporation	37
2.12.2 Plasmid extraction and restriction enzyme digestion	37
2.13 SDS-polyacrylamide gel electrophoresis.....	38
2.14 Study of L-phenylalanine production by pBLPTG or pBLPTG* & pYF clone....	41
2.14.1 L-phenylalanine production	41
2.14.2 Product determination by HPLC.....	42
2.15 Experimental design for L-phenylalanine production using response surface methodology (RSM).....	42
CHAPTER III RESULTS AND DISCUSSIONS.....	45
3.1. Amplification of <i>aroG</i> wild-type and <i>aroG</i> ^{fbr}	45
3. 2 Construction of pBLPTG and pBLPTG*	48
3.3 Nucleotide sequencing	50
3.4 Co-transformation of pBLPTG* & pYF into <i>E. coli</i> BL21(DE3)	57
3.5 Plasmid extraction and restriction enzyme digestion analysis	58
3.6 Protein expression of <i>E. coli</i> harboring pBLPTG or pBLPTG* & pYF.....	60
3.7 L-Phe production	62
3.8 Optimization of medium component using response surface methodology (RSM).....	65
CHAPTER IV CONCLUSIONS.....	69
REFERENCES	71
APPENDICES.....	79
APPENDIX A Restriction map of pRSFDuet-1	80
APPENDIX B Standard curve for protein determination by Lowry's method.....	81
APPENDIX C Preparation for denaturing polyacrylamide gel electrophoresis.....	82

APPENDIX D Preparation for agarose gel electrophoresis and HPLC mobile phase	86
APPENDIX E Standard curve for L-phenylalanine determination by HPLC	87
APPENDIX F Chromatogram of L-phenylalanine.....	88
APPENDIX G The sequencing chromatogram of <i>aroG</i> in pBLPTG using primers F_DuetUP_aroG_Intr (A) and R_Duet (B)	91
APPENDIX H The sequencing chromatogram of <i>aroG</i> ^{fbr} L175D in pBLPTG*L175D using primers F_DuetUP_aroG_Intr (A) and R_Duet (B).....	93
APPENDIX I The sequencing chromatogram of <i>aroG</i> ^{fbr} Q151A in pBLPTG*Q151A using primers F_DuetUP_aroG_Intr (A) and R_Duet (B).....	95
APPENDIX J The sequencing chromatogram of <i>aroG</i> ^{fbr} Q151L in pBLPTG*Q151L using primers F_DuetUP_aroG_Intr (A) and R_Duet (B).....	97
APPENDIX K The sequencing chromatogram of <i>aroG</i> ^{fbr} Q151N in pBLPTG*Q151N using primers F_DuetUP_aroG_Intr (A) and R_Duet (B).....	99
VITA.....	101

LIST OF TABLES

	Page
Table 1 Experimental matrices for central composite design	20
Table 2 Plasmids used in this work	26
Table 3 The oligonucleotide primers used for PCR amplification	27
Table 4 The oligonucleotide primers used for DNA sequencing	27
Table 5 Molecular weight of each protein in recombinant plasmid pBLPTG	41
Table 6 Level of different process variable in coded level for L-Phe Production	43
Table 7 Experimental design obtained by CCD matrix	44
Table 8 Experimental design and result of central composite design for L-Phe production	67

LIST OF FIGURES

	Page
Figure 1 Pathway of aromatic amino acid biosynthesis and its regulation in <i>E. coli</i>	7
Figure 2 The inhibitor-binding site of DHAP synthase	11
Figure 3 Aromatic amino acid biosynthetic pathway using glycerol as carbon source in <i>E. coli</i> BL21(DE3)	12
Figure 4 Diagram of expression vectors and co-expression strategies	14
Figure 5 Respiratory metabolism of glycerol in <i>E. coli</i>	17
Figure 6 Map of pAroG or pAroG* (SnapGene 1.1.3)	28
Figure 7 Simulation of <i>Bam</i> HI and <i>Hind</i> III digested pAroG or pAroG* (pDRAW32 revision 1.1.134)	28
Figure 8 The construction of pBLPTG or pBLPTG*	32
Figure 9 Map of <i>Xho</i> I in pBLPTG or pBLPTG* (SnapGene 1.1.3.4)	36
Figure 10 The simulation of <i>Xho</i> I digested pBLPTG* (pDRAW32 revision 1.1.134)	36
Figure 11 The illustration of pYF and pBLPTG* in <i>E. coli</i> BL21 (DE3)	37
Figure 12 The simulation of recombinant plasmids digested with <i>Bam</i> HI ...	39
Figure 13 <i>Bam</i> HI and <i>Hind</i> III pattern of pAroG and pAroG*	46
Figure 14 Amplification of <i>aroG</i> and each <i>aroG</i> ^{fbr}	47
Figure 15 Restriction pattern of pBLPTG and pBLPTG* digested by <i>Xho</i> I	49
Figure 16 The nucleotide sequence and deduced amino acid sequence of <i>aroG</i> in pBLPTG	51
Figure 17 The nucleotide sequence and deduced amino acid sequence of <i>aroGL175D</i> in pBLPTG*	52
Figure 18 The nucleotide sequence and deduced amino acid sequence of <i>aroGQ151A</i> in pBLPTG*	53

Figure 19 The nucleotide sequence and deduced amino acid sequence of <i>aroG</i> Q151L in pBLPTG*	54
Figure 20 The nucleotide sequence and deduced amino acid sequence of <i>aroG</i> Q151N in pBLPTG*	55
Figure 21 The deduced amino acid sequence of <i>aroG</i> compare to <i>aroG</i> ^{fbr} in pBLPTG and pBLPTG*	56
Figure 22 The screening of pBLPTG and pBLPTG* & pYF in <i>E. coli</i> BL21(DE3) in agar plate supplemented with 30 µg/mL of kanamycin and 10 µg/mL of chloramphenicol	57
Figure 23 Restriction pattern of pBLPTG and pBLPTG* & pYF digested by <i>Bam</i> HI	59
Figure 24 SDS-PAGE analyses of the recombinant proteins	61
Figure 25 The growth curve of recombinant clones and L-Phe production in minimum medium	64
Figure 26 Response surface and contour plot for the interactive effect of glycerol and ammonium sulfate on L-Phe production	68

LIST OF ABBREVIATION

A	absorbance, 2'-deoxyadenosine (in a DNA sequence)
AroB	3-dehydroquinate synthase
<i>aroB</i>	3-dehydroquinate synthase gene
AroF	L-tyrosine-feedback inhibited DAHP synthase
<i>aroF</i>	L-tyrosine-feedback inhibited DAHP synthase gene
<i>aroF^{fbr}</i>	L-tryptophan-feedback resistant DAHP synthase gene
AroG	L-phenylalanine-feedback inhibited DAHP synthase
<i>aroG</i>	L-phenylalanine-feedback inhibited DAHP synthase gene
<i>aroG^{fbr}</i>	L-phenylalanine-feedback resistant DAHP synthase gene
AroH	L-tryptophan-feedback inhibited DAHP synthase
<i>aroH</i>	L-tryptophan-feedback inhibited DAHP synthase gene
AroL	shikimate kinase II
<i>aroL</i>	shikimate kinase II gene
bp	base pairs
BSA	bovine serum albumin
C	2'-deoxycytidine (in a DNA sequence)
°C	degree Celsius
Da	Dalton
DNA	deoxyribonucleic acid

dNTP	2'-deoxynucleoside 5'-triphosphate
EC	Enzyme Commission
EDTA	ethylene diamine tetraacetic acid
G	2'-deoxyguanosine (in a DNA sequence)
GlpF	glycerol facilitator
<i>glpF</i>	glycerol facilitator gene
GlpFK	glycerol facilitator and glycerol kinase
<i>glpFK</i>	glycerol facilitator and glycerol kinase genes
GlpK	glycerol kinase
<i>glpK</i>	glycerol kinase gene
HPLC	high-performance liquid chromatography
IPTG	isopropyl- β -D-thiogalactoside
kb	kilobase pairs in duplex nucleic acid, kilobases in single-stranded nucleic acid
kDa	kiloDalton
K_m	Michaelis constant
KOH	potassium hydroxide
L	liter
L-Phe	L-phenylalanine
L-Trp	L-tryptophan
L-Tyr	L-tyrosine

LB	Luria-Bertani
μg	microgram
μL	microliter
μM	micromolar
M	mole per liter (molar)
mg	milligram
min	minute
mL	milliliter
mM	millimolar
MW	molecular weight
N	normal
NAD^+	nicotinamide adenine dinucleotide (oxidized)
NADH	nicotinamide adenine dinucleotide (reduced)
NADPH	nicotinamide adenine dinucleotide phosphate (reduced)
ng	nanogram
nm	nanometer
OD	optical density
PAGE	polyacrylamide gel electrophoresis
PCR	polymerase chain reaction
PheA	chorismate mutase/ prephenate dehydratase
<i>pheA</i>	chorismate mutase/ prephenate dehydratase gene

<i>pheA</i> ^{fbr}	feedback resistant chorismate mutase/ prephenate dehydratase
PheDH	phenylalanine dehydrogenase
<i>pheDH</i>	phenylalanine dehydrogenase gene
PMSF	phenyl methyl sulfonyl fluoride
RNase	ribonuclease
SDS	sodium dodecyl sulfate
T	2'-deoxythymidine (in a DNA sequence)
TE	Tris-EDTA buffer
TEMED	<i>N, N, N', N'</i> -tetramethyl ethylene diamine
TktA	transketolase
<i>tktA</i>	transketolase gene
<i>T_m</i>	melting temperature, melting point
UV	ultraviolet
v/v	volume by volume
vvm	volumes of air per volume of liquid per minute
w/w	weight by weight
YddG	aromatic amino acid exporter
<i>yddG</i>	aromatic amino acid exporter gene

CHAPTER I

INTRODUCTION

1.1 Amino acid

Amino acids are organic compound that consists of a basic amino group ($-\text{NH}_2$), an acidic carboxyl group ($-\text{COOH}$), and an organic R-group or called as side chain. The amino acids differ from each other in the particular chemical structure of the R-group (Nelson, 2007). Amino acids are essential for every metabolic process. They are utilized in living cells for protein synthesis under the control of genes and play important role as the building blocks of protein and as metabolic intermediate (Barret and Elmore, 2004, Mitsushashi, 2014).

On the basis of the dietary requirement for amino acids to support growth, amino acids are traditionally classified as nutritionally essential or nonessential for animals and humans. Among the 20 standard proteinogenic amino acids, the nine essential amino acids (valine, leucine, isoleucine, lysine, threonine, methionine, histidine, phenylalanine, and tryptophan) play role as key positions because they cannot be synthesized by animals and humans but need to be supplemented with food or feed (Mitsushashi, 2014). The non-proteinogenic amino acids are not required to form the proteins but these amino acids play a vital role as precursor or metabolic intermediates (Barret and Elmore, 2004).

Amino acids have been found in various applications for the biotechnology production (Wendisch, 2014). They are attractive and promising biochemical agent

since their applicability ranges from foods, animal feed additives as well as intermediates in chemical industry, flavor enhancers and ingredients in cosmetic to specialty nutrients in pharmaceutical and medical fields (D'Este et al., 2018). The increasing demand of amino acid market was stimulated since the production of monosodium glutamate (MSG) in 1970 (Sano, 2009, D'Este et al., 2018). Indeed, in 2008 the amino acids reached the largest share of the market which was around USD 5.4 billion (März, 2009). The worldwide market of amino acid used as feed additives is largest segment of total amino acid (lysine, methionine, threonine, and tryptophan) (Mitsubishi, 2014, Leuchtenberger et al., 2005). The food segment shares smaller market which determined by three amino acids: L-glutamic acid, L-aspartic acid and L-phenylalanine. L-glutamic acid is well known in the form of the flavor enhancer mono sodium glutamate (MSG). L-aspartic acid and L-phenylalanine are commonly used as starting materials for the peptide artificial sweetener (aspartame) (Leuchtenberger et al., 2005).

The market of amino acid is increasing due to the growing world population and high demand of animal products. This condition drives strain optimization and amino acid process intensification (Wendisch, 2014). Amino acids can be produced through three different processes: extraction, chemical synthesis and microbial processes (enzymatic synthesis and fermentation) (D'Este et al., 2018). However, the industrial processes to produce amino acids still need to be optimized with the aim of finding more cost-effective and sustainable routes to produce amino acids. Firstly,

Corynebacterium glutamicum has been used safely in food biotechnology then *Escherichia coli* is continuously improved using metabolic engineering approaches (Wendisch, 2014). This thesis focused on the production of L-phenylalanine by the recombinant *E. coli* clones.

1.2 L-phenylalanine

L-phenylalanine (L-Phe, $C_9H_{11}NO_2$; MW: 165.192 g/mol), is an essential aromatic amino acid in human (provided by food). It can be consumed from protein foods, such as meat, cottage cheese and wheat germ. L-Phe plays a key role in the biosynthesis of other amino acids and important in the structure and function of many proteins and enzymes. L-Phe is converted to tyrosine which used in the biosynthesis of dopamine and noradrenaline (norepinephrine) neurotransmitters. L-Phe is highly concentrated in the human brain and plasma. In pharmaceutical industry, the psychotropic drugs, (mescaline, morphine, codeine and papaverine) also have phenylalanine as a constituent (NCBI, 2017).

Furthermore, L-Phe is also used as additive in the food and feed industry as well as in pharmaceutical active compounds like HIV protease inhibitor, anti-inflammatory drugs and renin inhibitors (Bongaerts et al., 2001, Sprenger, 2007). In food industry, L-Phe is commonly used as flavor enhancer, but produced predominantly for the production of the low-calorie sweetened aspartame (L-aspartyl-L-phenylalanine methyl ester) and is increasingly being used in diet drinks or food (Ager et al., 1998, Bongaerts et al., 2001). Aspartame or artificial sugar commonly used as substitution

sugar, because it can give about 160 - 180 times sweeter than sucrose; so less of aspartame can be used to give the same level of sucrose (Ager et al., 1998).

Nowadays, the Essential Amino Acid Association in Japan estimated that more than 2.3 million tons of amino acids per year were produced in 2000 by using bacteria or bacterial enzymes (Suzuki, 2013). In 2007, it has been reported that the L-Phe market was 12, 650 ton/year which consumed USD 198 million (Demain, 2007).

1.3 L-phenylalanine production

L-phenylalanine can be synthesized by chemical reaction, enzymatic process and fermentation. For the large-scale production, L-Phe is mostly produced by fermentation processes based on L-Phe-producing mutants, especially metabolically engineered strains of *C. glutamicum* or *E. coli*. These strains are well known as economically superior to the alternatives of the chemical synthesis (Ikeda, 2006, Sprenger, 2007). The enzymatic process is based on the action of an enzyme or a combination of them to catalyze the production of the desired amino acids. The main advantage of the enzymatic process is it can produce optically pure D and L-amino acids in higher concentrations and lower by-products formation (Ikeda, 2003).

In development of industrial process, *E. coli* gives the advantages of high growth and production rates combined with high yields by using simple media which are suitable for product recovery efficiently (Gerigk et al., 2002). Hence, using recombinant *E. coli* strains is a great deal on the L-Phe process development and

many research works have been patented (Kim et al., 1994, Lim et al., 1995, Sprenger et al., 1998).

The higher L-Phe concentrations of 34 g/L, 46 g/L and 50 g/L were achieved (Ruffer et al., 2004, Konstantinov et al., 1991, Backman et al., 1990) with metabolically engineered strains of *E. coli* with glucose as a carbon source. It also has been reported that the production of L-Phe were achieve 0.58 g/L, 0.74 g/L, and 13.4 g/L (Khamduang et al., 2009, Ratchaneeladdajit, 2014, Weiner et al., 2014) from engineered *E. coli* strains using glycerol as a carbon source.

1.4 L-phenylalanine biosynthesis pathway in *E. coli*

The biosynthesis of L-Phe has ten reactions from the condensation of phosphoenolpyruvate (PEP) and erythrose-4-phosphate (E4P) (Bongaerts et al., 2001) (Figure 1). The first committed step and most tightly regulated reaction is the condensation of phosphoenolpyruvate (PEP) from glycolysis pathway and erythrose 4-phosphate (E4P) from pentose phosphate pathway (PPP) to form 3-dehydroxy-D-arabino-heptulosonate 7-phosphate (DAHP) by three isoenzymes of DAHP synthase (Bongaerts et al., 2001).

In the second step of pathway, DHAP is converted into 3-dehydroquinate (DHQ) which catalyzed by DHQ synthase (encoded by *aroB*). Subsequently, DHQ dehydratase (encoded by *aroD*) catalyzes the dehydration of DHQ to form 3-dehydroshikimate (DHS). The next step is the reduction of DHS to shikimate (SHIK) by shikimate dehydrogenase (encoded by *aroE* and *ydiB*) (Michel et al., 2003). SHIK is

then phosphorylated to yield shikimate 3-phosphate (S3P). This reaction is catalyzed by shikimate kinase I and II (encoded by *aroK* and *aroL*, respectively).

The next step is condensation of S3P and the second molecule of PEP to yield 5-enolpyruvoyl shikimate 3-phosphate (EPSP). This reaction is catalyzed by EPSP synthase (encoded by *aroA*). The EPSP is then converted to form chorismate (CHA). This reaction is catalyzed by chorismate synthase (encoded by *aroC*). The DHQ synthase (encoded by *aroB*) and shikimate kinase (encoded by *aroL* or *aroK*) were identified as the rate-limiting enzymes for aromatic amino acid biosynthesis pathway in *E. coli* (Dell and Frost, 1993). The central pathway branches at CHA to permit the terminal pathways that are specific for relevant aromatic amino acid (L-Phe or L-Tyr or L-Trp) (Bongaerts et al., 2001, Maeda and Dudareva, 2012). Chorismate (CHA) is then converted to prephenate (PPA). The L-Phe biosynthesis pathway is branched at prephenate (PPA) by the activity of the bifunctional enzymes chorismate mutase/prephenate dehydratase (CM-PDT, encoded by *pheA*) for L-Phe and chorismate mutase/prephenate dehydrogenase (encoded by *tyrA*) for L-Tyr. PheA catalyzes a conversion of chorismate to phenylpyruvate (PPY) through prephenate (PPA) intermediate.

The last step of L-Phe biosynthesis is a transamination reaction into phenylpyruvate (PPY) with amino donor glutamate to yield L-Phe. This reaction is catalyzed by three amino transferases encoded by *tyrB*, *aspC* and *ilvE* (Chao et al., 1999, Rodriguez et al., 2014).

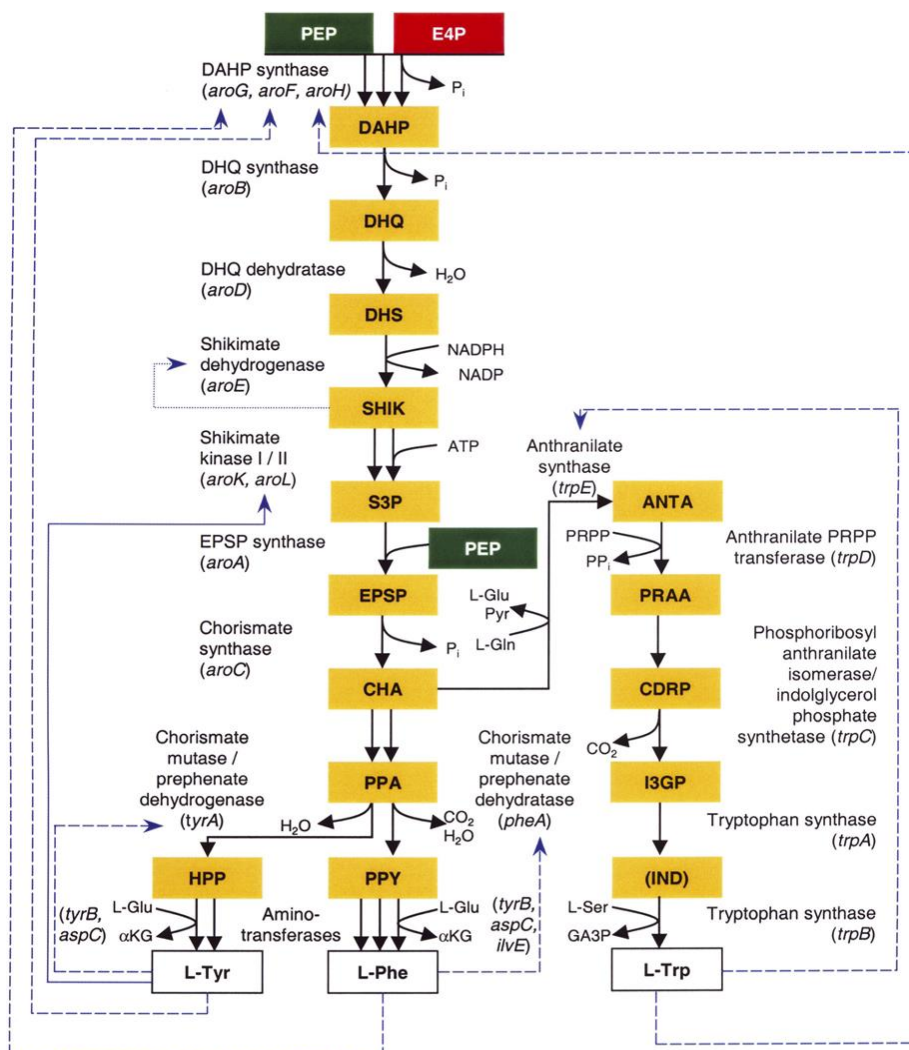


Figure 1 Pathway of aromatic amino acid biosynthesis and its regulation in *E. coli*

To indicate the type of regulation, different types of lines are used: - - -, transcriptional and allosteric control exerted by the aromatic amino acid end products; · · ·, allosteric control only; —, transcriptional control only. Abbreviations used: ANTA, anthranilate; α KG, α -ketoglutarate; CDRP, 1-(*o*-carboxyphenylamino)-1-deoxyribulose 5-phosphate; CHA, chorismate; DAHP, 3-deoxy-d-arobino-heptulosonate 7-phosphate; DHQ, 3-dehydroquinatate; DHS, 3-dehydroshikimate; EPSP, 5 *enol*pyruvylshikimate 3-phosphate; E4P, erythrose 4-phosphate; GA3P, glyceraldehyde 3-phosphate; HPP, 4-hydroxyphenylpyruvate, I3GP, indole 3-glycerolphosphate; IND, indole; L-Gln, L-glutamine; L-Glu, L-glutamate; L-Phe, L-phenylalanine; L-Ser, L-serine; L-Trp, L-tryptophan; L-Tyr, L-tyrosine; PEP,

phosphoenolpyruvate; PPA, prephenate; PPY, phenylpyruvate; PRAA, phosphoribosyl anthranilate; PRPP, 5-phosphoribosyl-*a*-pyrophosphate; Pyr, pyruvate; SHIK, shikimate; S3P, shikimate 3-phosphate.

Source: (Bongaerts et al., 2001)

1.5 Metabolic engineering for biosynthesis of L-phenylalanine in *E. coli*

The biosynthesis of L-Phe is one of the most complicated amino acid synthesis pathways. There are some key enzymes and pivotal genes involve in the route (Pittard, 1996). Several enzymes of the aromatic amino acid biosynthetic pathway are subjected to feedback regulation (Liu et al., 2014). *E. coli* strains for L-Phe production have been constructed with recombinant DNA technology. Several strategies are used for improvement of L-Phe production including overexpression of possible rate-limiting enzyme(s) and/or genetically switch off the feedback inhibition enzyme (Liu et al., 2013, Liu et al., 2014).

Some works have been studied on the characterization of the feedback-resistant DAHP synthases (DS) and chorismate mutase-prephenatedehydratase (CM-PDT) in L-Phe biosynthesis (Backman et al., 1990, Ikeda, 2006, Zhou et al., 2010). DAHP synthases (DS) is the first committed step in aromatic metabolites encoded by each of three paralog genes *aroF*, *aroG*, and *aroH* (encodes for AroF, AroG and AroH, respectively). These enzymes are subjected to feedback inhibition by its end products of L-tyrosine (L-Tyr), L-phenylalanine (L-Phe), and L-tryptophan (L-Trp), respectively (Rodriguez et al., 2014). The AroL is the dominant isoenzyme with high affinity to the

substrate. The K_m value of AroL is 100-fold lower than AroK (De Feyter, 1987). About 80% of total DHAPS activity is contributed by AroG, 15% from AroF, and remaining activity corresponds to AroH (Herrmann, 1995). The second rate-limiting step in the L-Phe biosynthesis is the conversion of chorismate to phenylpyruvate, via prephenate catalyzed by a bifunctional enzyme chorismate mutase prephenate dehydratase (CM-PDT) encoded by *pheA*. This enzyme is also sensitive to feedback inhibition mediated by allosteric binding of L-Phe (Pittard, 1996, Zhang et al., 1998). Gerigk and coworkers used recombinant *E. coli* carrying feedback-resistant *pheA* (*pheA^{fbr}*) and feedback-resistant *aroF* (*aroF^{fbr}*) to synthesize L-Phe in 20 L bioreactor and achieved more than 30 g/L of L-Phe (Gerigk et al., 2002). It also has been reported that the construction of genetically modified *E. coli* strain with *pheA^{fbr}* and *aroF^{fbr}*, with L-Phe titer of 50 g/L was achieved after 36 h (Backman et al., 1990). Liu and coworkers demonstrated the replacing of Asp146 with Asn in AroG (AroG15) gave a thermostable mutant. The engineered *E. coli* expressing *aroG15*, *pheA^{fbr}*, *ydiB*, *aroK*, *tyrB* and *yddG* improved the excretion of L-Phe into the medium at higher rate of 47.0 g/L and less intracellular of L-Phe accumulated (Liu et al., 2014).

In aromatic amino acid producing strains, DAHP synthase activity is strongly reduced as a result of feedback control by the end products. To overcome allosteric inhibition in the pathway, amino acid substitution have been successfully constructed to relieve feedback inhibition (De Boer and Dijkhuizen, 1990). The proposed binding site of Phe in DAHPS demonstrated by nine mutations; Pro19,

Asp146, Met147, Ile148, Pro150, Gln151, Ala154, Gly178, and Ser180 can eliminate or strongly reduce feedback inhibition (Shumilin et al., 1999).

Hu and coworkers investigated the feedback inhibition site of AroG using the proposed possible L-Phe binding site for feedback inhibition from 3D structure of AroG co-crystallized with the substrate PEP (Figure 2A). The enzyme activity assay showed that the amino acid replacement at Pro150, L175, L179, F209 and V221 completely or partially relieved feedback inhibition. Among these mutants, L175D was mostly resistant to feedback inhibition. It remained 83.5% of relative enzymatic activity at 1 mM L-Phe. Moreover, specific enzymatic activity of L175D at 0 mM Phe increased significantly (4.46 U/mg) when compared with wild-type AroG (2.70 U/mg) (Hu et al., 2003).

In our previous work, UCSF Chimera Program was used to determine amino acid residues at regulatory site of AroG from *E. coli* that interact with Phe. Crystal structure of AroG complexed with Mn^{2+} , PEP and Phe (PDB ID 1KFL) resulted from X-ray diffraction at resolution 2.8 Å was used. The result showed that Gln151 forms hydrogen bond with Phe (Figure 2B). This amino acid residue has not been reported before. Thus 3 expected feedback-resistant AroG (AroG^{fbr}) were achieved by replacing Gln151 with Ala (Q151A), Leu (Q151L), and Asn (Q151N). L175D that was reported by Hu *et al* (2003) was also performed. These four *aroG*^{fbr} were successfully constructed and cloned into pRSFDuet-1 (pAroG*) (Kanoksinwuttipong, 2014).

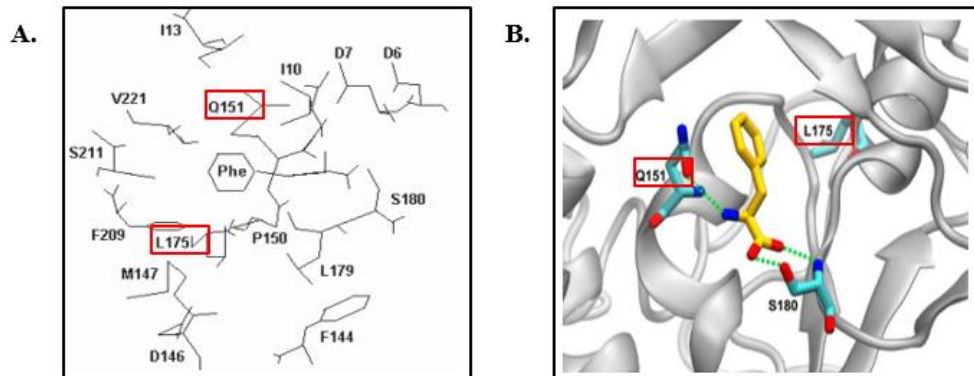


Figure 2 The inhibitor-binding site of DHAP synthase

(A) L175 and Q151 residues of DAHP synthase are within Van Der Waals contact of the bound phenylalanine. (B) The 3D structure of AroG complexed with Mn^{2+} , PEP and Phe (PDB ID 1KFL). Q151 interacts with Phe using hydrogen bond.

Source: (Hu et al., 2003, Kanoksinwuttipong, 2014)

Moreover, Thongchuang and coworkers co-expressed phenylalanine dehydrogenase gene (*phedh*) from *Bacillus lentus*, glycerol facilitator gene (*glpF*), and aromatic amino acid exporter (*yddG*) from *E. coli* in pRSFDuet-1 (pPYF). The fermentation of pPYF clone in glycerol medium showed that the maximum L-Phe production was 280 mg/L in the shake flasks (Thongchuang et al., 2012). Then, co-expression of *aroB*, *aroL* and *tktA* which encode 3-dehydroquinate synthase, shikimate kinase II, and transketolase, respectively, with the former three genes was performed. The recombinant pPTFBLY clone produced 429 mg/L of L-Phe at the rate of 3.36 mg/L/h (Thongchuang, 2011) (Figure 3).

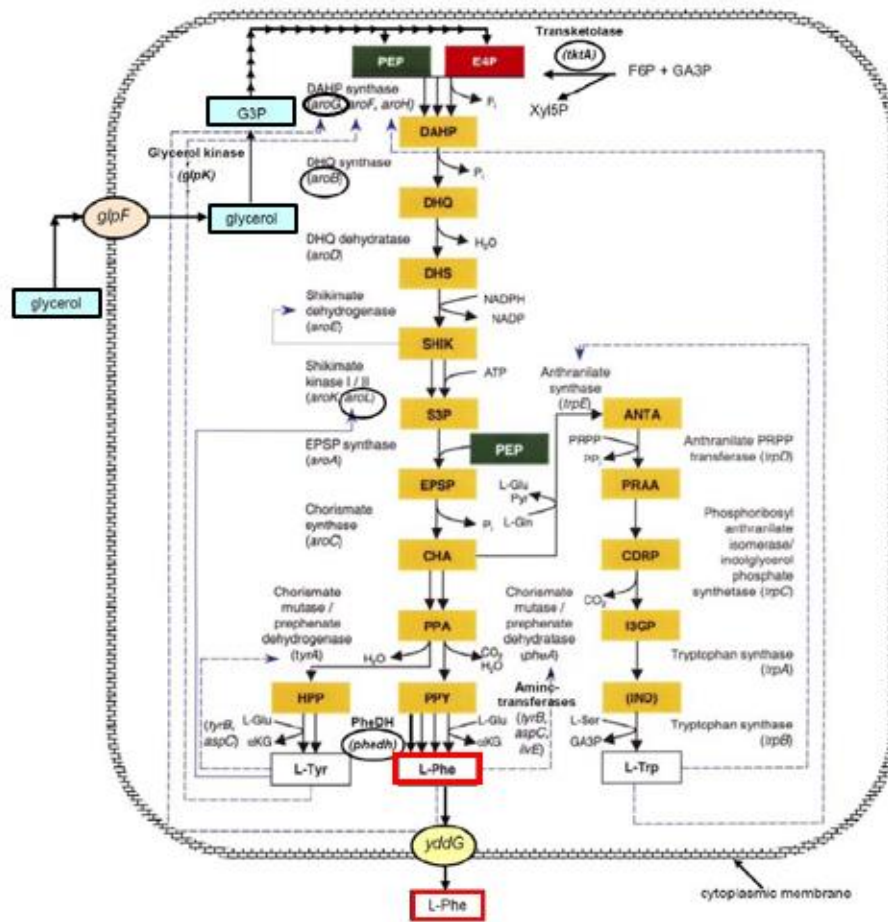


Figure 3 Aromatic amino acid biosynthetic pathway using glycerol as carbon source in *E. coli* BL21(DE3)

Source: Thongchuan, 2011

However, the morphology of this recombinant clone was different from normal shape. The smaller and flat colonies were formed on agar plate with undulate margin. The different morphology of colony might occur from the basal level expression of membrane-associated protein (*yddG* and *glpF*). The trans-membrane protein YddG and GlpF are relatively hydrophobic and believed to be toxic to cell

when express at high level (Thongchuang et al., 2012). The phenomenon was reported in over-production of seven membrane proteins in *E. coli*-bacteriophage T7 RNA polymerase expression system. When expression of the target membrane protein was induced, most of the *E. coli* BL21(DE3) host cell died (Miroux and Walker, 1996). Therefore, expressing these genes in dual plasmid system may overcome this problem.

1.6 Two plasmid-mediated co-expression in *E. coli*

Recently, many researchers are interested in production of protein complex by co-expression. This technique is used to produce various active soluble protein such as intracellular protein, secreted proteins and intracellular/ extracellular domain of membrane protein (Kerrigan et al., 2011) Co-expression involves the transformant with several plasmids that have compatible *ori* of replication and antibiotic selection. Many strategies can be achieved for protein partner co-expression via a single expression vector or multiple expression vectors, via a single ORF or multiple ORFs (Kerrigan et al., 2011, Hanzlowsky et al., 2006).

A multi-vector co-expression system utilizes two or more expression vectors, each expressing one or two component proteins as illustrated in Figure 4 (Kerrigan et al., 2011). In eukaryotic cells for stable expression, multiple vectors can be selected via different selectable markers, either via episomal maintenance or genomic insertion. In *E. coli*, co-expression via this strategy requires each vector contain a different origin of replication (*ori*) and a different selectable marker.

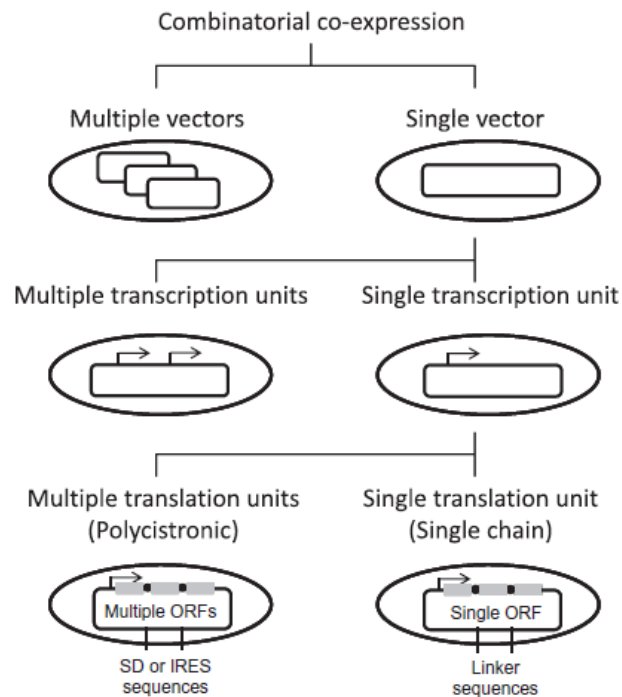


Figure 4 Diagram of expression vectors and co-expression strategies

The diagram depicts expression vectors and strategies for co-expression in *E. coli*. Ovals represent *E. coli* cell, and rectangles represent expression vectors. Bent arrows represent individual expression cassettes, and shaded rectangles are for individual ORFs. The round dots represent either ribosome binding sites or linker sequences, as indicated. Each vector can be used alone or in combination with others. SD, Shine-Dalgarno sequence; IRES, internal ribosome entry site; ORF, open reading frame.

Source: (Kerrigan et al., 2011)

Dzivenu and coworkers constructed the bacterial co-expression vectors to produce the substantial amounts of recombinant multi protein complexes. They used two different plasmid pOKD4 and pOKD5 (kanamycin and ampicillin resistant, respectively) which are derivatives of pACYC177 and pET26b. The result showed that the efficacy and versatility of this co-expression vectors were successfully

constructed for the production of active DFF40/DFF45 heterodimeric protein complex in *E. coli* (Dzivenu et al., 2004).

Yang and coworkers successfully co-expressed the human DNA fragmentation factor (DFF) in *E. coli* using two incompatible plasmids. The two subunits of DFF45 and DFF40 were cloned into two incompatible vectors pET-21a with ampicillin resistance and pET-28a with kanamycin resistance, respectively. In the presence of the two antibiotics, the DFF45 and DFF40 were co-expressed successfully which product contained of soluble parts for both DFF45 and DFF40 (Yang et al., 2001).

In our laboratory, the increasing L-Phe production was reported by dual plasmid system. The first plasmid was pRSFDuet-1 harboring four important genes in L-Phe biosynthesis pathway (*aroB*, *aroL*, *phedh* and *tktA*). This recombinant plasmid was co-transformed with pBAD33 vector containing a glycerol uptake gene (*glpF*) and an aromatic amino acid exporter gene (*yddG*) into *E. coli* BL21(DE3). The production of L-Phe with rate of 746 mg/L was achieved. L-Phe yield was about 1.7 fold compare to the fermentation using one expression vector (Thongchuang, 2011, Ratchaneeladdajit, 2014).

1.7 Using glycerol as a carbon source

Glycerol can be synthesized by microbial fermentation or chemical synthesis from petrochemical feedstock. In the traditional process of the latter, glycerol is released as a by-product during the hydrolysis of fats (Wang et al., 2001, Da Silva et al., 2009). Glycerol has become an inexpensive and abundant carbon source due to

its generation by-product of biodiesel fuel production. With every 100 lb of biodiesel produced by trans-esterification of vegetable oils or animal fats, 10 lb of crude glycerol is generated (Yazdani and Gonzalez, 2007). The availability of glycerol has increased significantly due to the production of biodiesel worldwide. As a consequence, prices of glycerol have fallen (Demirbas and Balat, 2006). Therefore, glycerol has also been considered as a feedstock for new industrial fermentations (Wang et al., 2001). One of advantages of using glycerol is its bioconversion to high value compounds through microbial fermentation. Glycerol is not only inexpensive and abundant, but its greater degree of reduction than sugars offers the opportunity to obtain reduced chemicals, as succinate, ethanol, xylitol, propionate, hydrogen, etc. at higher yields than those obtained using sugars (Dharmadi et al., 2006).

Compared to the conventionally fermentation used glucose and sucrose, glycerol is efficient low-cost carbon source. The initial step of glycerol utilization in *E. coli* is the uptake of glycerol molecule into the cytoplasm via protein-mediated glycerol facilitator (GlpF) encoded by the *glpF* (Sweet et al., 1990). Glycerol is trapped by an ATP-dependent glycerol kinase (GlpK) to yield glycerol- 3-phosphate (G3P) (Zwaig et al., 1970) which is then oxidized by a membrane-bound ubiquinone-8 (UQ8)-dependent G3P dehydrogenase (GlpD) to dihydroxyacetone phosphate (DHAP) that enters glycolysis (Murarka et al., 2008) (Figure 5).

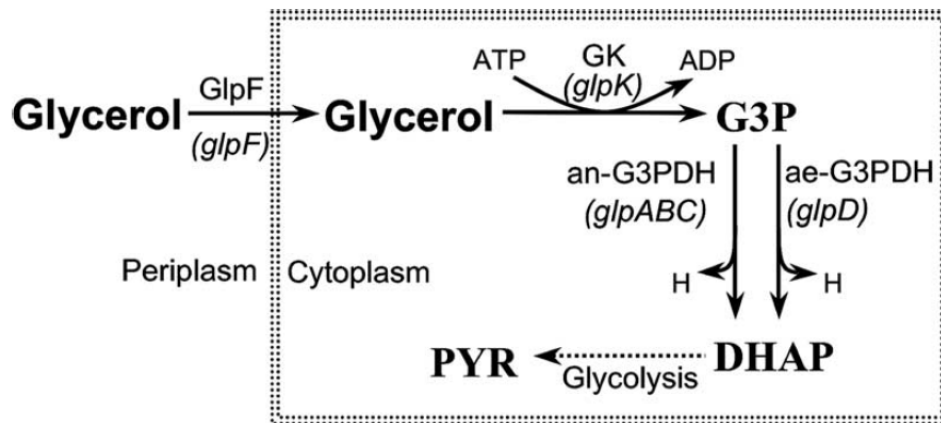


Figure 5 Respiratory metabolism of glycerol in *E. coli*

Glycerol dissimilation in the presence of electron acceptors is mediated by an ATP-dependent glycerol kinase (GK, coded for by *glpK*) and two respiratory G3PDHs (aerobic and anaerobic enzymes, encoded by *glpD* and *glpABC*, respectively). Abbreviations: DHAP, dihydroxyacetone phosphate; GK, glycerol kinase; ae-G3PDH, an-G3PDH, aerobic G3PDH; H, reducing equivalents (H = NADH/NADPH/FADH₂); PYR, pyruvate.

Source: (Murarka et al., 2008)

Another limiting step in glycerol metabolism is the necessity for a gluconeogenic formation of glucose 6-phosphate (G6P), specifically the reaction from fructose 1,6-biphosphate (F1,6BP) to fructose-6-phosphate (F6P) (Marr, 1991). This reaction is catalyzed by the enzyme fructose-1,6-bisphosphatase (FBPase). *E. coli* has two isoenzymes (FBPase I and FBPase II) encoded by the *fbp* and *glpX*, respectively (Donahue et al., 2000). Whereas PEP formation from glycerol can occur via the lower glycolytic pathway, E4P formation requires functions of the pentose phosphate pathway (PPP) and a connection from gluconeogenesis to the PPP. Thus, the enzyme

transketolase (encoded by *tktA*) could play a major role in provision of the precursor E4P when *E. coli* cells grow on glycerol (Sprenger, 2007, Gottlieb et al., 2014).

Khamduang and coworkers reported that the yield of L-phenylalanine production by recombinant *E. coli* in glycerol medium was twice when compared to values attained use glucose or sucrose as carbon source (Khamduang et al., 2009). In 2012, it has been reported that the production of L-Phe in engineered *E. coli* harboring *pheDh*, *yddg* and *glpF* using glycerol as carbon source attained 280 mg/L (Thongchuang et al., 2012). Gottlieb and coworker reported that the combination of *glpX* and *tktA* in recombinant *E. coli* using glycerol could achieve the L-Phe production at 0.37 g/L/h (Gottlieb et al., 2014).

1.8 Response surface methodology for optimization of L-Phe

Cell growth and the accumulation of metabolic products in fermentation are strongly influenced by medium compositions such as carbon sources, nitrogen sources, growth factors, and inorganic salts. The traditional 'one-factor' technique used for optimizing a multivariable system not only is time-consuming, but also may result in wrong conclusions (Oh et al., 1995, Li et al., 2002). Response surface methodology (RSM) is an empirical modeling technique for designing experiments, building models, evaluating the effects of factors, and searching optimum conditions of factors for desirable responses. RSM is used to estimate the relationship between the set of controllable experimental factors and the observed results. In completed with computing software, RSM has been successfully applied in many areas of

biotechnology such as optimization of a cultural medium (Ooijkaas et al., 1999, Li et al., 2002).

There are five steps in the application of RSM for optimization as follows: (1) selection of independent variables of major effects on studies and delimitation of the experimental substance related to the objective of the study; (2) choice the experimental design; (3) calculation the model of experimental data; (4) the evaluation of the model; (5) optimization the values for each variable (Bezerra et al., 2008).

In the RSM, a central composite design (CCD) was optimized for fitting the quadratic models, and the number of experimental points in the CCD was sufficient to test the statistical validity of the fitted model, or to uncover the model's lack of fit (Li et al., 2002, Ghosh et al., 2014).

The full uniformly rotatable CCD presents the characteristics as follows (Bezerra et al., 2008):

- (1) requiring an experiment number according to $N = k^2 + 2k + Cp$, where k is the factor number and (Cp) is the replicate number of the central point;
- (2) α -values depend on the number of variables and can be calculated by $\alpha = 2^{(k-p)/4}$.

For two, three, and four variables, they are, respectively, 1.41, 1.68, and 2.00;

- (3) all factors are studied in five levels ($-\alpha$, -1 , 0 , $+1$, $+\alpha$) (Table 1).

Table 1 Experimental matrices for central composite design

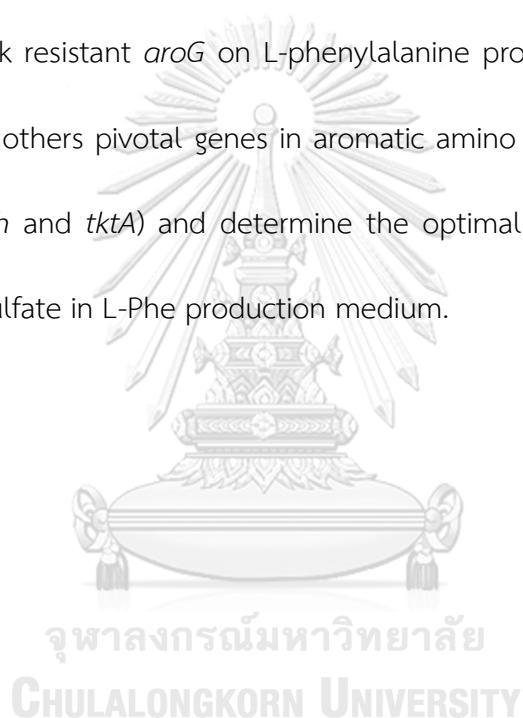
(a) two variables and (b) three variables

a			b			
	X_1	X_2		X_1	X_2	X_3
Factorial design	-1	-1	Factorial design	-1	-1	-1
	1	-1		1	-1	-1
	-1	1		-1	1	-1
	1	1		1	1	-1
Axial points	$-\alpha$	0	Axial points	-1	-1	1
	α	0		1	-1	1
	0	$-\alpha$		-1	1	1
	0	α		1	1	1
Central point	0	0	Central point	α	0	0
				α	0	0
				0	α	0
				0	α	0
				0	0	α
				0	0	α
			Central point	0	0	0

Source: (Bezerra et al., 2008)

1.9 Objective of the research

In our previous works, Ratchaneeladdajit (2014) successfully constructed dual plasmid system of pBLPT (pRSFDuet-1 harboring *phedh*, *tktA*, *aroB* and *aroL*) and pYF (pBAD33 harboring *glpF* and *yddG* in *E. coli* BL21(DE). The highest of L-Phe production at 746 mg/L was observed when the minimum medium containing 3.1 % glycerol and 6.3% ammonium sulfate was used. This study aimed to observe the effect of *aroG* and feedback resistant *aroG* on L-phenylalanine production in recombinant *E. coli* harboring the others pivotal genes in aromatic amino acid biosynthesis pathway (*aroB*, *aroL*, *phedh* and *tktA*) and determine the optimal concentration of glycerol and ammonium sulfate in L-Phe production medium.



CHAPTER II

MATERIALS AND METHODS

2.1 Equipments

- Autoclave (MLS-3020, SANYO electric Co., Ltd., Japan)
- Autopipette (Pipetman, Gilson, France)
- Benchtop centrifuge (SorvallBiofuge Primo, Kendro Laboratory Products L.P., USA)
- Bioreactor (BioFloIIc, New Brunswick Scientific, USA)
- Chirex3126 (D)-penicillaminesize 150 mm dimension 4.6 mm (Phenomenex, USA)
- Dry bath incubator (MD-01N, Major Science, USA)
- Electrophoresis unit (Gelmate 2000, TOYOBO Co., Ltd., Japan)
- Electroporator (MicroPulser™electroporator, Bio-Rad Laboratories, Inc., USA)
- Gel Doc (BioDoc-It® Imaging System with M-20 UV Transilluminator, UVP®, Inc., USA)
- High Performance Liquid Chromatography (Shimadzu, Japan)
- Magnetic hotplate stirrer (CH-1E, Nickel Electro-Clifton, UK)
- Micro centrifuge (22R, Beckman coulter, USA)
- pH meter (S20-K SevenEasy™, Mettler-Toledo, Switzerland)
- Refrigerated centrifuge (Avanti J-30I High-Performance Centrifuge, Beckman Coulter, Inc., USA)
- Shaking incubator (Excella E24R, New Brunswick Scientific, USA)
- Spectrophotometer (Biospectrometer, Eppendorf, Germany)
- Thermosblock Reactor (MD-01-220, Major Science,USA)
- Thermo cycler (T100™ Thermal cycler, Biorad, USA)
- UV Transilluminator (MacroVue™ UV-25, Hoefer Inc., USA)
- Vacuum/pressure pump (Model number. WP6111560, Millipore Inc., USA)
- Vortex mixer (Top mix FB15024, Thermo Fisher Scientific Inc., USA)

2.2 Disposable materials

Membrane filter (PTFE, sterile, ANPEL Laboratory Technologies (Shanghai) Inc.

Membrane filter (NYLON membrane filters, 0.45 μm , 47 mm, Vertical Chromatography Co., Ltd., Thailand)

Microcentrifuge tube (1.5 mL microcentrifuge tube, MCT-150, Axygen Inc., USA)

PCR tube (0.2 mL thin-wall domed-cap PCR tube, PCR-02D-C, Axygen Inc., USA)

Pipette tip (10 μL , 200 μL and 1000 μL pipette tip, Axygen Inc., USA)

Syringe (3 mL, 5 mL and 20 mL disposable syringe, Nissho Nipro Co., Ltd., Japan)

2.3 Markers

λ DNA/*Hind*III marker (#SM0102, Thermo Fisher, USA)

GeneRuler 1 kb DNA ladder (#SM0311, Thermo Fisher, USA)

TriColor protein ladder (10-180kDa) (Biotechrabbit, Germany)

2.4 Kits

GenepHlow™ Gel/PCR kit (DFH100, Geneaid, Biotech Ltd, Taiwan)

Presto™ mini plasmid kit (PDH100, Geneaid, Biotech Ltd, Taiwan)

2.5 Chemicals

Agar, bacteriological grade (Himedia, India)

Agarose (Serva, Germany)

Ammonium sulphate (Carlo Erba, Italy)

Arabinose (Acros Organics, USA)

Bovine serum albumin (Sigma, USA)

Bromphenol blue (Merck, Germany)

Calcium chloride (Scharlau, Spain)

Chloramphenicol (Nacalaitesque, Japan)

Chloroform (Lab Scan, Thailand)

Copper sulfate (Carlo Erba, Italy)

Ethyl alcohol absolute (Carlo Erba, Italy)

Ethylenediaminetetraacetic acid disodium salt, EDTA (Merck, Germany)

Ferrous sulfate (Fluka, Switzerland)

Glacial acetic acid (Carlo Erba, Italy)

Glucose (Carlo Erba, Italy)

Glycerol (Ajax Finechem, Australia)

Isopropyl- β -D-thiogalactopyranoside (IPTG), dioxane free (US Biological, UK)

Kanamycin (Sigma, Switzerland)

L-phenylalanine (Sigma, USA)

Magnesium chloride (Carlo Erba, Italy)

Manganese (II) sulphate monohydrate (Carlo Erba, Italy)

Methanol, HPLC grade (Merck, Germany and LAB SCAN, Thailand)

Pancreatic digest of casein (Criterion, USA)

Phenol (BDH, UK)

Potassium dihydrogen phosphate (Carlo Erba, Italy)

Potassium hydroxide (Ajax Finechem, Australia)

Sodium chloride (Carlo Erba, Italy)

Sodium citrate (Carlo Erba, Italy)

Sodium hydroxide (Carlo Erba, Italy)

RedSafe™ Nucleic acid staining solution 20.000x (Intron Biotechnology, Hongkong)

Thiamine-HCl (Sigma, USA)

Tri-sodium citrate dehydrate (Scharlau, Spain)

Yeast extract (Scharlau, Spain)

Zinc sulfate (BDH, England)

Other common chemicals were products obtained from Sigma, USA; BDH, UK; Fluka, Switzerland; Merck, Germany; Ajax Finechem, Australia; Carlo Erba, Italy; and Lab Scan, Thailand.

2.6 Enzymes and restriction enzymes

Pfu DNA polymerase (Biotechrabbit, Germany)

Taq DNA polymerase (Apsalagen, Thailand)

Restriction enzymes (New England BioLabs, Inc., USA)

T4 DNA ligase (New England BioLabs, Inc., USA)

2.7 Bioinformatics tools

<https://www.ebi.ac.uk/Tools/msa/clustalo/> (Multiple Sequence Alignment)

<https://www.ebi.ac.uk/Tools/psa/> (Pairwise Sequence Alignment)

DE_6.08 (Design experiment for Response Surface Methodology (RSM))

ExPASy/translate tool

Genetyx_version7

pDRAW32 revision 1.1.134

SnapGene 1.1.3

2.8 Bacterial strains and plasmids

E. coli Top10, genotype $F^- mcrA \Delta(mrr-hsdRMS-mcrBC) \Phi80lacZ\Delta M15 \Delta lacX74 recA1 araD139 \Delta(ara leu) 7697 galU galK rpsL$ (StrR) *endA1 nupG*, was used as host for cloning of pAroG*, pBLPT, pBLPTG* and pYF.

E. coli BL21(DE3), genotype: $F^- ompT hsdSB (r_B^- mB^-) gal dcm$ (DE3), was used as host for expression of recombinant plasmid of pRSFDuet-1 vector (The restriction map of pRSFDuet-1 is shown in Appendix A) and pYF. All plasmids are listed in Table 2.

For short-term storage, all constructed recombinant strains were maintained on Luria-Bertani (LB) agar (1% peptone from casein, 0.5% yeast extract, 0.5% NaCl and

1.5% agar, pH 7.0) containing either 10 µg/mL chloramphenicol and/or 30 µg/mL kanamycin depending on the selective marker on plasmid. Agar plates were incubated at 37 °C for 18 h and then stored at 4 °C. For the long-term storage, as much as 0.5 mL of 50% glycerol stock and 0.5 mL of overnight culture of each strains were prepared and storage at -80 °C.

Table 2 Plasmids used in this work

Plasmids	Characteristics	Reference
pAroG	pRSFDuet-1 with <i>aroG</i> under <i>T7lac</i> promoter	Kanoksinwuttipong, 2015
pAroG*	pRSFDuet-1 with <i>aroG^{fbr}</i> (L175D, Q151A, Q151L and Q151N), inserted under <i>T7lac</i> promoter	Kanoksinwuttipong, 2015
pBLPT	pRSFDuet-1 with each <i>phedh</i> , <i>tktA</i> , <i>aroB</i> and <i>aroL</i> preceded by <i>T7lac</i> promoter	Ratchaneeladdajit, 2014
pYF	pBAD33 with each <i>yddG</i> and <i>glpF</i> under <i>ara</i> promoter	Ratchaneeladdajit, 2014
pBLPTG	pRSFDuet-1 with each <i>phedh</i> , <i>tktA</i> , <i>aroB</i> , <i>aroL</i> and <i>aroG</i> preceded by <i>T7lac</i> promoter	This study
pBLPTG*	pRSFDuet-1 with each <i>phedh</i> , <i>tktA</i> , <i>aroB</i> , <i>aroL</i> and <i>aroG^{fbr}</i> preceded by <i>T7lac</i> promoter	This study

2.9 Oligonucleotides

Oligonucleotide synthesis was performed by Integrated DNA technology, Singapore. The oligonucleotides used for polymerase chain reaction (PCR) amplification and DNA sequencing are shown in Table 3 and Table 4, respectively.

Table 3 The oligonucleotide primers used for PCR amplification

Primer	Sequence (5' to 3')	T _m (°C)
F_T7_Pacl_aroG	CCT TAA TTA ATC CCT TAT GCG ACT CCT GCA TTA GG	61.1
R_AvrII_aroG	ACT CCT AGG TTA CCC GCG ACG CGC TTT CAC T	68.2

Table 4 The oligonucleotide primers used for DNA sequencing

Primer	Sequence (5' to 3')	T _m (°C)
F_DuetUP_aroG_Intr	TTC GCG CTG TAG TTA GGC TCT TTA CCG	61.3
R_Duet	CGC TTA TGT CTA TTG CTG GTT TAC CGG	59.4

2.10 Amplification of *aroG* wild-type and *aroG*^{fbr}

2.10.1 Plasmid extraction

LB medium 5 mL containing 30 µg/mL kanamycin was inoculated with a single colony of *E. coli* Top10 harboring previously constructed pAroG and pAroG* (4,851 bp); pAroG*L175D, pAroG*Q151A, pAroG*Q151L and pAroG*Q151N. The culture was then incubated at 37 °C overnight with shaking at 250 rpm. After that, cell pellet was cultivated by centrifugation at 5,000 x g for 2 min at room temperature. Then, plasmid was extracted using Presto™ mini plasmid kit (Geneaid Biotech). *Bam*HI and *Hind*III digestion analysis was performed to show that *aroG* or *aroG*^{fbr} was correctly inserted into pRSFDuet-1. Map of pAroG and pAroG* created by SnapGene1.1.3 and *Bam*HI and *Hind*III digestion pattern created by pDRAW32 revision1.1.134 are shown

in Figure 6 and Figure 7, respectively. The obtained plasmids were used as DNA template for *aroG* or *aroG*^{fb} PCR amplification.

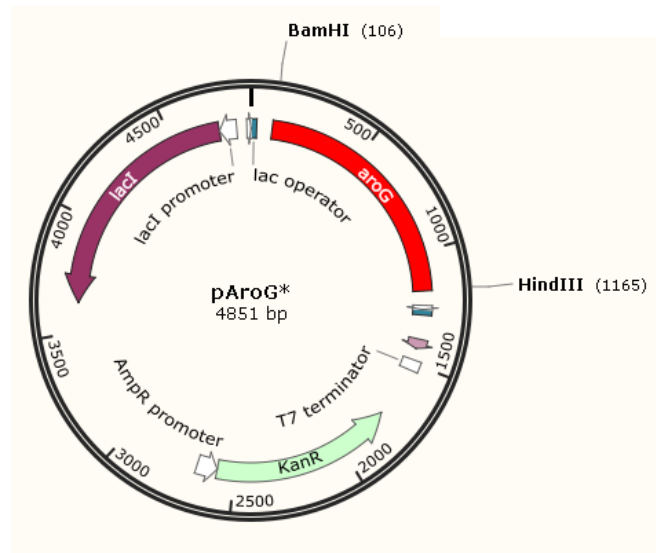


Figure 6 Map of pAroG or pAroG* (SnapGene 1.1.3)

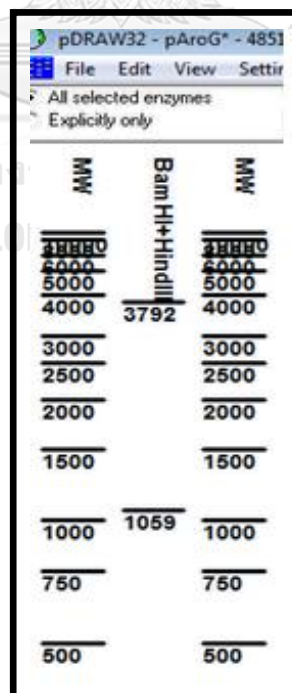


Figure 7 Simulation of *Bam*HI and *Hind*III digested pAroG or pAroG* (pDRAW32 revision 1.1.134)

2.10.2 Agarose gel electrophoresis

DNA samples were separated and analyzed by electrophoresis using agarose gel containing 0.8% (w/v) agarose in 1x TBE buffer (89 mM Tris-HCl, 8.9 mM boric acid and 2.5 mM EDTA, pH 8.0). The gel was added directly with 20.000x RedSafe™ Nucleic acid staining solution (Intron Biotechnology, Hongkong). The DNA samples were mixed with 6x loading buffer (30% glycerol and 0.25% bromphenol blue), then loaded into the gel. Electrophoresis was performed at 100 volts. The DNA bands were detected by exposing the gel to UV light. The concentration and molecular weight of DNA samples were compared with those of the DNA markers (λ DNA/*Hind*III marker and GeneRuler 1 kb DNA ladder).

2.10.3 PCR amplification of *aroG* wild-type and *aroG*^{fbr}

The complete fragment of *aroG* and *aroG*^{fbr} under T7 promoter were amplified from pAroG and pAroG*, respectively using forward and reverse primers: F_T7_Pacl_aroG and R_AvrII_aroG as listed in Table 2.2. The forward primer was designed from 5' end of T7 promoter and the reverse primer sequence was designed based on 3' end of *aroG*. PCR reaction mixture for total volume of 50 μ L contained 1.0 ng of DNA template, 0.2 mM dNTP mix, 10 pmole of each primer, 1x *Pfu* reaction buffer, 1x PCR enhancer and 2.5 U of *Pfu* DNA polymerase. The PCR step was initiated by pre-denaturation at 95 °C for 2 min, 25 cycles of denaturation at 95 °C for 30 sec, annealing at 62 °C for 45 sec and extension at 72 °C for 2.5 min and the last

final extension at 72 °C for 5 min. The *aroG* and *aroG^{fbr}* fragments (1,214 bp) were purified by PCR clean up protocol using GenepHlow™ Gel/PCR kit (Geneaid, Biotech).

2.11 Construction of pBLPTG and pBLPTG*

The recombinant plasmid pBLPTG and pBLPTG* containing *aroB*, *aroL*, *phedh*, *tktA* and *aroG* or *aroG^{fbr}* were constructed using pBLPT (containing *aroB*, *aroL*, *phedh* and *tktA*) and *aroG* or *aroG^{fbr}* fragment. Each *aroG* and *aroG^{fbr}* fragment was inserted into pBLPT at *PacI* and *AvrII* sites and the recombinant plasmid was transformed to *E. coli* Top10. The transformants were selected on LB agar containing 30 µg/ml of kanamycin. The transformed cells in master plates were further identified by colony PCR. The positive clones were then verified with *XhoI*. Sequencing of *aroG* in pBLPTG and *aroG^{fbr}* in pBLPTG* were done using F_DuetUP_aroG_Intr and R_Duet primers as listed in Table 3.

2.11.1 Vector DNA preparation

E. coli Top10 containing pBLPT (8,695 bp) was cultured in LB medium supplemented with 30 µg/mL of kanamycin. pBLPT was then extracted as described in section 2.10.1. The pBLPT was linearized with *PacI* and *AvrII*. The reaction mixture for digestion containing 1 µg of DNA vector pBLPT, 1x CutSmart NEBuffer, 10 U of *AvrII*, in a total volume of 40 µL was incubated at 37 °C for 1 h. Electrophoresis was performed as described in section 2.10.2. The linearized DNA fragment then was purified using Gel Extraction protocol of GenepHlow™ Gel/PCR kit. After that the purified fragment was digested with *PacI*. The reaction mixture for digestion

containing 1 µg of DNA purified fragment, 1x CutSmart NEBuffer, 10 U of *PacI*, in a total volume of 25 µL was incubated at 37 °C for 1 h. The linear DNA fragment of pBLPT (8,691 bp) was recovered and concentrated using PCR clean up protocol of GenepHlow™ Gel/PCR kit.

2.11.2 Insert DNA preparation

Each of the purified *aroG* or *aroG^{fbr}* gene fragments from section 2.10.3 was digested with *PacI* and *AvrII*. The reaction mixture for digestion consisting of 1 µg of gene fragment, 1x CutSmart NEBuffer, and 10 U of *PacI* and 10 U of *AvrII* in a total volume of 20 µL was incubated at 37 °C for 18 h. The DNA fragment (1,214 bp) was purified using PCR clean up protocol of GenepHlow™ Gel/PCR kit.

2.11.3 Ligation of vector and insert DNA

Each of the insert DNA gene fragments from section 2.11.2 was ligated into the pBLPT from section 2.11.1, the ratio of vector to insert is of 1:3. The ligation mixture of 20 µL consisting of 100 ng of vector DNA, 50 ng of the insert DNA gene fragment, 1x T4 DNA ligase buffer and 10 U of T4 DNA ligase was incubated overnight at 16°C, followed by heat inactivation 65 °C for 10 min. This obtained ligation reaction was further used for transformation to *E. coli* Top10. The construction of recombinant plasmid pBLPTG and pBLPTG* (9,905 bp) are shown in Figure 8. The sequence of *aroG* and *aroG^{fbr}* gene and its T7 promoter were confirmed by DNA sequencing.

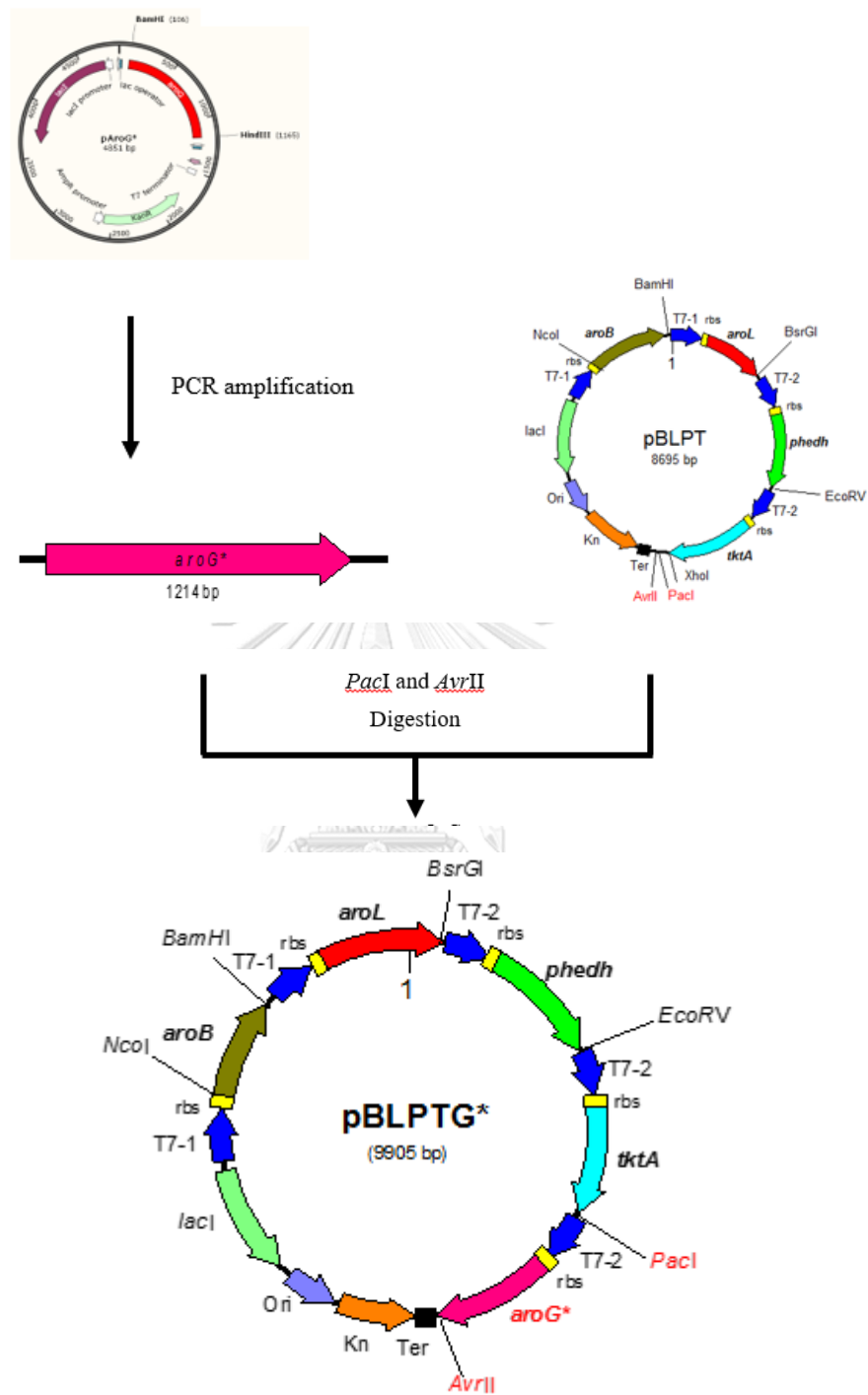


Figure 8 The construction of pBLPTG or pBLPTG*

2.11.4 Transformation of recombinant plasmid

2.11.4.1 Preparation of competent cell

A single colony of *E. coli* Top10 was grown in 100 mL of LB medium at 37 °C for 24 h with shaking at 250 rpm, then the 50 mL of starter was inoculated to 1 liter of LB medium and continued the incubation until optical density at 600 nm reached 0.3-0.4. The culture medium was then chilled on ice for 30 min and centrifuged at 3,000xg for 15 min at 4 °C. The supernatant was discarded, then the cell pellets were washed with cold distilled water about 1.5-2 medium volumes. The cell pellets were washed in 10 mL of 10% cold glycerol then centrifuged at 8,000xg for 10 min at 4 °C. Finally, the cell pellets were resuspended with 10% cold glycerol until a final volume of 2-3 mL. As much as 50 µL of cell suspension was aliquoted into 1.5 mL microcentrifuge tube and stored at -80 °C.

2.11.4.2 Electroporation

In electrophoration, 0.1 cm cuvette was used and chilled on ice. The competent cells from -80 °C were thawed on ice. After that, 20 µL of ligation mixture from pBLPTG or pBLPTG* was mixed with 50 µL competent cells and incubated on ice for 1 min then transferred to a cold cuvette. After that, the cuvette was placed into electroporation chamber and one pulse for electroporation was applied. About 0.5 mL of LB medium was added quickly to the cells and suspended with pipette. The cell suspension was then transferred to 1.5 mL new autoclaved tube and incubated at 37 °C for 1 h with shaking. About 0.2 mL cell suspension was

finally spread on LB agar plate containing 30 µg/mL kanamycin and incubated at 37 °C for 18 h. The transformed cells containing recombinant plasmid growing on these selective plates were picked and replicated onto the new LB agar plates containing 30 µg/mL of kanamycin called as the master plates.

2.11.5 Selection of recombinant clone

2.11.5.1 Rapid selection by colony PCR

The transformed colonies in master plates from above section were identified if each clone contained recombinant plasmid by colony PCR. Each of the *aroG* or *aroG^{fbr}* under T7 promoter was amplified using forward and reverse primers: F_T7_Pacl_aroG and R_AvrII_aroG, respectively. PCR reaction mixture for total volume of 25 µL contained a single colony of recombinant clone, 0.2 mM dNTP mix, 0.5 mM MgCl₂, 10 pmole of each primer, 1x reaction buffer, and 2.5 U of *Taq* DNA polymerase. The PCR step was initiated by pre-denaturation (94°C, 3 min), 25 cycles of denaturation (94°C, 1 min), annealing (62 °C, 1 min), and extension (72 °C, 1 min 15 sec), and the last final extension (72 °C, 10 min).

Each of PCR products was subjected to an agarose gel electrophoresis. Clones containing desired recombinant plasmid were picked and cultured in LB medium containing 30 µg/mL of kanamycin. After that, the plasmids were extracted and confirmed again by restriction enzyme digestion as described below.

2.11.5.2 Plasmid extraction and restriction enzyme digestion

E. coli Top10 harboring desired recombinant plasmid was grown in 5 mL of LB medium containing 30 µg/mL of kanamycin at 37 °C for 18 h at 250 rpm. After that, cell pellet was cultivated by centrifugation at 5,000 × g for 2 min at room temperature. Then, plasmid was extracted using Presto™ mini plasmid kit (Geneaid Biotech). The plasmids then were completely digested with *Xho*I. The sizes of digested recombinant plasmids were estimated by agarose gel electrophoresis compared with *M*HindIII and 1 kb DNA marker. The position of *Xho*I in pBLPTG* at 5,220 bp (in the plasmid vector part) and 6,389 bp in insert part (*aroG* or *aroG*^{fbn}) as shown in Figure 9. The simulation of *Xho*I digested pBLPTG or pBLPTG* by pDRAW32 revision 1.1.134 is shown in Figure 10 (8,736 and 1,169 bp).

2.11.6 Nucleotide sequencing

The positive recombinant plasmids were sent to Bioneer, Korean for sequencing. The obtained nucleotide sequences were compared with DNA sequence in NCBI database by CLUSTALW online program.

2.12 Co-transformation of pBLPTG or pBLPTG* and pYF into *E. coli* BL21(DE3)

The pYF containing *glpF* and *yddG* under *ara* promoter as shown in Figure 11 was co-transformed with pBLPTG or pBLPTG* into competent *E. coli* BL21 (DE3) as described in section 2.11.4.2. The transformants were then spread on LB agar containing 30 µg/ml of kanamycin and 10 µg/ml chloramphenicol. Existence of pBLPTG or pBLPTG* & pYF plasmids in *E. coli* were confirmed by *Bam*HI digestion.

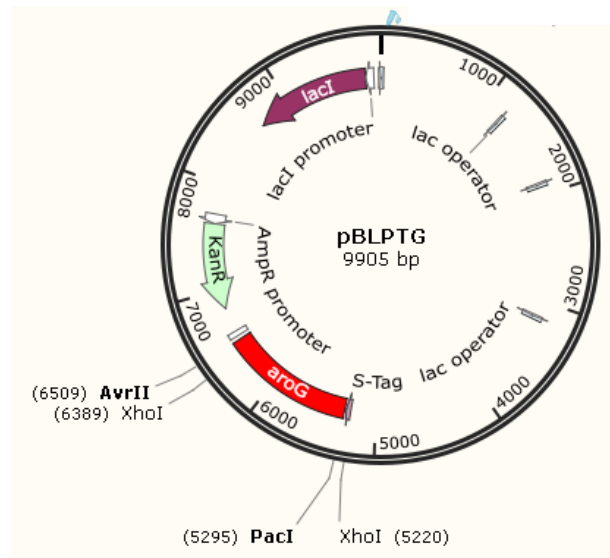


Figure 9 Map of *XhoI* in pBLPTG or pBLPTG* (SnapGene 1.1.3.4)

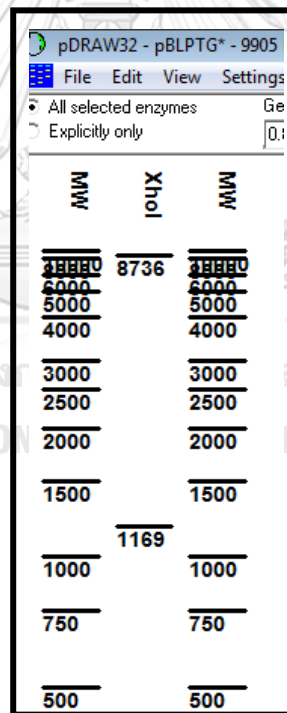


Figure 10 The simulation of *XhoI* digested pBLPTG* (pDRAW32 revision 1.1.134)

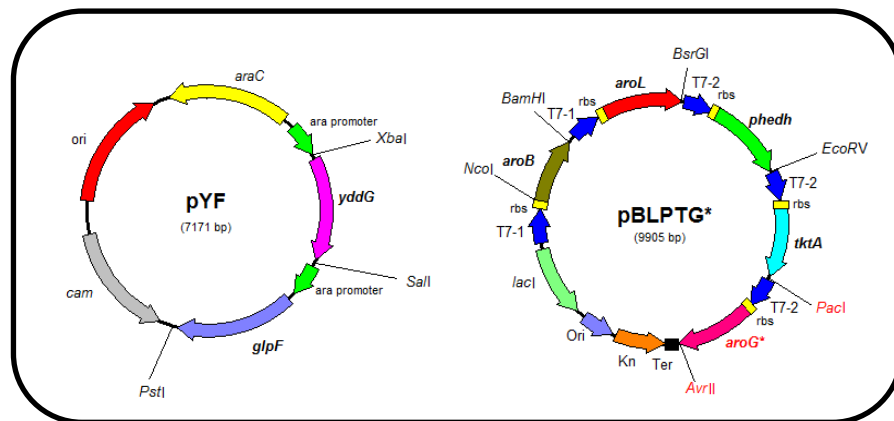


Figure 11 The illustration of pYF and pBLPTG* in *E. coli* BL21 (DE3)

2.12.1 Electroporation

In electroporation, 0.1 cm cuvette was used and chilled on ice. The competent cells from $-80\text{ }^{\circ}\text{C}$ were thawed on ice. After that, 1- 50 $\text{ng}/\mu\text{L}$ of recombinant pBLPTG or pBLPTG* and pYF were mixed with 50 μL competent cells and incubated on ice for 1 min then transferred to a cold cuvette. After that, the cuvette was placed into electroporation chamber and one pulse for electroporation was applied. About 0.5 mL of LB medium was added quickly to the cells and suspended with pipette. The cell suspension was then transferred to 1.5 mL new autoclaved tube and incubated at $37\text{ }^{\circ}\text{C}$ for 1 h with shaking. About 0.2 mL cell suspension finally was spread on LB agar plate containing 30 $\mu\text{g}/\text{mL}$ kanamycin and 10 $\mu\text{g}/\text{mL}$ of chloramphenicol then incubated at $37\text{ }^{\circ}\text{C}$ for 18 h.

2.12.2 Plasmid extraction and restriction enzyme digestion

E. coli BL21(DE3) harboring desired recombinant clones of pBLPTG or pBLPTG* and pYF were grown in 5 mL of LB medium containing 30 $\mu\text{g}/\text{mL}$ of kanamycin and 10 $\mu\text{g}/\text{mL}$ of chloramphenicol at $37\text{ }^{\circ}\text{C}$ for 18 h at 250 rpm. After that,

cell pellet was cultivated by centrifugation at 5,000 x g for 2 min at room temperature. Then, plasmid was extracted using Presto™ mini plasmid kit (Geneaid Biotech). The plasmids then were completely digested with *Bam*HI. The position of *Bam*HI in pBLPTG* is at 1,160 bp (in the plasmid vector part) and 5,450 bp (in the insert part). The simulation of pBLPTG or pBLPTG* digested by *Bam*HI (5,615 and 4,290 bp) using pDRAW32 revision 1.1.134 is shown in Figure 12.A. The position of *Bam*HI in pYF is at 1,327 bp and 2,306 bp. The simulation of pYF digested by *Bam*HI (6,104 and 979 bp) using pDRAW32 revision 1.1.134 is shown in Figure 12.B. So, if the host cell *E. coli* BL21(DE3) contained these both recombinant plasmids (pBLPTG* and pYF), after *Bam*HI digestion, the predicted fragment by pDRAW32 revision 1.1.134 would be 6,104; 5,615; 4,290 and 979 bp as shown in Figure 12.C. The sizes of digested recombinant plasmids were estimated by agarose gel electrophoresis compared with λ HindIII and 1 kb DNA marker.

2.13 SDS-polyacrylamide gel electrophoresis

Recombinant proteins were analyzed by SDS-PAGE (Bollag et al., 1996). Protein expression was induced by 2 methods. The first method; protein expression was induced at 37 °C for 5 h in LB medium. *E. coli* BL21(DE3) cells containing the recombinant plasmid were cultured in 5 mL of LB medium supplemented with 30 µg/mL of kanamycin and/or 10 µg/L chloramphenicol at 37 °C for 18 h. The seed culture was inoculated (5% v/v) to LB medium 50 mL and incubation was continued until OD600 was about 0.6. IPTG and/or arabinose were added to a final

concentration of 1 mM and 0.02%, respectively and the cultivation was continued for 5 h. The cells were harvested by centrifugation at 5,000xg for 10 min and stored at -20 °C for further analysis.

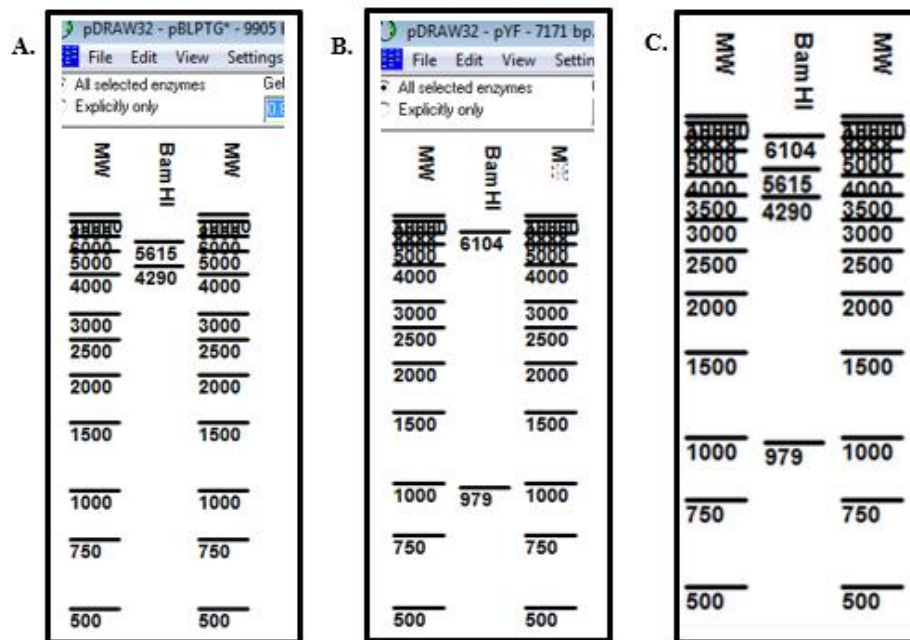


Figure 12 The simulation of recombinant plasmids digested with *Bam*HI

(A) pBLPTG or pBLPTG* (B) pYF and (C) pBLPTG* and pYF (pDRAW32 revision 1.1.134)

The second method; protein expression was induced at 25 °C for 16 h in TB medium. Terrific Broth is a nutritionally rich medium for the growth of bacteria and improvement of the yields in recombinant *E. coli*. In TB medium containing tryptone, yeast extract, potassium phosphate and glycerol, the strains can extend the growth phase. Different from glucose, glycerol is not fermented to acetic acid, so that this can prevent decreasing in pH during the growth phase and cell death due to loss of pH of the culture (Green and Sambrook, 2012). *E. coli* BL21(DE3) cells containing the

recombinant plasmids were cultured in 5 mL of LB medium supplemented with 30 µg/ml of kanamycin and/or 10 µg/L chloramphenicol at 37 °C for 12 h. After that 2.5 mL of seed culture was inoculated into 50 mL TB medium and incubation was continued. When OD₆₀₀ was about 1.0, IPTG and/or arabinose were added to a final concentration of 0.5 mM and 0.02%, respectively. The cultivation was continued in 25 °C for 16 h. The cells were then harvested by centrifugation at 5,000 x g for 10 min.

After that the cells were suspended in lysis buffer (100 mM phosphate buffer pH 7.4, 1 mM EDTA pH 8, 0.1 mM phenylmethylsulfonyl fluoride, and 0.01% 2-mercaptoethanol) and broken by sonication. Cell debris was eliminated by centrifugation at 10,000 x g for 15 min. Thereafter, the protein separation and visualization were carried out with 12.5 % acrylamide gel.

The slab gel system consisted of 0.1% SDS (w/v) in 12.5% separating gel and 5% stacking gel. The cells pellet were resuspended in 0.25 g/mL of the 1x sample buffer (312.5 mM Tris-HCl pH 6.8, 50% (v/v) glycerol, 1% (w/v) bromophenol blue) and boiled for 5 min. After centrifugation at 10,000xg for 10 min, 30 µg/µL of each sample was loaded to the gel. The cell extract of *E. coli* BL21(DE3) containing pRSFDuet-1 under induction with IPTG was loaded as reference of protein pattern. Tricolor Protein Ladder was used as the protein molecular weight marker. After electrophoresis, the gel was stained with Coomassie blue solution and then destained by destaining solution (Appendix C). The molecular weight of each protein

was calculated by using http://www.bioinformatics.org/sms/prot_mw.html as listed in

Table 5.

Table 5 Molecular weight of each protein in recombinant plasmid pBLPTG

Protein	Number of amino acid residue	MW (kDa)
TktA	663	72.19
PheDH	380	41.34
AroB	362	38.89
AroG	350	38.01
YddG	293	31.54
GlpF	281	29.78
AroL	174	19.15

2.14 Study of L-phenylalanine production by pBLPTG or pBLPTG* & pYF clone

L-Phe production of pBLPTG* & pYF clones in minimum medium were studied in comparison with pBLPTG & pYF clone.

2.14.1 L-phenylalanine production

The recombinant clones were cultured in minimum medium pH 7.0 containing (g/L): 31 glycerol, 63 (NH₄)₂SO₄, 0.3 MgSO₄·7H₂O, 1.5×10⁻² CaCl₂·2H₂O, 3.0 KH₂PO₄, 12 K₂HPO₄, 1.0 NaCl, 7.5×10⁻² FeSO₄·7H₂O/1.0 Na-citrate, 7.5×10⁻³ thiamine·HCl, and 1.5 ml/L trace element solution (TES) containing (g/L): 2.0 Al₂(SO₄)₃·18H₂O, 7.5×10⁻¹ CoSO₄·7H₂O, 2.5 CuSO₄·5H₂O, 5.0×10⁻¹ H₃BO₃, 24 MnSO₄·7H₂O, 3.0×10⁻¹ Na₂MoO₄·2H₂O, 2.5 NiSO₄·6H₂O, 15 ZnSO₄·7H₂O (Ratchaneeladdajit, 2014). Shake flask fermentation was carried out in 500 ml Erlenmeyer flask containing 100 ml of medium inoculated with 5% (v/v) of overnight

seed culture from 100 ml of LB medium containing 30 µg/ml of kanamycin and 10 µg/ml chloramphenicol. The cultures were shaken at 37 °C and 250 rpm. One ml of cell suspension was taken for measuring the optical density at 600 nm. After OD₆₀₀ reached 0.6, the samples were induced by addition of 0.02% arabinose. After that, 1 ml of cell suspension was taken every 24 h for measuring OD₆₀₀ and supernatant was harvested by centrifugation at 5,000 x g for 15 min and stored at -20 °C for L-Phe determination. The experiments were performed in triplicate.

2.14.2 Product determination by HPLC

Supernatant samples were passed through 0.22 µm syringe filter set. The filtrates were analyzed by HPLC technique using Chirex 3126 (D) - penicillamine column. Two mM copper sulfate and methanol at the ratio of 75:25 was used as a mobile phase. The column was operated at flow rate 0.7 ml/min and peaks were detected at 254 nm. L-Phe was quantified by comparison with the standard curve (Appendix E).

2.15 Experimental design for L-phenylalanine production using response surface methodology (RSM)

Response surface methodology (RSM) is a collection of statistical techniques for designing experiments, building models, evaluating the effects of factors, and searching optimum conditions of factors for desirable responses. Response surface methodology uses statistical techniques for designing experiments, building models, evaluating the interactive effects of variables, and pointing the optimum conditions. The major medium components for L-Phe production was optimized using RSM

(Ratchaneeladdajit, 2014). In this study, two medium components; glycerol (as a carbon source) and ammonium sulfate (as nitrogen source) were used as independent variables and the maximum of L-Phe production was used as a criteria.

A central composite design (CCD) with five center points was used to conduct the experiment. In CCD, each two factors have five level ($-\alpha$, -1, 0, +1, + α) as shown in Table 6. Level of different process variable in percentage is shown in Table 7. As preliminary, the best level concentration of independent variable for RSM were determine by varying concentration of glycerol and ammonium sulfate (data not shown). Then, the zero level of independent variable; glycerol and ammonium sulfate were set at 4.5 and 5.0 (% w/v), respectively. The program DE_6.08 was used to build the model, analyze and evaluate the data. Data validation was calculated by comparing the value of observed data from experimental dan predicted data calculated by DE_6.08.

Table 6 Level of different process variable in coded level for L-Phe production

Variable	Coded level				
	-1.414	-1	0	1	1.414
Glycerol (% w/v)	2.38	3.00	4.50	6.00	6.62
Ammonium sulfate (% w/v)	2.17	3.00	5.00	7.00	7.83

Table 7 Experimental design obtained by CCD matrix

Run	Variable coded		Glycerol (% w/v)	Ammonium sulfate (% w/v)
	X ₁	X ₂		
1	-1	-1	3.00	3.00
2	1	-1	6.00	3.00
3	-1	1	3.00	7.00
4	1	1	6.00	7.00
5	-1.414	0	2.38	5.00
6	1.414	0	6.62	5.00
7	0	-1.414	4.50	2.17
8	0	1.414	4.50	7.83
9	0	0	4.50	5.00
10	0	0	4.50	5.00
11	0	0	4.50	5.00
12	0	0	4.50	5.00
13	0	0	4.50	5.00

CHAPTER III

RESULTS AND DISCUSSIONS

3.1. Amplification of *aroG* wild-type and *aroG*^{fbr}

pAroG and pAroG* (pRSFDuet-1 harboring each of L175D, Q151A, Q151L and Q151N) were used as sources of *aroG* and *aroG*^{fbr}. Firstly, the pAroG and pAroG* (4,951 bp) were extracted from *E. coli* Top 10 as described in section 2.10.1. The plasmids were verified by digestion. As shown in Figure 13, DNA fragment of 3,792 and 1,059 bp were obtained when pAroG, pAroG*L175D, pAroG*Q151A, pAroG*Q151L and pAroG*Q151N were digested with *Bam*HI and *Hind*III. The patterns were the same as that predicted by pDRAW revision 1.1.134 which is shown in Figure 7. The result confirmed that *aroG* or *aroG*^{fbr} correctly inserted under T7lac promoter and ribosome binding site of pRSFDuet-1.

The *aroG* and *aroG*^{fbr} were then amplified from pAroG and pAroG* using F_T7_Pacl_aroG and R_AvrII_aroG primers. The fragment of *aroG* and *aroG*^{fbr} are shown in Figure 14. The 1,214 bp PCR products were then purified by PCR clean up protocol using GenepHlow™ Gel/PCR kit according to the protocol.

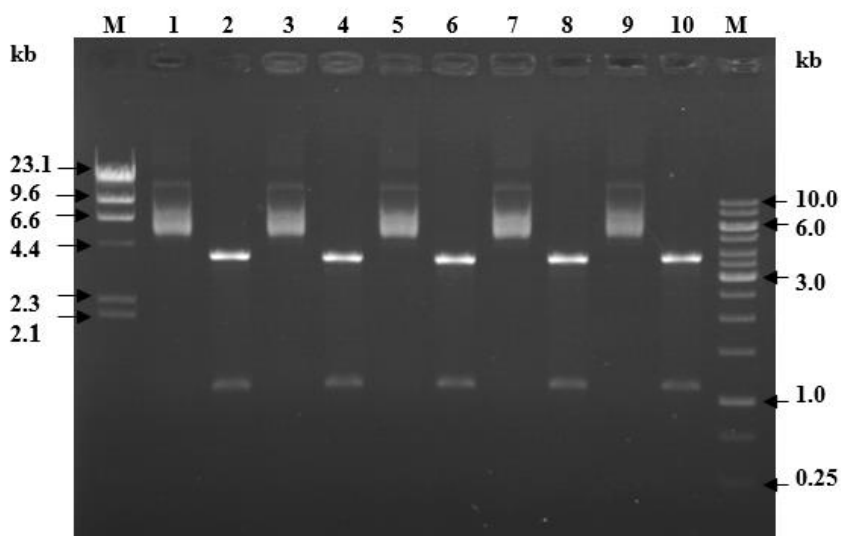


Figure 13 *Bam*HI and *Hind*III pattern of pAroG and pAroG*

- Lane M = λ /*Hind*III DNA marker
- Lane 1 = undigested pAroG
- Lane 2 = *Bam*HI and *Hind*III digested pAroG
- Lane 3 = undigested pAroG*L175D
- Lane 4 = *Bam*HI and *Hind*III digested pAroG*L175D
- Lane 5 = undigested pAroG*Q151A
- Lane 6 = *Bam*HI and *Hind*III digested pAroG*Q151A
- Lane 7 = undigested pAroG*Q151L
- Lane 8 = *Bam*HI and *Hind*III digested pAroG*Q151L
- Lane 9 = undigested pAroG*Q151N
- Lane 10 = *Bam*HI and *Hind*III digested pAroG*Q151N
- Lane m = 1 kb DNA ladder

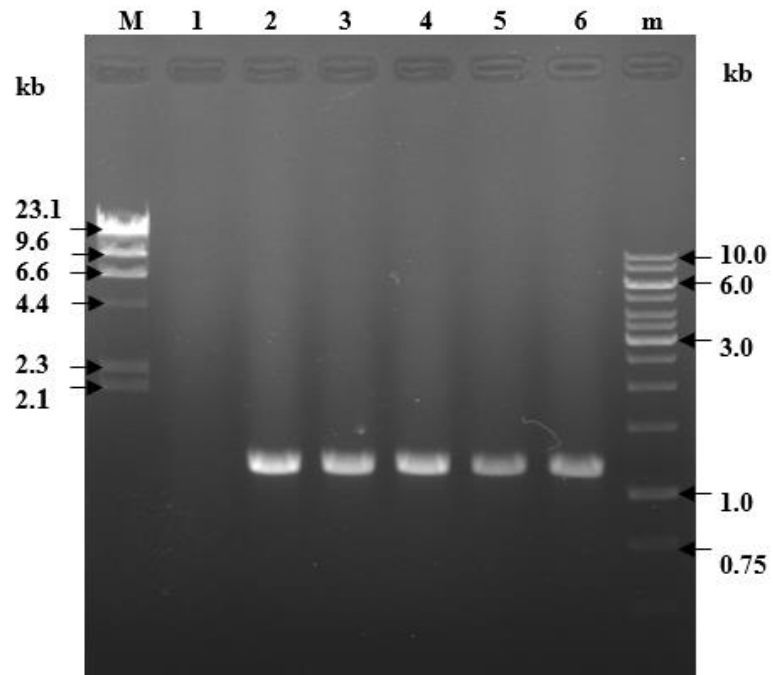


Figure 14 Amplification of *aroG* and each *aroG*^{fbr}

Lane M = λ HindIII DNA marker

Lane 1 = PCR negative control

Lane 2 = *aroG*

Lane 3 = *aroG*^{fbrL175D}

Lane 4 = *aroG*^{fbrQ151A}

Lane 5 = *aroG*^{fbrQ151L}

Lane 6 = *aroG*^{fbrQ151N}

Lane m = 1 kb DNA ladder

3. 2 Construction of pBLPTG and pBLPTG*

The recombinant plasmid pBLPTG and pBLPTG* were constructed using the genes from pBLPT (containing *aroB*, *aroL*, *phedh* and *tktA*) and PCR product of *aroG* or each *aroG*^{fbr} as described in section 2.11. The PCR product of *aroG* and each *aroG*^{fbr} from section 3.1 as well as plasmid vector pBLPT were digested with *PacI* and *AvrII*. After purification, *aroG* and each *aroG*^{fbr} (1,214 bp) were then ligated to pBLPT (8,691 bp). The obtained recombinant plasmids pBLPTG and pBLPTG* (9,905 bp) were transformed into *E. coli* Top10. After that these recombinant plasmids were extracted and digested by *XhoI* to verify that each of *aroG* and *aroG*^{fbr} was correctly inserted into pBLPT as predicted by pDRAW32 version 1.1.134 (Figure 10).

When pBLPT was digested with *PacI* and *AvrII*, the single DNA fragment 8,691 bp was obtained (Figure 15, lane 2). Lane 3 showed the PCR product of *aroG* fragment about 1,214 bp after digested with *PacI* and *AvrII*. The digestion of pBLPTG with *XhoI* gave two DNA fragments of 8,736 and 1,169 bp as shown in lane 5 which corresponded to *PacI* and *AvrII* digested pBLPT and PCR product of *aroG*. Digestion of pBLPTG*L175D, pBLPTG*Q151A, pBLPTG*Q151L and pBLPTG*Q151N also gave the same pattern (lane 7, 9, 11 and 13). The results showed that the pBLPTG and pBLPTG* were successfully constructed.

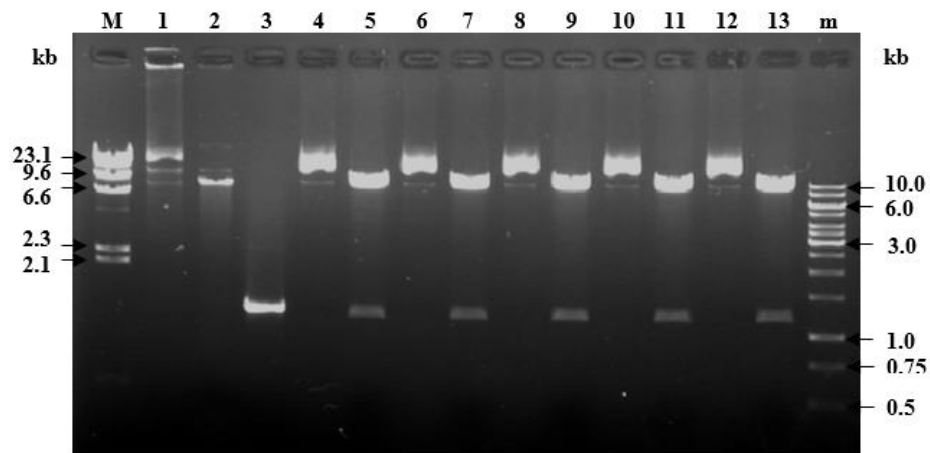


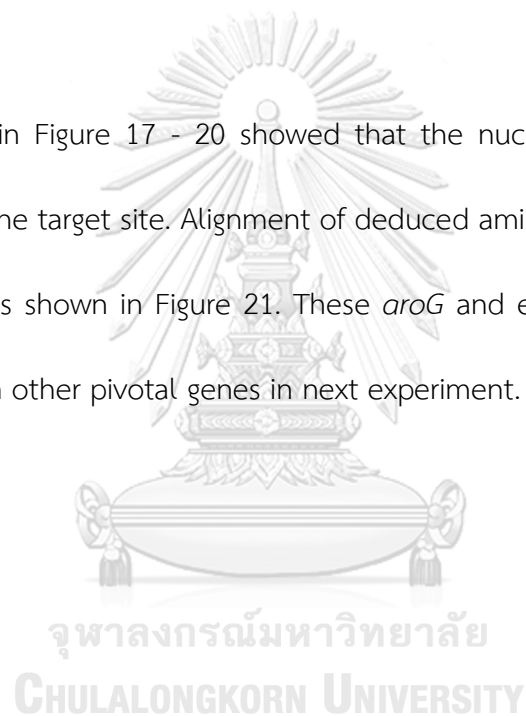
Figure 15 Restriction pattern of pBLPTG and pBLPTG* digested by *Xho*I

- Lane M = λ HindIII DNA marker
- Lane 1 = undigested pBLPT
- Lane 2 = *Pac*I and *Avr*II digested pBLPT
- Lane 3 = PCR product of *aroG*
- Lane 4 = undigested pBLPTG
- Lane 5 = *Xho*I digested pBLPTG
- Lane 6 = undigested pBLPTG*L175D
- Lane 7 = *Xho*I digested pBLPTG*L175D
- Lane 8 = undigested pBLPTG*Q151A
- Lane 9 = *Xho*I digested pBLPTG*Q151A
- Lane 10 = undigested pBLPTG* Q151L
- Lane 11 = *Xho*I digested pBLPTG* Q151L
- Lane 12 = undigested pBLPTG* Q151N
- Lane 13 = *Xho*I digested pBLPTG* Q151N
- Lane m = 1 kb DNA ladder

3.3 Nucleotide sequencing

To verify the sequences before using in the next experiment, the obtained pBLPTG and each pBLPTG* were sent to Bioneer, Korean for sequencing. F_DuetUP_aroG_Intr primer designed from *aroG* internal sequence and R_Duet primer from pRSFDuet-1 sequence were used. The obtained nucleotide sequences were converted to amino acid sequence and analyzed by Genetyx-Win version 3.1 programs.

The results in Figure 17 - 20 showed that the nucleotide substitutions were occurred only at the target site. Alignment of deduced amino acid sequences of *aroG* and each *aroG*^{fbr} is shown in Figure 21. These *aroG* and each *aroG*^{fbr} were used for co-expression with other pivotal genes in next experiment.



```

-171          CGCAGCTTAATTAA TCCCTTATGCGACTCCTGCATTAGGAAATTAATACGA
-120 CTCACTATAGGGGAATTGTGAGCGGATAACAATTCCCTGTAGAATAATTTTGTTTAAC
-60  TTTAATAAGGAGATATACCATGGGCAGCAGCCATCACCATCATCACCACAGCCAGGATCC

1    ATGAATTATCAGAACGACGATTTACGCATCAAAGAAATCAAAGAGTTACTTCCCTCTGTC
M N Y Q N D D L R I K E I K E L L P P V
61  GCATTGCTGGAAAAATCCCCGCTACTGAAAATGCCGGAATACGGTTGCCCATGCCCGA
A L L E K F P A T E N A A N T V A H A R
121 AAAGCGATCCATAAGATCCTGAAAGGTAATGATGATCGCCTGTTGGTTGTGATTGGCCCA
K A I H K I L K G N D D R L L V V I G P
181 TGCTCAATTCATGATCCTGTGCGGCAAAAGAGTATGCCACTCGCTTGGCGTCCGCT
C S I H D P V A A K E Y A T R L L A L R
241 GAAGAGCTGAAAGATGAGCTGAAAATCGTAATGCGCGTCTATTTTAAAAGCCGCTACC
E E L K D E L E I V M R V Y F E K P R T
301 ACGGTGGGCTGAAAGGGCTGATTAACGATCCGCATATGGATAATAGCTTCCAGATCAAC
T V G W K G L I N D P H M D N S F Q I N
361 GACGGTCTGCGTATAGCCCGTAAATTGCTGCTTGATATTAACGACAGCGGTCTGCCAGCG
D G L R I A R K L L L D I N D S G L P A
421 GCAGGTGAATTCCTCGATATGATCACTCCTCAATATCTCGCTGACCTGATGAGCTGGGGC
A G E F L D M I T P Q Y L A D L M S W G
481 GCAATTGGCGCAGTACCACCGAATCGCAGGTGCACCGGAACGGCATCAGGGCTTTCT
A I G A R T T E S Q V H R E L A S G L S
541 TGTCCGGTCCGCTTCAAAAATGGCACCGGACGGTACGATTAAGTGGCTATCGATGCCATT
C P V G F K N G T D G T I K V A I D A I
601 AATGCGCCGGTGCGCCGACTTCTCCTGTCCGTAACGAAATGGGGGCATTCCGCGATT
N A A G A P H C F L S V T K W G H S A I
661 GTGAATACCAGCGTAACGGCGATTGCCATATCATTCTGCGCGGGTAAAGAGCCTAAC
V N T S G N G D C H I I L R G G K E P N
721 TACAGCGCAAGCACGTTGCTGAAGTGAAGAAGGGCTGAACAAAGCAGGCCTGCCAGCA
Y S A K H V A E V K E G L N K A G L P A
781 CAGGTGATGATCGATTCAGCCATGCTAACTCGTCCAAACAATTCAAAAAGCAGATGGAT
Q V M I D F S H A N S S K Q F K K Q M D
841 GTTTGTGCTGACGTTTGCCAGCAGATTGCCGGTGGCGAAAAGGCCATTATTGGCGTGATG
V C A D V C Q Q I A G G E K A I I G V M
901 GTGAAAGCCATCTGGTGAAGGCAATCAGAGCCTCGAGAGCGGGGAGCCGCTGGCCTAC
V E S H L V E G N Q S L E S G E P L A Y
961 GGTAAGAGCATACCGATGCCTATCGGCTGGGAAGATACCGATGCTCTGTACGTCAA
G K S I T D A C I G W E D T D A L L R Q
1021 CTGGCGAATGCAGTGAAGCGCGTCGCGGGTAACTAGGCTGCTGCCACCGCTGAGCAAT
L A N A V K A R R G *

```

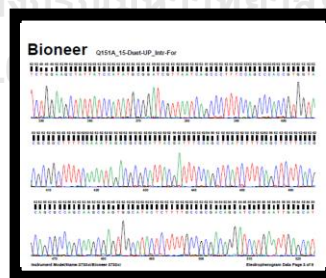


Figure 16 The nucleotide sequence and deduced amino acid sequence of *aroG* in pBLPTG

The T7 promoter, *lac* operator and ribosome binding site are indicated in red, blue and green respectively. The restriction site of *PacI* and *AvrII* are indicated in pink and purple, respectively. This sequence addressed to *aroG* wild-type without point mutation. Complete chromatogram of *aroG* is shown in Appendix G.

```

-171          CGCAGCTTAATTAA TCCCTTATGCGACTCCTGCATTAGGAAATTAATACGA
-120 C T C A C T A T A G G G G A A T T G T G A G C G G A T A A C A A T T C C C C T G T A G A A A T A A T T T T G T T A A C
-60 T T T A A T A A G G A G A T A T A C C A T G G G C A G C A G C C A T C A C C A T C A T C A C C A C A G C C A G G A T C C

1   ATGAATTATCAGAACGACGATTTACGCATCAAAGAAATCAAAGAGTTACTTCCTCCTGTC
M   N   Y   Q   N   D   D   L   R   I   K   E   I   K   E   L   L   P   P   V
61  GCATTGCTGGAAAAATCCCCGCTACTGAAAATGCCGGAATACGGTTGCCCATGCCCGA
A   L   L   E   K   F   P   A   T   E   N   A   A   N   T   V   A   H   A   R
121 AAAGCGATCCATAAGATCCTGAAAGGTAATGATGATCGCCTGTTGGTTGTGATTGGCCCA
K   A   I   H   K   I   L   K   G   N   D   D   R   L   L   V   V   I   G   P
181 TGCTCAATTCATGATCCTGTGCGGGCAAAGAGTATGCCACTCGCTTGCTGGCGCTGCGT
C   S   I   H   D   P   V   A   A   K   E   Y   A   T   R   L   L   A   L   R
241 GAAGAGCTGAAAGATGAGCTGAAAATCGTAATGCGCGTCTATTTTAAAAGCCGCGTACC
E   E   L   K   D   E   L   E   I   V   M   R   V   Y   F   E   K   P   R   T
301 ACGGTGGGCTGAAAGGGCTGATTAACGATCCGCATATGGATAATAGCTTCCAGATCAAC
T   V   G   W   K   G   L   I   N   D   P   H   M   D   N   S   F   Q   I   N
361 GACGGTCTGCGTATAGCCCGTAAATTGCTGCTTGATATTAACGACAGCGGTCTGCCAGCG
D   G   L   R   I   A   R   K   L   L   L   D   I   N   D   S   G   L   P   A
421 GCAGGTGAGTTTCTCGATATGATCACCCACAATATCTCGCTGACCTGATGAGCTGGGGC
A   G   E   F   L   D   M   I   T   P   Q   Y   L   A   D   L   M   S   W   G
481 GCAATTGGCGCAGTACCACCGAATCGCAGGTGCACCGCGAAGATCGCGTCTGGTCTTTCT
A   I   G   A   R   T   T   E   S   Q   V   H   R   E   D   A   S   G   L   S
541 TGTCCGGTCCGCTTCAAAAATGGCACCCGCGTACGATTAAAGTGCGTATCGATGCCATT
C   P   V   G   F   K   N   G   T   D   G   T   I   K   V   A   I   D   A   I
601 AATGCCGCCGGTGGCGCCGACTGCTTCCTGTCCGTAACGAAATGGGGCATTCCGGCGATT
N   A   A   G   A   P   H   C   F   L   S   V   T   K   W   G   H   S   A   I
661 GTGAATACCAGCGGTAACGGCGATTGCCATATCATTCTGCGCGGGTAAAGAGCCTAAC
V   N   T   S   G   N   G   D   C   H   I   I   L   R   G   G   K   E   P   N
721 TACAGCGGAAGCACGTTGCTGAAGTGAAGAAGGGCTGAACAAAGCAGGCCTGCCAGCA
Y   S   A   K   H   V   A   E   V   K   E   G   L   N   K   A   G   L   P   A
781 CAGGTGATGATCGATTTACGCCATGCTAACTCGTCCAACAATTCAAAAAGCAGATGGAT
Q   V   M   I   D   F   S   H   A   N   S   S   K   Q   F   K   K   Q   M   D
841 GTTGTGCTGACGTTTGCCAGCAGATTGCCGGTGGCGAAAAGGCCATTATTGGCGTGATG
V   C   A   D   V   C   Q   Q   I   A   G   G   E   K   A   I   I   G   V   M
901 GTGAAAGCCATCTGGTGAAGCAATCAGAGCCTCGAGAGCGGGGAGCCGCTGGCCTAC
V   E   S   H   L   V   E   G   N   Q   S   L   E   S   G   E   P   L   A   Y
961 GGTAAGAGCATCCCGATGCCTGCATCGGCTGGGAAGATACCGATGCTCTGTTACGTCAA
G   K   S   I   T   D   A   C   I   G   W   E   D   T   D   A   L   L   R   Q
1021 CTGGCGAATGCAGTGAAGCGCGTCGCGGGTAACTAGGCTGCTGCCACCGCTGAGCAAT
L   A   N   A   V   K   A   R   R   G   *

```

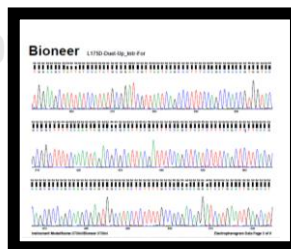


Figure 17 The nucleotide sequence and deduced amino acid sequence of *aroGL175D* in pBLPTG*

The T7 promoter, *lac* operator and ribosome binding site are indicated in red, blue and green respectively. The restriction site of *PacI* and *AvrII* are indicated in pink and purple, respectively. The point mutation of Leu175Asp (CTG→GAT) is underlined with mutated amino acid residue in yellow. Complete chromatogram of Leu175Asp is shown in Appendix H.

```

-171          CGCAGCTTAATTAA TCCCTTATGCGACTCCTGCATTAGGAAATTAATACGA
-120  CTCACTATAGGGGAATTGTGAGCGGATAACAATTCCCTGTAGAAATAATTTTGTTTAAC
-60   TTTAATAAGGAGATATACCATGGGCAGCAGCCATCACCATCATCACCACAGCCAGGATCC

1     ATGAATTATCAGAACGACGATTTACGCATCAAAGAAATCAAAGAGTTACTTCTCTCTGTC
    M N Y Q N D D L R I K E I K E L L P P V
61   GCATTGCTGGAAAAATCCCCGCTACTGAAAATGCCGGAATACGGTTGCCCATGCCCGA
    A L L E K F P A T E N A A N T V A H A R
121  AAAGCGATCCATAAGATCCTGAAAGGTAATGATGATCGCCTGTTGGTTGTGATTGGCCCA
    K A I H K I L K G N D D R L L V V I G P
181  TGCTCAATTCATGATCCTGTGCGGCAAAAGAGTATGCCACTCGCTTGGCGCTGCGT
    C S I H D P V A A K E Y A T R L L A L R
241  GAAGAGCTGAAAGATGAGCTGAAAATCGTAATGCGCGTCTATTTTAAAAGCCGCTACC
    E E L K D E L E I V M R V Y F E K P R T
301  ACGGTGGGCTGAAAGGGCTGATTAACGATCCGCATATGGATAATAGCTTCCAGATCAAC
    T V G W K G L I N D P H M D N S F Q I N
361  GACGGTCTGCGTATAGCCCGTAAATTGCTGCTTGATATTAACGACAGCGGTCTGCCAGCG
    D G L R I A R K L L L D I N D S G L P A
421  GCAGGTGAATTCCTCGATATGATCACTCCTGCC TATCTCGCTGACCTGATGAGCTGGGGC
    A G E F L D M I T P A Y L A D L M S W G
481  GCAATTGGCGCAGTACCACCGAATCGCAGGTGCACCGCGAATGGCATCAGGGCTTTCT
    A I G A R T T E S Q V H R E L A S G L S
541  TGTCCGGTCCGCTTCAAAAATGGCACCGACGGTACGATTAAAGTGGCTATCGATGCCATT
    C P V G F K N G T D G T I K V A I D A I
601  AATGCCGCCGGTGCGCCGACTTCTCCTGTCCGTAACGAAATGGGGCATTCCGCGATT
    N A A G A P H C F L S V T K W G H S A I
661  GTGAATACCAGCGTAACGGCGATTGCCATATCATTCTGCGCGCGGTAAAGAGCCTAAC
    V N T S G N G D C H I I L R G G K E P N
721  TACAGCGGAAGCACGTTGCTGAAGTGAAGAAGGGCTGAACAAAGCAGGCCTGCCAGCA
    Y S A K H V A E V K E G L N K A G L P A
781  CAGGTGATGATCGATTTCAGCCATGCTAACTCGTCCAAACAATTCAAAAAGCAGATGGAT
    Q V M I D F S H A N S S K Q F K K Q M D
841  GTTTGTGCTGACGTTTGCCAGCAGATTGCCGGTGGCGAAAAGGCCATTATTGGCGTGATG
    V C A D V C Q Q I A G G E K A I I G V M
901  GTGGAAAGCCATCTGGTGAAGGCAATCAGAGCCTCGAGAGCGGGGAGCCGCTGGCCTAC
    V E S H L V E G N Q S L E S G E P L A Y
961  GGTAAGAGCATCACCGATGCCTCGATCGGCTGGGAAGATACCGATGCTCTGTTACGTCAA
    G K S I T D A C I G W E D T D A L L R Q
1021 CTGGCGAATGCAGTGAAGCGCGTCGCGGGTAACTAGGCTGCTGCCACCGCTGAGCAAT
    L A N A V K A R R G *

```

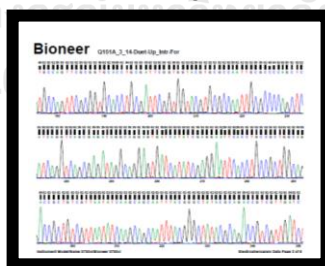


Figure 18 The nucleotide sequence and deduced amino acid sequence of *aroGQ151A* in pBLPTG*

The T7 promoter, *lac* operator and ribosome binding site are indicated in red, blue and green respectively. The restriction site of *PacI* and *AvrII* are indicated in pink and purple, respectively. The point mutation of Gln151Ala (CAA→GCC) is underlined with mutated amino acid residue in yellow. Complete chromatogram of Gln151Ala is shown in Appendix I.

```

-171          CGCAGCTTAATTAA TCCCTTATGCGACTCCTGCATTAGGAAATTAATACGA
-120 C T C A C T A T A G G G G A A T T G T G A G C G G A T A A C A A T T C C C C T G T A G A A A T A A T T T T G T T A A C
-60 T T T A A T A A G G A G A T A T A C C A T G G G C A G C A G C C A T C A C C A T C A T C A C C A C A G C C A G G A T C C

1   ATGAATTATCAGAACGACGATTTACGCATCAAAGAAATCAAAGAGTTACTTCTCTCTGTC
   M N Y Q N D D L R I K E I K E L L P P V
61  GCATTGCTGGAAAAATCCCCGCTACTGAAAATGCCGGAATACGGTTGCCCATGCCCGA
   A L L E K F P A T E N A A N T V A H A R
121 AAAGCGATCCATAAGATCCTGAAAGGTAATGATGATCGCCTGTTGGTTGTGATTGGCCCA
   K A I H K I L K G N D D R L L V V I G P
181 TGCTCAATTCATGATCCTGTGCGGCAAAAGAGTATGCCACTCGCTTGGCGTCCGT
   C S I H D P V A A K E Y A T R L L A L R
241 GAAGAGCTGAAAGATGAGCTGAAAATCGTAATGCGCGTCTATTTTAAAAGCCGCTACC
   E E L K D E L E I V M R V Y F E K P R T
301 ACGGTGGGCTGAAAGGGCTGATTAACGATCCGCATATGGATAATAGCTTCCAGATCAAC
   T V G W K G L I N D P H M D N S F Q I N
361 GACGGTCTGCGTATAGCCCGTAAATGCTGCTTGATATTAACGACAGCGGTCTGCCAGCG
   D G L R I A R K L L L D I N D S G L P A
421 GCAGGTGAATTCCTCGATATGATCACTCCTCTG T A T C T C G C T G A C C T G A T G A G C T G G G G C
   A G E F L D M I T P L Y L A D L M S W G
481 GCAATTGGCGCAGTACCACCGAATCGCAGGTGCACCGCGAATGGCATCAGGGCTTTCT
   A I G A R T T E S Q V H R E L A S G L S
541 TGTCGGTCCGGCTTCAAAAATGGCACCGACGGTACGATTAAAGTGGCTATCGATGCCATT
   C P V G F K N G T D G T I K V A I D A I
601 AATGCCGCCGGTGCGCCGACTGCTTCTGTCGTAACGAAATGGGGCATTCCGCGATT
   N A A G A P H C F L S V T K W G H S A I
661 GTGAATACCAGCGTAACGGCGATTGCCATATCATTCTGCGCGCGGTAAAGAGCCTAAC
   V N T S G N G D C H I I L R G G K E P N
721 TACAGCGGAAGCACGTTGCTGAAGTGAAGAAGGGCTGAACAAAGCAGGCCTGCCAGCA
   Y S A K H V A E V K E G L N K A G L P A
781 CAGGTGATGATCGATTTAGCCATGCTAACTCGTCCAACAATTCAAAAGCAGATGGAT
   Q V M I D F S H A N S S K Q F K K Q M D
841 GTTTGTGCTGACGTTTGCCAGCAGATTGCCGGTGGCGAAAAGGCCATTATTGGCGTGATG
   V C A D V C Q Q I A G G E K A I I G V M
901 GTGGAAAGCCATCTGGTGAAGGCAATCAGAGCCTCGAGAGCGGGGAGCCGCTGGCCTAC
   V E S H L V E G N Q S L E S G E P L A Y
961 GGTAAGAGCATACCGATGCCTCGATCGGCTGGGAAGATACCGATGCTCTGTTACGTCAA
   G K S I T D A C I G W E D T D A L L R Q
1021 CTGGCGAATGCAGTGAAGCGCGTCGCGGGTAA C T A G G C T G C T G C C A C C G C T G A G C A A T
      L A N A V K A R R G *

```

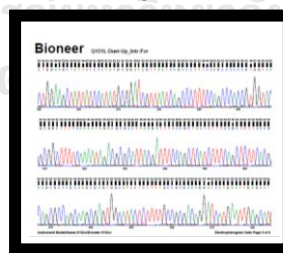


Figure 19 The nucleotide sequence and deduced amino acid sequence of *aroGQ151L* in pBLPTG*

The T7 promoter, *lac* operator and ribosome binding site are indicated in red, blue and green respectively. The restriction site of *PacI* and *AvrII* are indicated in pink and purple, respectively. The point mutation of Gln151Leu (CAA→CTG) is underlined with mutated amino acid residue in yellow. Complete chromatogram of Gln151Leu is shown in Appendix J.


```

-171          CGCAGCTTAATTAA TCCCTTATGCGACTCCTGCATTAGGAAATTAATACGA
-120 CTCACTATAGGGGAATTGTGAGCGGATAACAATTCCCTGTAGAAATAATTTTGTTTAAC
-60  TTTAATAAGGAGATATACCATGGGCAGCAGCCATCACCATCATCACCACAGCCAGGATCC

1    ATGAATTATCAGAACGACGATTTACGCATCAAAGAAATCAAAGAGTTACTTCCCTCTGTC
    M N Y Q N D D L R I K E I K E L L P P V
61  GCATTGCTGGAAAAATCCCCGCTACTGAAAATGCCGGAATACGGTTGCCCATGCCCGA
    A L L E K F P A T E N A A N T V A H A R
121 AAAGCGATCCATAAGATCCTGAAAGGTAATGATGATCGCCTGTTGGTTGTGATTGGCCCA
    K A I H K I L K G N D D R L L V V I G P
181 TGCTCAATTCATGATCCTGTGCGGCAAAAGAGTATGCCACTCGCTTGGCGTGCCT
    C S I H D P V A A K E Y A T R L L A L R
241 GAAGAGCTGAAAGATGAGCTGAAAATCGTAATGCGCGTCTATTTTAAAAGCCGCTACC
    E E L K D E L E I V M R V Y F E K P R T
301 ACGGTGGGCTGAAAGGGCTGATTAACGATCCGCATATGGATAATAGCTTCCAGATCAAC
    T V G W K G L I N D P H M D N S F Q I N
361 GACGGTCTGCGTATAGCCCGTAAATTGCTGCTTGATATTAACGACAGCGGTCTGCCAGCG
    D G L R I A R K L L L D I N D S G L P A
421 GCAGGTGAATTCCTCGATATGATCACTCCTAAT TATCTCGCTGACCTGATGAGCTGGGGC
    A G E F L D M I T P N Y L A D L M S W G
481 GCAATTGGCGCAGTACCACCGAATCGCAGGTGCACCGGAACGGCATCAGGGCTTTCT
    A I G A R T T E S Q V H R E L A S G L S
541 TGTCCGGTCCGCTTCAAAAATGGCACCGGACGGTACGATTAAGTGGCTATCGATGCCATT
    C P V G F K N G T D G T I K V A I D A I
601 AATCCGCGCGGTGCGCCGACTGCTTCCCTGTCGTAACGAAATGGGGCATTCCGCGGATT
    N A A G A P H C F L S V T K W G H S A I
661 GTGAATACCAGCGTAACGGCGATTGCCATATCATTCTGCGCGCGGTAAAGAGCCTAAC
    V N T S G N G D C H I I L R G G K E P N
721 TACAGCGGAAGCACGTTGCTGAAGTGAAGAAGGGCTGAACAAGCAGGCCTGCCAGCA
    Y S A K H V A E V K E G L N K A G L P A
781 CAGGTGATGATCGATTCAGCCATGCTAACTCGTCAAACAATTCAAAAAGCAGATGGAT
    Q V M I D F S H A N S S K Q F K K Q M D
841 GTTTGTGCTGACGTTTGCCAGCAGATTGCCGGTGGCGAAAAGGCCATTATTGGCGTGATG
    V C A D V C Q Q I A G G E K A I I G V M
901 GTGGAAAGCCATCTGGTGAAGGCAATCAGAGCCTCGAGAGCGGGGAGCCGCTGGCCTAC
    V E S H L V E G N Q S L E S G E P L A Y
961 GGTAAGAGCATCACCGATGCCTCGATCGGGAAGATAACCGATGCTCTGTTACGTCAA
    G K S I T D A C I G W E D T D A L L R Q
1021 CTGGCGAATGCAGTGAAGCGCGTCGCGGGTAACTAGGCTGCTGCCACCGCTGAGCAAT
    L A N A V K A R R G *

```

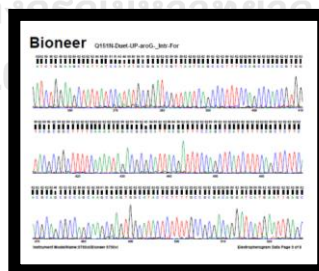


Figure 20 The nucleotide sequence and deduced amino acid sequence of *aroGQ151N* in pBLPTG*

The T7 promoter, *lac* operator and ribosome binding site are indicated in red, blue and green respectively. The restriction site of *PacI* and *AvrII* are indicated in pink and purple, respectively. The point mutation of Gln151Asn (CAA→AAT) is underlined with mutated amino acid residue in yellow. Complete chromatogram of Gln151Asn is shown in Appendix K.

CLUSTAL O(1.2.4) multiple sequence alignment

```

Q151N  MNYQNDDLRIKEIKELLPPVALLEKFPATENAANTVAHARKAIHKILKGNDDRLLVVIGP 60
Q151L  MNYQNDDLRIKEIKELLPPVALLEKFPATENAANTVAHARKAIHKILKGNDDRLLVVIGP 60
Q151A  MNYQNDDLRIKEIKELLPPVALLEKFPATENAANTVAHARKAIHKILKGNDDRLLVVIGP 60
aroG   MNYQNDDLRIKEIKELLPPVALLEKFPATENAANTVAHARKAIHKILKGNDDRLLVVIGP 60
L175D  MNYQNDDLRIKEIKELLPPVALLEKFPATENAANTVAHARKAIHKILKGNDDRLLVVIGP 60
*****

Q151N  CSlHDPVAAKEYATRLLALREELKDELEIVMRVYFEKPRTTVGWKGLINDPHMDSNFQIN 120
Q151L  CSlHDPVAAKEYATRLLALREELKDELEIVMRVYFEKPRTTVGWKGLINDPHMDSNFQIN 120
Q151A  CSlHDPVAAKEYATRLLALREELKDELEIVMRVYFEKPRTTVGWKGLINDPHMDSNFQIN 120
aroG   CSlHDPVAAKEYATRLLALREELKDELEIVMRVYFEKPRTTVGWKGLINDPHMDSNFQIN 120
L175D  CSlHDPVAAKEYATRLLALREELKDELEIVMRVYFEKPRTTVGWKGLINDPHMDSNFQIN 120
*****

Q151N  DGLRIARKLLLDINDSGLPAAGEFLDMITPNYLADLMSWGAIGARTTESQVHRELASGLS 180
Q151L  DGLRIARKLLLDINDSGLPAAGEFLDMITPLYLADLMSWGAIGARTTESQVHRELASGLS 180
Q151A  DGLRIARKLLLDINDSGLPAAGEFLDMITPAYLADLMSWGAIGARTTESQVHRELASGLS 180
aroG   DGLRIARKLLLDINDSGLPAAGEFLDMITPOYLADLMSWGAIGARTTESQVHRELASGLS 180
L175D  DGLRIARKLLLDINDSGLPAAGEFLDMITPOYLADLMSWGAIGARTTESQVHRELASGLS 180
*****

Q151N  CPVGFKNGTDGTIKVAIDAINAAGAPHCFLSVTKWGHSAIVNTSGNGDCHIILLRGGKEPN 240
Q151L  CPVGFKNGTDGTIKVAIDAINAAGAPHCFLSVTKWGHSAIVNTSGNGDCHIILLRGGKEPN 240
Q151A  CPVGFKNGTDGTIKVAIDAINAAGAPHCFLSVTKWGHSAIVNTSGNGDCHIILLRGGKEPN 240
aroG   CPVGFKNGTDGTIKVAIDAINAAGAPHCFLSVTKWGHSAIVNTSGNGDCHIILLRGGKEPN 240
L175D  CPVGFKNGTDGTIKVAIDAINAAGAPHCFLSVTKWGHSAIVNTSGNGDCHIILLRGGKEPN 240
*****

Q151N  YSAKHVAEVKEGLNKAGLPAQVMIDFSHANSSKQFKKQMDVCADVCQQIAGGEKAIIIGVM 300
Q151L  YSAKHVAEVKEGLNKAGLPAQVMIDFSHANSSKQFKKQMDVCADVCQQIAGGEKAIIIGVM 300
Q151A  YSAKHVAEVKEGLNKAGLPAQVMIDFSHANSSKQFKKQMDVCADVCQQIAGGEKAIIIGVM 300
aroG   YSAKHVAEVKEGLNKAGLPAQVMIDFSHANSSKQFKKQMDVCADVCQQIAGGEKAIIIGVM 300
L175D  YSAKHVAEVKEGLNKAGLPAQVMIDFSHANSSKQFKKQMDVCADVCQQIAGGEKAIIIGVM 300
*****

Q151N  VESHLVEGNQSLESGEPLAYGKSITDACIGWEDTDALLRQLANAVKARRG 350
Q151L  VESHLVEGNQSLESGEPLAYGKSITDACIGWEDTDALLRQLANAVKARRG 350
Q151A  VESHLVEGNQSLESGEPLAYGKSITDACIGWEDTDALLRQLANAVKARRG 350
aroG   VESHLVEGNQSLESGEPLAYGKSITDACIGWEDTDALLRQLANAVKARRG 350
L175D  VESHLVEGNQSLESGEPLAYGKSITDACIGWEDTDALLRQLANAVKARRG 350
*****

```

Figure 21 The deduced amino acid sequence of *aroG* compare to *aroG^{fbr}* in pBLPTG and pBLPTG*

The mutagenesis of L175D, Q151A, Q151L and Q151N are indicated in yellow.

3.4 Co-transformation of pBLPTG* & pYF into *E. coli* BL21(DE3)

The next step of the experiment was co-transformation of recombinant plasmid pYF and pBLPTG or pBLPTG* into competent *E. coli* BL21 (DE3) as described in section 2.12. The recombinant clones were screened using LB agar supplemented with 30 µg/mL of kanamycin for pRSFDuet-1 derivative and 10 µg/mL of chloramphenicol for pBAD33 derivative. Recombinant *E. coli* harboring pYF or pBLPTG*Q151N were used as control. After incubated overnight at 37 °C, no colony of control strains was observed while the expected transformant of pBLPTG or pBLPTG* & pYF grew well (Figure 22). Therefore, those growing colonies should harbor both co-transformant plasmids.

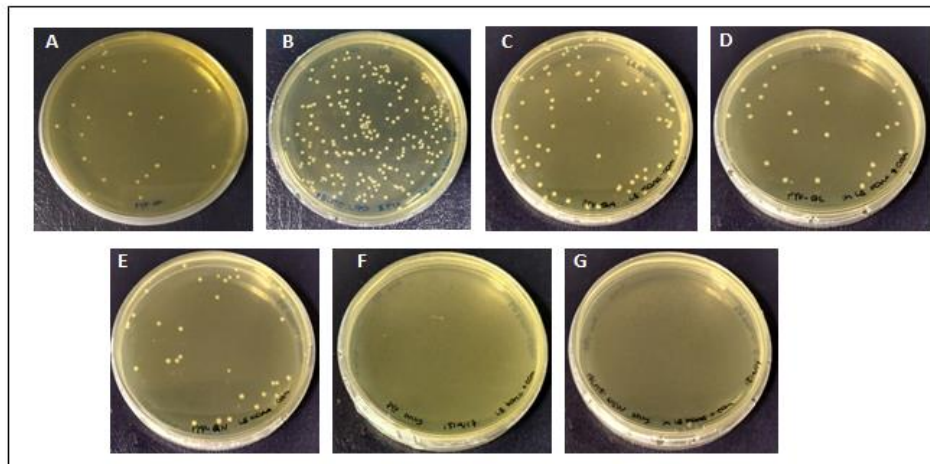


Figure 22 The screening of pBLPTG and pBLPTG* & pYF in *E. coli* BL21(DE3) in agar plate supplemented with 30 µg/mL of kanamycin and 10 µg/mL of chloramphenicol.

(A) Recombinant *E. coli* harboring pBLPTG & pYF (B) Recombinant *E. coli* harboring pBLPTG*L175D & pYF (C) Recombinant *E. coli* harboring pBLPTG*Q151A & pYF (D) Recombinant *E. coli* harboring pBLPTG*Q151L & pYF (E) Recombinant *E. coli* harboring

pBLPTG*Q151N & pYF (F) Recombinant *E. coli* harboring pYF (G) Recombinant *E. coli* harboring pBLPTG*Q151N.

3.5 Plasmid extraction and restriction enzyme digestion analysis

The transformants obtained from section 3.4 were grown in LB containing 30 µg/mL of kanamycin and 10 µg/mL of chloramphenicol. The recombinant plasmids were extracted and *Bam*HI digestion was performed. The result of plasmid digestion is shown in Figure 23. Digestion of the recombinant plasmid pYF with *Bam*HI gave two DNA fragments of 6,104 and 979 bp (lane 2). The recombinant plasmid pBLPTG showed 5,615 and 4,290 bp DNA fragments after *Bam*HI digestion (lane 4). Lane 6 showed four DNA fragments after *Bam*HI digestion of pBLPTG & pYF with size about 6,104; 5,615; 4,290 and 979 bp which corresponded to *Bam*HI digested fragments of pYF and pBLPTG. Though the 6,104 and 5,615 bp of bands were not well separated, the intensity of the band was thicker when compared to that of the control. Lane 8, 10, 12 and 14 showed the same pattern for pBLPTG*L175D, pBLPTG*Q151A, pBLPTG*Q151L and pBLPTG*Q151N with pYF, respectively. Thus, the result indicated that both recombinant plasmid pBLPTG or pBLPTG* & pYF were successfully transformed into *E. coli* BL21(DE3).

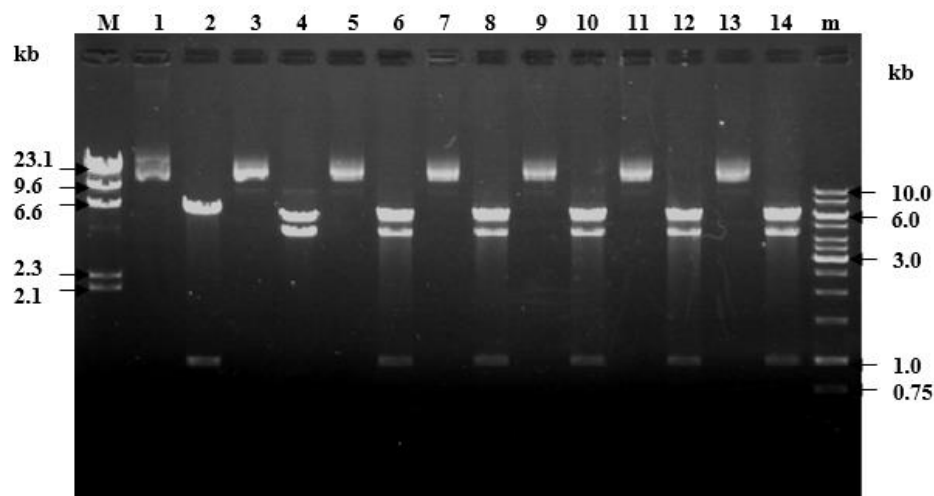


Figure 23 Restriction pattern of pBLPTG and pBLPTG* & pYF digested by *Bam*HI

- Lane M = λ HindIII DNA marker
 Lane 1 = undigested pYF
 Lane 2 = *Bam*HI digested pYF
 Lane 3 = undigested pBLPTG
 Lane 4 = *Bam*HI digested pBLPTG
 Lane 5 = undigested pBLPTG & pYF
 Lane 6 = *Bam*HI digested pBLPTG & pYF
 Lane 7 = undigested pBLPTG*L175D & pYF
 Lane 8 = *Bam*HI digested pBLPTG*L175D & pYF
 Lane 9 = undigested pBLPTG*Q151A & pYF
 Lane 10 = *Bam*HI digested pBLPTG*Q151A & pYF
 Lane 11 = undigested pBLPTG*Q151L & pYF
 Lane 12 = *Bam*HI digested pBLPTG*Q151L & pYF
 Lane 13 = undigested pBLPTG*Q151N & pYF
 Lane 14 = *Bam*HI digested pBLPTG*Q151N & pYF
 Lane m = 1 kb DNA ladder

3.6 Protein expression of *E. coli* harboring pBLPTG or pBLPTG* & pYF

SDS-PAGE is an electrophoretic method that separates proteins based on their molecular weight. Figure 24.A showed the protein expression at 37 °C for 5 h in LB medium. Figure 24.B showed the protein expression at 25 °C for 16 h in TB medium. Terrific Broth (TB), a highly enriched medium was used to improve yields in recombinant *E. coli*.

The proteins of strain harboring pRSFDuet-1 or pBAD33 were used as the control group (lane 2 and 3). In both figures, the protein bands of TktA (72.2 kDa), PheDH (41.4 kDa), AroB (38.9 kDa), and AroL (19.2 kDa) could be observed in all recombinant clones (lane 4-9), while these bands did not exist in the control strains (lane 1-3). The protein band of YddG and GlpF with approximately 31.6 and 29.8 kDa, respectively, could not be detected in both gels. This similar result was also found by Ratchaneeladdajit (2014) when pBLPT & pYF clone was used. Thongchuang and coworkers (2012) also found that the membrane proteins of YddG and GlpF from the cell extract was insufficient to be detected on Commasie Blue stained. In another work, the expression of these genes has proven to be detect radiolabeling (Seol and Shatkin, 1992).

However, the band of AroG at approximately 38 kDa also could not be observed in both figures. This could be due to the interference of AroB that has similar size. In addition, it was found that the protein expression of recombinant allosteric enzyme is quite low. Rastegari and coworker found that the expression of allosteric

aspartokinase under Ptac promoter of pEKEx2 showed very faint band (Rastegari et al., 2013).

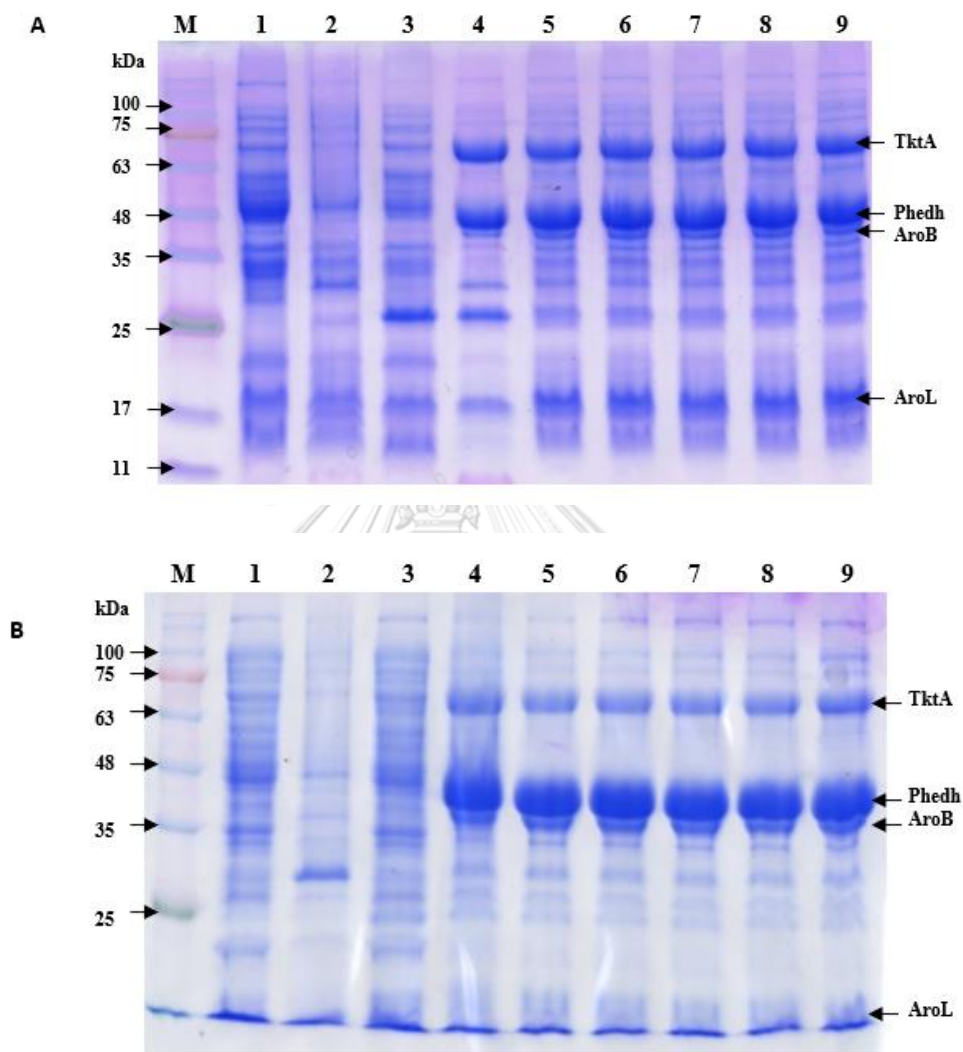


Figure 24 SDS-PAGE analyses of the recombinant proteins

(A) Protein expression was induced at 37 °C for 5 h in LB medium. (B) Protein expression was induced at 25 °C for 16 h in TB medium. Lane M: tricolor ladder (10-180 kDa); lane 1: *E. coli* BL21(DE3) wild-type; lane 2: *E. coli* BL21(DE3)/pRSFDuet-1; lane 3: *E. coli* BL21(DE3)/pBAD33; lane 4: *E. coli* BL21(DE3)/pBLPT & pYF; lane 5: *E. coli* BL21(DE3)/pBLPTG & pYF; lane 6: *E. coli* BL21(DE3)/pBLPTG*L175D & pYF; lane 7:

E. coli BL21(DE3)/pBLPTG*Q151A & pYF; lane 8: *E. coli* BL21(DE3)/pBLPTG*Q151L & pYF; lane 9: *E. coli* BL21(DE3)/pBLPTG*Q151N & pYF

3.7 L-Phe production

Each of recombinant clones was cultured in the minimum medium containing 3.1% (w/v) glycerol as a carbon source (Ratchaneeladdajit, 2014). Determination of cell growth by measurement OD at 600 nm revealed that growth of control recombinant clone pBLPT & pYF (harboring six genes) was higher when compared to pBLPTG & pYF (harboring seven genes). The cell growth of each clone exhibited the exponential phase until 96 h, then remaining constant. Among the recombinant pBLPTG or pBLPTG* & pYF clones, the cell growth of pBLPTG & pYF was the highest. Each recombinant clone of pBLPTG* & pYF showed no significant difference in growth (Figure 25A). Liu and coworker performed fermentation of *aroG* mutants which shared the same expression frame-work (promoter/transcription factor/RBS/terminator/plasmid/host strain) and culture condition. The work reported that their expression levels were in the averages (Liu et al., 2013).

The L-Phe production was tightly correlated with phase of cell growth, which reached the maximum concentration at the start of stationary phase (Figure 25B). Liu and coworker (2013) reported that in fed-batch fermentation of *E. coli* harboring *pheA^{fbr}* and *aroG^{fbr}*, the production of L-Phe was correlated with the cell growth, which exhibiting the maximum concentration after the exponential growth phase. In six days fermentation, the pBLPTG*Q151L & pYF and pBLPTG*Q151N & pYF clones

could produce the highest L-Phe at 1.8 g/L following by pBLPTG*L175D & pYF clone (0.6 g/L) and pBLPTG*Q151A & pYF clone (0.58 g/L). pBLPTG*Q151L & pYF and PBLPTG*Q151N & pYF mutants produced 7.7 fold of that obtained from the wild-type control pBLPTG & pYF, while L-Phe yield from pBLPTG*L175D & pYF and pBLPTG*Q151A & pYF were 2.7 and 2.5 fold, respectively. Ding and coworker, improved the titer and yield of L-Phe by introducing two mutations in *aroG* (Ding et al., 2014). The *E. coli* strain carrying the *aroG*8/15 allele produced a phenylalanine titer of 26.78 g/L and 116% improvement over the control L-Phe overproducing strain (12.41 g/L). In this study, the results of fermentation under glycerol as a carbon source indicated that the modification of the *aroG* through the introduction of point mutation at Gln151 in regulatory (R) domain to Leu and Asn could lead to strong resistance to feedback inhibition. According to the result, the changes of amino acid group could successfully disrupt the hydrogen bond interaction between *aroG* and Phe in L-Phe binding site.

Although the concentration of L-Phe from control pBLPT & pYF was relatively low compared with the highest concentration of 746 mg/L reported previously by Ratchaneeladdajit, (2014), the production of L-Phe by recombinant *E. coli* was significantly improved by expression of *aroG*^{fbr} in the pBLPTG. In addition, the titer and yield of L-Phe can be improved by optimizing the fermentation parameters (Gerigk et al., 2002, Zhou et al., 2011), or performing in situ product recovery (Ruffer et al., 2004).

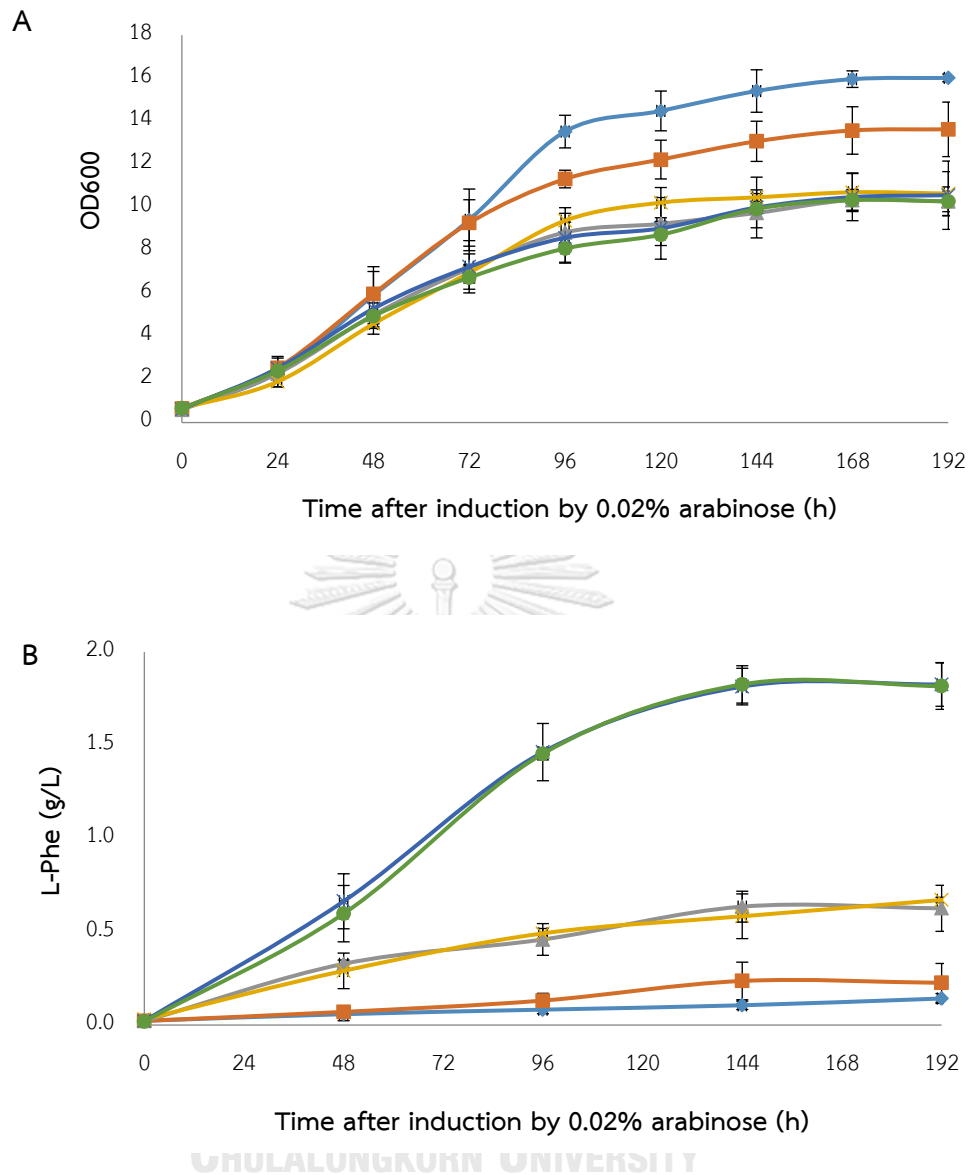


Figure 25 The growth curve of recombinant clones and L-Phe production in minimum medium

(A) The growth curve (B) L-Phe production in minimum medium. pYF & pBLPT (diamond), pYF & pBLPTG (boxes), pYF & pBLPTG*L175D (triangles), pYF & pBLPTG*Q151A (crosses), pYF & pBLPTG*Q151L (double crosses), pYF & pBLPTG*Q151N (circles). The data were obtained from three independent experiments.

In another parallel study, the crude extract of recombinant clone pAroG*Q151L showed the highest DAHP synthase activity in the present of 5 mM L-Phe (Yenyuvadee, 2016). Therefore, for the next experiment the recombinant clone pBLPTG*Q151L & pYF was selected for optimization of medium component using response surface methodology (RSM).

3.8 Optimization of medium component using response surface methodology (RSM)

In this study, the levels of the two independent variables (glycerol and ammonium sulfate) were studied. Thirteen experiments were carried out according to the condition as indicated in Table 8. The L-Phe yield from thirteen experiments is listed in observed column. The experimental result showed that the highest of L-Phe yield was found with the high concentration of glycerol (6.62% w/v). In six days fermentation, the maximum L-Phe yield was 2.14 g/L at 6.62% of glycerol and 5% of ammonium sulfate. The predicted column was calculated by the D.E 6.0.8 program using the data from observed result. The L-Phe yield of 1.88 g/L was predicted at 6.62 (% w/v) of glycerol and 5 (% w/v) of ammonium sulfate.

The value of coefficient of determination (R^2) of this experiment was 0.82. This can be indicated that the 82% of the variability in the response can be explained in the model, while the remaining 18% can be attributed to unknown. The R^2 value is the proportion of variability in response values accounted by the model. The value of R^2 is always in between 0.0 and 1.0. The R^2 value which close to 1.0 indicated that

the model is accurate and predicts better response (Thi Nguyen and Tran, 2018). However, the model with higher R^2 value always does not mean that model is accurate. The higher R^2 value also is resulted by addition of non-significant extra variables in the model. Therefore, it could be possible of a model having higher R^2 value with poor prediction of response (Hegde et al., 2013).

The relationship between the response and the experimental variables can be graphically illustrated by response surface plot (Figure 26.A). The maximum point in surface plot indicated the significant interaction between two variables. The elliptical plot of glycerol versus ammonium sulfate concentration is shown in contour plot (Figure 26.B).

Based on the experimental data using response surface methodology and prediction by D.E 6.0.8 program, the optimization and solution given for glycerol and ammonium sulfate was 6:4.24 (% w/v). The predicted value for L-Phe yield was 2.0 g/L.

When the pBLPTG*Q151L & pYF was cultured in minimum medium containing (g/L): 60 glycerol, 42.4 $(\text{NH}_4)_2\text{SO}_4$, 0.3 $\text{MgSO}_4 \cdot 7\text{H}_2\text{O}$, 1.5×10^{-2} $\text{CaCl}_2 \cdot 2\text{H}_2\text{O}$, 3.0 KH_2PO_4 , 12 K_2HPO_4 , 1.0 NaCl, 7.5×10^{-2} $\text{FeSO}_4 \cdot 7\text{H}_2\text{O}$ /1.0 Na-citrate, 7.5×10^{-3} thiamine·HCl, and 1.5 mL/L trace element solution (TES) containing (g/L): 2.0 $\text{Al}_2(\text{SO}_4)_3 \cdot 18\text{H}_2\text{O}$, 7.5×10^{-1} $\text{CoSO}_4 \cdot 7\text{H}_2\text{O}$, 2.5 $\text{CuSO}_4 \cdot 5\text{H}_2\text{O}$, 5.0×10^{-1} H_3BO_3 , 24 $\text{MnSO}_4 \cdot 7\text{H}_2\text{O}$, 3.0 $\text{Na}_2\text{MoO}_4 \cdot 2\text{H}_2\text{O}$, 2.5 $\text{NiSO}_4 \cdot 6\text{H}_2\text{O}$, 15 $\text{ZnSO}_4 \cdot 7\text{H}_2\text{O}$ at 37 °C after induction with 0.02% arabinose for 6 days, the observed maximum L-Phe production at 2.03 g/L was obtained.

Table 8 Experimental design and result of central composite design for L-Phe production

Run	Variable coded		Glycerol (% w/v)	(NH ₄) ₂ SO ₄ (% w/v)	L-Phe (g/L)	
	X ₁	X ₂			Observed	Predicted
1	-1	-1	3.00	3.00	1.40	1.41
2	1	-1	6.00	3.00	1.51	1.83
3	-1	1	3.00	7.00	1.61	1.36
4	1	1	6.00	7.00	1.09	1.16
5	-1.414	0	2.38	5.00	1.54	1.72
6	1.414	0	6.62	5.00	2.14	1.88
7	0	-1.414	4.50	2.17	1.54	1.33
8	0	1.414	4.50	7.83	0.67	0.82
9	0	0	4.50	5.00	1.92	1.96
10	0	0	4.50	5.00	1.94	1.96
11	0	0	4.50	5.00	2.13	1.96
12	0	0	4.50	5.00	1.98	1.96
13	0	0	4.50	5.00	1.86	1.96

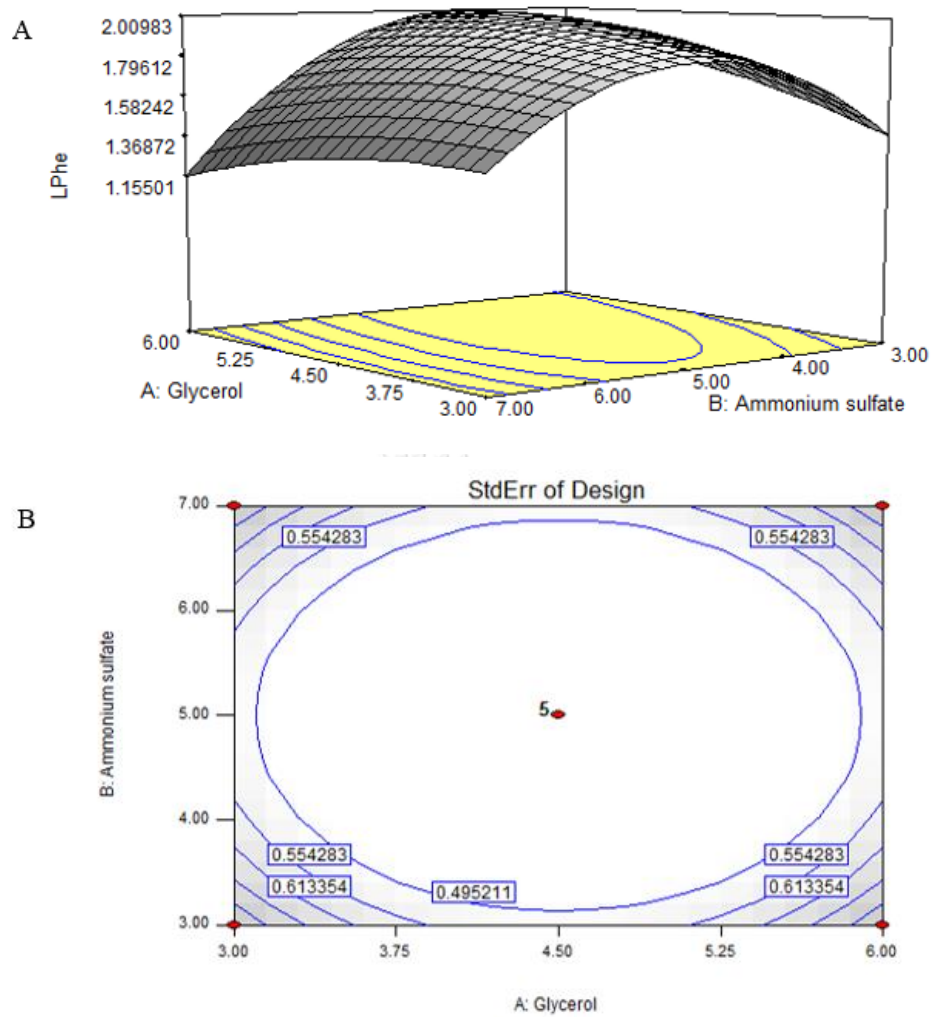


Figure 26 Response surface and contour plot for the interactive effect of glycerol and ammonium sulfate on L-Phe production

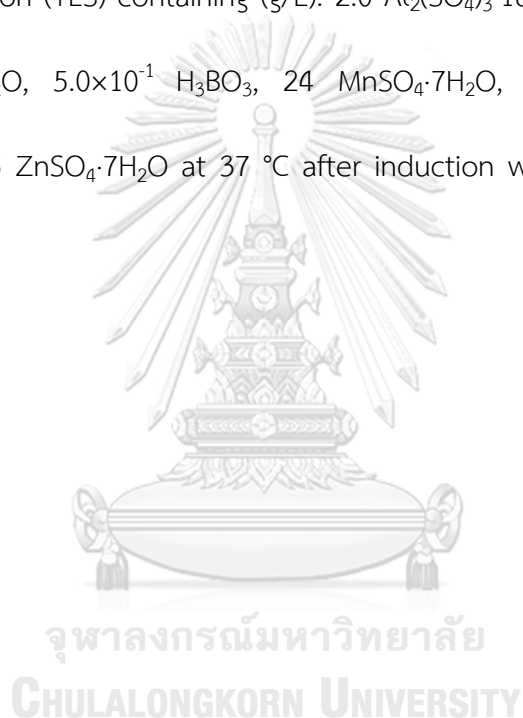
(A) Surface plot (B) Contour plot

CHAPTER IV

CONCLUSIONS

1. The recombinant plasmid pBLPTG and each of pBLPTG* harboring five genes (*aroB* encoding 3-dehydroquinate synthase, *aroL* encoding shikimate kinase II, *phedh* encoding phenylalanine dehydrogenase, *tktA* encoding transketolase and *aroG* encoding 3-dehydroxy-D-arabino-heptulosonate 7-phosphate (DAHP synthase) were successfully constructed under T7lac promoter of pRSFDuet-1.
2. The pBAD33 harboring *glpF* (glycerol facilitator) and *yddG* (aromatic amino acid exporter) inserted under *ara* promoter (pYF) was co-transformed with pBLPTG or pBLPTG* and expressed in *E. coli* BL21 (DE3).
3. In six days fermentation, the pBLPTG*Q151L & pYF and pBLPTG*Q151N & pYF clones could produce the highest L-Phe at 1.8 g/L following by pBLPTG*L175D & pYF clone (0.6 g/L) and pBLPTG*Q151A & pYF clone (0.58 g/L).
4. The recombinant clone pBLPTG*Q151L & pYF and pBLPTG*Q151N & pYF mutants produced 7.7 fold of that obtained from the wild-type control pBLPTG & pYF, while L-Phe yield from pBLPTG*L175D & pYF and pBLPTG*Q151A & pYF were 2.7 and 2.5 fold, respectively. This result revealed that substitution of Leu and Asn at Gln151 could well relieve the feedback inhibition, therefore, elevated the L-Phe production.

5. After optimization using response surface methodology (RSM), the highest L-Phe production at 2.03 mg/L was obtained when the *E. coli* harboring pBLPTG*Q151L & pYF was cultured in minimum medium containing (g/L): 60 glycerol, 42.4 $(\text{NH}_4)_2\text{SO}_4$, 0.3 $\text{MgSO}_4 \cdot 7\text{H}_2\text{O}$, 1.5×10^{-2} $\text{CaCl}_2 \cdot 2\text{H}_2\text{O}$, 3.0 KH_2PO_4 , 12 K_2HPO_4 , 1.0 NaCl, 7.5×10^{-2} $\text{FeSO}_4 \cdot 7\text{H}_2\text{O}$ /1.0 Na-citrate, 7.5×10^{-3} thiamine-HCl, and 1.5 mL trace element solution (TES) containing (g/L): 2.0 $\text{Al}_2(\text{SO}_4)_3 \cdot 18\text{H}_2\text{O}$, 7.5×10^{-1} $\text{CoSO}_4 \cdot 7\text{H}_2\text{O}$, 2.5 $\text{CuSO}_4 \cdot 5\text{H}_2\text{O}$, 5.0×10^{-1} H_3BO_3 , 24 $\text{MnSO}_4 \cdot 7\text{H}_2\text{O}$, 3.0 $\text{Na}_2\text{MoO}_4 \cdot 2\text{H}_2\text{O}$, 2.5 $\text{NiSO}_4 \cdot 6\text{H}_2\text{O}$, 15 $\text{ZnSO}_4 \cdot 7\text{H}_2\text{O}$ at 37 °C after induction with 0.02% arabinose for 6 days.



REFERENCES

- AGER, D. J., PANTALEONE, D. P., HENDERSON, S. A., KATRITZKY, A. R., PRAKASH, I. & WALTERS, D. E. 1998. Commercial, synthetic nonnutritive sweeteners. *Angewandte Chemie*, 37, 1802-1817.
- BACKMAN, K., O'CONNOR, M. J., MARUYA, A., RUDD, E., MCKAY, D., BALAKRISHNAN, R., RADJAI, M., DIPASQUANTONIO, V., SHODA, D. & HATCH, R. 1990. Genetic engineering of metabolic pathways applied to the production of phenylalanine. *Annals New York Academic of Science*, 589, 16-24.
- BARRET, G. C. & ELMORE, D. T. 2004. *Amino Acids and Peptides*, United Kingdom, Cambridge University Press 2004.
- BEZERRA, M. A., SANTELLI, R. E., OLIVEIRA, E. P., VILLAR, L. S. & ESCALEIRA, L. A. 2008. Response surface methodology (RSM) as a tool for optimization in analytical chemistry. *Talanta*, 76, 965-77.
- BOLLAG, D. M., ROZYCKI, M. D. & EDELSTEIN, S. J. 1996. *Protein methods*, New York, USA, John Wiley-Liss, Inc.
- BONGAERTS, J., KRAMER, M., MULLER, U., RAEVEN, L. & WUBBOLTS, M. 2001. Metabolic engineering for microbial production of aromatic amino acids and derived compounds. *Metabolic Engineering*, 3, 289-300.
- CHAO, Y. P., LAI, Z. J., CHEN, P. & CHERN, J. T. 1999. Enhanced conversion rate of L-phenylalanine by coupling reactions of aminotransferases and phosphoenolpyruvate carboxykinase in *Escherichia coli* K-12. *Biotechnology Progress*, 15, 453-8.
- D'ESTE, M., MORALES, M. A. & ANGELIDAKI, I. 2018. Amino acids production focusing on fermentation technologies - A review. *Biotechnology Advances*, 36, 14-25.
- DA SILVA, G. P., MACK, M. & CONTIERO, J. 2009. Glycerol: a promising and abundant carbon source for industrial microbiology. *Biotechnology Advances*, 27, 30-9.
- DE BOER, L. & DIJKHUIZEN, L. 1990. *Microbial and enzymatic processes for L-phenylalanine production*, Berlin, Heidelberg, Springer Berlin Heidelberg.
- DE FEYTER, R. 1987. Shikimate kinases from *Escherichia coli* K12. *Methods Enzymology*,

- 142, 355-61.
- DELL, K. A. & FROST, J. W. 1993. Identification and removal of impediments to biocatalytic synthesis of aromatics from D-glucose: rate-limiting enzymes in the common pathway of aromatic amino acid biosynthesis. *Journal of the American Chemical Society*, 115, 11581-11589.
- DEMAIN, A. L. 2007. Reviews: The business of biotechnology. *Industrial Biotechnology*, 3, 269-283.
- DEMIRBAS, M. F. & BALAT, M. 2006. Recent advances on the production and utilization trends of bio-fuels: A global perspective. *Energy Conversion and Management*, 47, 2371-2381.
- DHARMADI, Y., MURARKA, A. & GONZALEZ, R. 2006. Anaerobic fermentation of glycerol by *Escherichia coli*: a new platform for metabolic engineering. *Biotechnology Bioengineering*, 94, 821-9.
- DING, R., LIU, L., CHEN, X., CUI, Z., ZHANG, A., REN, D. & ZHANG, L. 2014. Introduction of two mutations into AroG increases phenylalanine production in *Escherichia coli*. *Biotechnology Letters*, 36, 2103-8.
- DONAHUE, J. L., BOWNAS, J. L., NIEHAUS, W. G. & LARSON, T. J. 2000. Purification and characterization of *glpX*-encoded fructose 1, 6-bisphosphatase, a new enzyme of the glycerol 3-phosphate regulon of *Escherichia coli*. *Journal of Bacteriology*, 182, 5624-7.
- DZIVENU, O. K., PARK, H. H. & WU, H. 2004. General co-expression vectors for the overexpression of heterodimeric protein complexes in *Escherichia coli*. *Protein expression and purification*, 38, 1-8.
- GERIGK, M. R., MAASS, D., KREUTZER, A., SPRENGER, G., BONGAERTS, J., WUBBOLTS, M. & TAKORS, R. 2002. Enhanced pilot-scale fed-batch L-phenylalanine production with recombinant *Escherichia coli* by fully integrated reactive extraction. *Bioprocess and Biosystem Engineering*, 25, 43-52.
- GHOSH, S., CHAKRABORTY, R., CHATTERJEE, A. & RAYCHAUDHURI, U. 2014. Optimization of media components for the production of palm vinegar using response surface methodology. *Journal of the Institute of Brewing*, 120, 550-558.
- GOTTLIEB, K., ALBERMANN, C. & SPRENGER, G. A. 2014. Improvement of L-phenylalanine

- production from glycerol by recombinant *Escherichia coli* strains: the role of extra copies of *glpK*, *glpX*, and *tktA* genes. *Microbial Cell Factories*, 13, 96.
- GREEN, M. R. & SAMBROOK, J. 2012. *Molecular cloning: a laboratory manual* New York, USA, Cold Spring Harbour Laboratory Press.
- HANZLOWSKY, A., JELENCIC, B., JAWDEKAR, G., HINKLEY, C. S., GEIGER, J. H. & HENRY, R. W. 2006. Co-expression of multiple subunits enables recombinant SNAPC assembly and function for transcription by human RNA polymerases II and III. *Protein expression and purification*, 48, 215-223.
- HEGDE, S., BHADRI, G., NARSAPUR, K., KOPPAL, S., OSWAL, P., TURMURI, N., JUMNAL, V. & HUNGUND, B. 2013. Statistical optimization of medium components by response surface methodology for enhanced production of bacterial cellulose by *Gluconacetobacter persimmonis*. *Journal Bioprocessing Biotechniques*, 4, 142.
- HERRMANN, K. M. 1995. The shikimate pathway: Early steps in the biosynthesis of aromatic compounds. *The Plant Cell*, 7, 907 – 919.
- HU, C., JIANG, P., XU, J., WU, Y. & HUANG, W. 2003. Mutation analysis of the feedback inhibition site of phenylalanine-sensitive 3-deoxy-D-arabino-heptulosonate 7-phosphate synthase of *Escherichia coli*. *Journal of Basic Microbiology*, 43, 399-406.
- IKEDA, M. 2003. Amino acid production processes. *Advances in Biochemical Engineering/Biotechnology*, 79, 1-35.
- IKEDA, M. 2006. Towards bacterial strains overproducing L-tryptophan and other aromatics by metabolic engineering. *Applied microbiology and biotechnology*, 69, 615-626.
- KANOKSINWUTTIPONG, N. 2014. *Construction of phenylalanine feedback-resistant 3-deoxy-D-arabino-heptulosonate-7-phosphate synthase* (Senior Project), Chulalongkorn University.
- KERRIGAN, J. J., XIE, Q., AMES, R. S. & LU, Q. 2011. Production of protein complexes via co-expression. *Protein Expression and Purification*, 75, 1-14.
- KHAMDUANG, M., PACKDIBAMRUNG, K., CHUTMANOP, J., CHISTI, Y. & SRINOPHAKUN, P. 2009. Production of L-phenylalanine from glycerol by a recombinant *Escherichia coli*. *Journal of Industrial Microbiology and Biotechnolgy*, 36, 1267-74.

- KIM, H. Y., RHYM, H., LEE, D. J., WON, C. H., LIM, B. L. & CHOI, H. G. 1994. *Method for production of L-phenylalanine by recombinant E. coli*. Miwon Co. Ltd., Korea. patent application.
- KONSTANTINOV, K. B., NISHIO, N., SEKI, T. & YOSHIDA, T. 1991. Physiologically motivated strategies for control of the fed-batch cultivation of recombinant *Escherichia coli* for phenylalanine production. *Journal of Fermentation and Bioengineering*, 71, 350-355.
- LEUCHTENBERGER, W., HUTHMACHER, K. & DRAUZ, K. 2005. Biotechnological production of amino acids and derivatives: current status and prospects. *Applied Microbiology and Biotechnology*, 69, 1-8.
- LI, C., BAI, J., CAI, Z. & OUYANG, F. 2002. Optimization of a cultural medium for bacteriocin production by *Lactococcus lactis* using response surface methodology. *Journal of Biotechnology*, 93, 27-34.
- LIM, B. L., RHYM, H., LEE, J. H., CHOI, T. Y., HWANG, E. N. & CHOI, H. K. 1995. *Method for production of L-phenylalanine by Escherichia coli mutant that is resistant to osmotic pressure*. Miwon Co. Ltd., Korea. patent application.
- LIU, S. P., LIU, R. X., XIAO, M. R., ZHANG, L., DING, Z. Y., GU, Z. H. & SHI, G. Y. 2014. A systems level engineered *E. coli* capable of efficiently producing L-phenylalanine. *Process Biochemistry*, 49, 751-757.
- LIU, S. P., XIAO, M., ZHANG, L., XU, J., DING, Z., GU, Z. & SHI, G. 2013. Production of L-phenylalanine from glucose by metabolic engineering of wild type *Escherichia coli* W3110. *Process Biochemistry*, 48, 413-419.
- MAEDA, H. & DUDAREVA, N. 2012. The shikimate pathway and aromatic amino acid biosynthesis in plants. *Annual Review of Plant Biology*, 63, 73-105.
- MARR, A. G. 1991. Growth rate of *Escherichia coli*. *Microbiological reviews*, 55, 316-333.
- MÄRZ, U. 2009. *World markets for fermentation ingredients* [Online]. Available: <http://www.bccresearch.com/market-research/food-and-beverage/fermentationingredients-fod020c.html> [Accessed September 25 2018].
- MICHEL, G., ROSZAK, A. W., SAUVÉ, V., MACLEAN, J., MATTE, A., COGGINS, J. R., CYGLER, M. & LAPHORN, A. J. 2003. Structures of shikimate dehydrogenase AroE and its Paralog YdiB. A common structural framework for different activities. *The*

Journal of biological chemistry, 278, 19463-19472.

- MIROUX, B. & WALKER, J. E. 1996. Over-production of proteins in *Escherichia coli*: mutant hosts that allow synthesis of some membrane proteins and globular proteins at high levels. *Journal of Molecular Biology*, 260, 289-98.
- MITSUHASHI, S. 2014. Current topics in the biotechnological production of essential amino acids, functional amino acids, and dipeptides. *Current Opinion in Biotechnology*, 26, 38-44.
- MURARKA, A., DHARMADI, Y., YAZDANI, S. S. & GONZALEZ, R. 2008. Fermentative utilization of glycerol by *Escherichia coli* and its implications for the production of fuels and chemicals. *Applied and Environmental Microbiology*, 74, 1124.
- NCBI. 2017. *Phenylalanine* [Online]. Available: <https://pubchem.ncbi.nlm.nih.gov/compound/6140> [Accessed October 13, 2017].
- NELSON, D. L. 2007. *Lehninger principles of biochemistry*, New York, W H Freeman and Co.
- OH, S., RHEEM, S., SIM, J., KIM, S. & BAEK, Y. 1995. Optimizing conditions for the growth of *Lactobacillus casei* YIT 9018 in tryptone-yeast extract-glucose medium by using response surface methodology. *Applied and Environmental Microbiology*, 61, 3809-14.
- OOIJKAAS, L. P., WILKINSON, E. C., TRAMPER, J. & BUITELAAR, R. M. 1999. Medium optimization for spore production of *Coniothyrium minitans* using statistically-based experimental designs. *Biotechnology and Bioengineering*, 64, 92-100.
- PITTARD, J. A. 1996. Biosynthesis of the aromatic amino acids. *Escherichia coli and Salmonella*. 2 nd ed. Washington DC, USA: ASM Press.
- RASTEGARI, H., CHIANI, M., AKBARZADEH, A., CHERAGHI, S., SAFFARI, Z., MEHRABI, M. R., FARHANGI, A. & GHASSEMI, S. 2013. Improvement in the production of L-lysine by overexpression of aspartokinase (ASK) in *C. glutamicum* ATCC 21799. *Tropical Journal of Pharmaceutical Research*, 12, 51 -56.
- RATCHANEELADDAJIT, P. 2014. *L-phenylalanine production by recombinant Escherichia coli under regulation of T7 and ara promoters* Master's Thesis, Chulalongkorn University.

- RODRIGUEZ, A., MARTNEZ, J. A., FLORES, N., ESCALANTE, A., GOSSET, G. & BOLIVAR, F. 2014. Engineering *Escherichia coli* to overproduce aromatic amino acids and derived compounds. *Microbial Cell Factories*, 13, 126.
- RUFFER, N., HEIDERSDORF, U., KRETZERS, I., SPRENGER, G. A., RAEVEN, L. & TAKORS, R. 2004. Fully integrated L-phenylalanine separation and concentration using reactive-extraction with liquid-liquid centrifuges in a fed-batch process with *E. coli*. *Bioprocess and Biosystem Engineering*, 26, 239-48.
- SANO, C. 2009. History of glutamate production. *The American Journal of Clinical Nutrition*, 90, 728S-732S.
- SEOL, W. & SHATKIN, A. J. 1992. *Escherichia coli* alpha-ketoglutarate permease is a constitutively expressed proton symporter. *Journal of Biological Chemistry* 267, 6409-13.
- SHUMILIN, I. A., KRETSINGER, R. H. & BAUERLE, R. H. 1999. Crystal structure of phenylalanine-regulated 3-deoxy-D-arabino-heptulosonate-7-phosphate synthase from *Escherichia coli*. *Structure*, 7, 865-875.
- SPRENGER, G., SIEWE, R., SAHM, H., KARUTZ, M. & SONKE, T. 1998. *Microbial preparation of substances from metabolism II*. Netherlands patent application WO-98/18937.
- SPRENGER, G. A. 2007. From scratch to value: engineering *Escherichia coli* wild type cells to the production of L-phenylalanine and other fine chemicals derived from chorismate. *Applied Microbiology and Biotechnology*, 75, 739-49.
- SUZUKI, H. 2013. Microbial production of amino acids and their derivatives for use in foods, nutraceuticals and medications. In: MCNEIL, B., ARCHER, D., GIAVASIS, I. & HARVEY, L. (eds.) *Microbial Production of Food Ingredients, Enzymes and Nutraceuticals*. Woodhead Publishing.
- SWEET, G., GANDOR, C., VOEGELE, R., WITTEKINDT, N., BEUERLE, J., TRUNIGER, V., LIN, E. C. & BOOS, W. 1990. Glycerol facilitator of *Escherichia coli*: cloning of *glpF* and identification of the *glpF* product. *Journal Bacteriology*, 172, 424-30.
- THI NGUYEN, H. Y. & TRAN, G. B. 2018. Optimization of Fermentation Conditions and Media for Production of Glucose Isomerase from *Bacillus megaterium* Using Response Surface Methodology. *Scientifica*, 2018, 11.

- THONGCHUANG, M. 2011. *Improvement of phenylalanine production in Escherichia coli by metabolic engineering process*. Ph.D. thesis, Chulalongkorn University
- THONGCHUANG, M., PONGSAWASDI, P., CHISTI, Y. & PACKDIBAMRUNG, K. 2012. Design of a recombinant *Escherichia coli* for producing L-phenylalanine from glycerol. *World Journal of Microbiology and Biotechnology*, 28, 2937-43.
- WANG, Z. X., ZHUGE, J., FANG, H. & PRIOR, B. A. 2001. Glycerol production by microbial fermentation: a review. *Biotechnology Advances*, 19, 201-23.
- WEINER, M., ALBERMANN, C., GOTTLIEB, K., SPRENGER, G. A. & WEUSTER-BOTZ, D. 2014. Fed-batch production of L-phenylalanine from glycerol and ammonia with recombinant *Escherichia coli*. *Biochemical Engineering Journal*, 83, 62 - 69.
- WENDISCH, V. F. 2014. Microbial production of amino acids and derived chemicals: synthetic biology approaches to strain development. *Current Opinion in Biotechnology*, 30, 51-8.
- YANG, W., ZHANG, L., LU, Z., TAO, W. & ZHAI, Z. 2001. A new method for protein coexpression in *Escherichia coli* using two incompatible plasmids. *Protein expression and purification*, 22, 472-478.
- YAZDANI, S. S. & GONZALEZ, R. 2007. Anaerobic fermentation of glycerol: a path to economic viability for the biofuels industry. *Current opinion in biotechnology*, 18, 213-219.
- YENYUVADEE, C. 2016. *Co-expression of feedback-resistant aroG and some important genes in L-phenylalanine biosynthesis pathway* (Senior Project) Chulalongkorn University.
- ZHANG, S., POHNERT, G., KONGSAEREE, P., WILSON, D. B., CLARDY, J. & GANEM, B. 1998. Chorismate mutase-prephenate dehydratase from *Escherichia coli*. Study of catalytic and regulatory domains using genetically engineered proteins. *Journal of Biological Chemistry*, 273, 6248-53.
- ZHOU, H., LIAO, X., LIU, L., WANG, T., DU, G. & CHEN, J. 2011. Enhanced L-phenylalanine production by recombinant *Escherichia coli* BR-42 (pAP-B03) resistant to bacteriophage BP-1 via a two-stage feeding approach. *Journal of Industrial Microbiology and Biotechnology*, 38, 1219-27.
- ZHOU, H., LIAO, X., WANG, T., DU, G. & CHEN, J. 2010. Enhanced L-phenylalanine

biosynthesis by co-expression of *pheA(fbr)* and *aroF(wt)*. *Bioresource Technology*, 101, 4151-6.

ZWAIG, N., KISTLER, W. S. & LIN, E. C. 1970. Glycerol kinase, the pacemaker for the dissimilation of glycerol in *Escherichia coli*. *Journal of Bacteriology*, 102, 753-9.

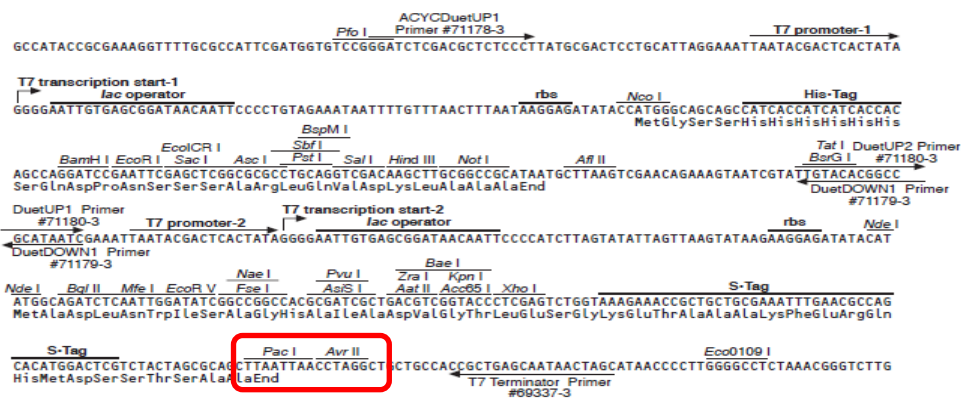
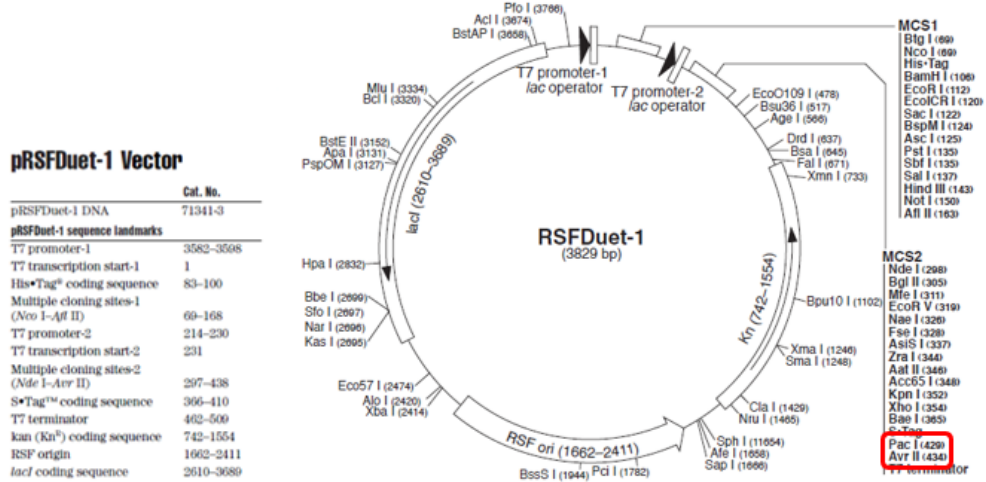




จุฬาลงกรณ์มหาวิทยาลัย
CHULALONGKORN UNIVERSITY

APPENDIX A

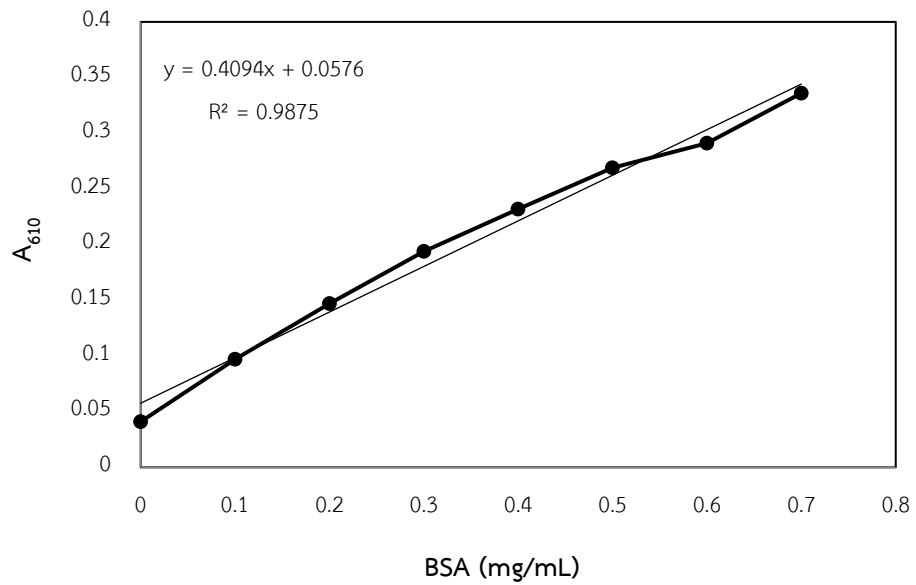
Restriction map of pRSFDuet-1



pRSFDuet-1 cloning/expression regions

APPENDIX B

Standard curve for protein determination by Lowry's method



APPENDIX C

Preparation for denaturing polyacrylamide gel electrophoresis

1. Stock solution

2 M Tris-HCl (pH 8.8)

Tris (hydroxymethyl)-aminomethane	24.2	g
-----------------------------------	------	---

Adjusted pH to 8.8 with 1N HCl and adjusted volume to 100 ml with distilled water.

1M Tris HCl (pH 6.8)

Tris (hydroxymethyl)-aminomethane	12.1	g
-----------------------------------	------	---

Adjusted pH to 6.8 with 1N HCl and adjusted volume to 100 ml with distilled water.

10% (w/v) SDS

Sodium dodecyl sulfate (SDS)	10	g
------------------------------	----	---

Added distilled water to a total volume to 100 ml.

50% Glycerol

100% glycerol	50	ml
---------------	----	----

Added distilled water to a total volume to 100 ml.

1% (w/v) Bromophenol blue

Bromophenol blue	100	mg
------------------	-----	----

Brought to 10 ml with distilled water and stirred until dissolved.

The aggregate dye was removed by filtration.

2. Working solution

Solution A (30% (w/v) acrylamide, 0.8% (w/v) bis-acrylamide)

Acrylamide	29.2	g
------------	------	---

N, N'-methylene-bis-acrylamide	0.8	g
--------------------------------	-----	---

Adjusted volume to 100 ml with distilled water

Filtered and stored in the dark bottle at 4°C

Solution B (1.5M Tris-HCl, pH 8.8 and 0.4% SDS)

2 M Tris-HCl (pH 8.8)	75	ml
10% (w/v) SDS	4	ml
Distilled water	21	ml

Solution C (0.5M Tris-HCl, pH 6.8 and 0.4% SDS)

1 M Tris-HCl (pH 6.8)	50	ml
10% (w/v) SDS	4	ml
Distilled water	46	ml

10% (w/v) Ammonium persulfate

Ammonium persulfate	0.5	g
Distilled water	5	ml

Electrophoresis buffer (25 mM Tris, 192 mM glycine and 0.1% (w/v) SDS)

Tris (hydroxymethyl)-aminomethane	3.0	g
Glycine	14.4	g
SDS	1	g

Dissolved and adjusted to total volume to 1 liter with distilled water

(The final pH should be approximately 8.3)

5x sample buffer (312.5 mM Tris-HCl pH 6.8, 50% (v/v) glycerol, 1% (w/v)

bromophenol blue

1 M Tris-HCl (pH 6.8)	0.6	ml
50% (v/v) Glycerol	5.0	ml
10% (w/v) SDS	2.0	ml
1% (w/v) Bromophenol blue	1.0	ml
β -Mercaptoethanol	0.5	ml
Distilled water	1.4	ml

Lysis buffer (89 mM Tris-HCl, 89 mM boric acid, 2.5 mM EDTA, pH 8.0, 2% SDS, 5% sucrose and 0.04% bromophenol blue)

1 M Tris-HCl (pH 8.0)	89	μ L
0.25 M Boric acid	356	μ L
0.5 M EDTA (pH 8.0)	5	μ L
25% (w/v) SDS	80	μ L
25% (w/v) Sucrose	200	μ L

20% (w/v) Bromophenol blue	2	μL
Sterile water	268	μL

Each of these components was put into a sterile 1.5 mL microcentrifuge tube and should be stored at -20 °C until used.

0.1 M IPTG stock solution

Dissolved 0.238 g of IPTG in 8 mL of distilled H₂O. Adjusted to a final volume 10 mL. Filter sterilized with a 0.22 μM syringe filter.

10% arabinose stock solution

Dissolved 1.0 g of arabinose in 8 mL of distilled H₂O. Adjusted to a final volume 10 mL. Filter sterilized with a 0.22 μM syringe filter.

3. SDS-PAGE

12.5 % Separating gel

Solution A	4.2	ml
Solution B	2.5	ml
Distilled water	3.3	ml
10% (w/v) Ammonium persulfate	60	μl
TEMED	10	μl

5.0 % Stacking gel

Solution A	0.67	ml
Solution C	1.0	ml
Distilled water	2.3	ml
10% (w/v) Ammonium persulfate	30	μl
TEMED	5	μl

4. Protein staining solution

Staining solution, 1 L

Coomassie brilliant blue R-250	1.0	g
Glacial acetic acid	100	ml
Methanol	450	ml
Distilled water	450	ml

Destaining solution, 1 L

Methanol	100	ml
Glacial acetic acid	100	ml
Distilled water	800	ml



APPENDIX D

Preparation for agarose gel electrophoresis and HPLC mobile phase

1. Electrophoresis buffer (10X TBE)

Tris (hydroxymethyl)-aminomethane	54	g
Boric acid	27.5	g
Ethylenediaminetetraacetic Acid, Disodium salt	9.3	g

Adjust volume to 1 L with deionized water

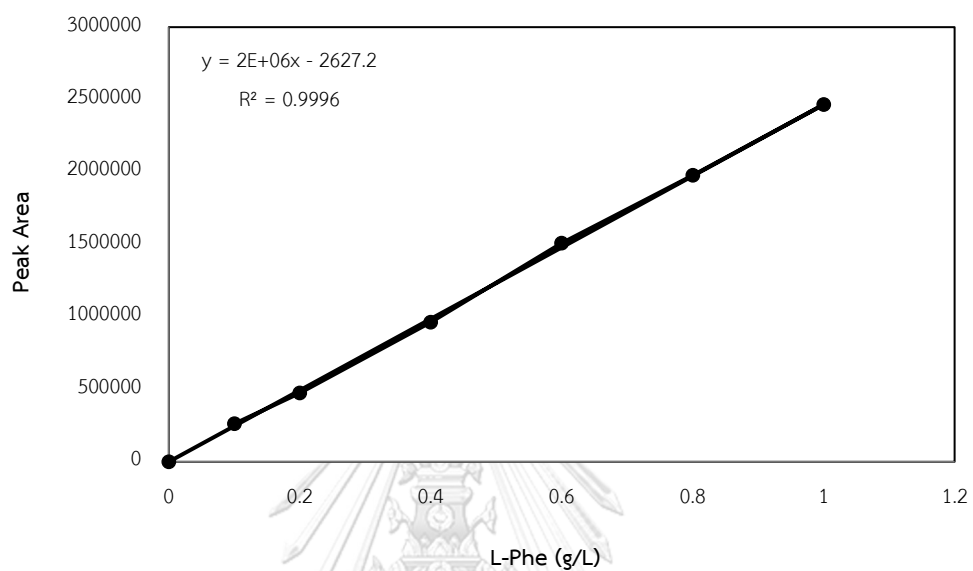
2. HPLC mobile phase (2mM Copper sulfate)

Copper sulfate	0.5	g
----------------	-----	---

Adjust to volume to 1 liter with ultrapure water and filtered for remove impurity that can be interfering in HPLC system

APPENDIX E

Standard curve for L-phenylalanine determination by HPLC



APPENDIX F

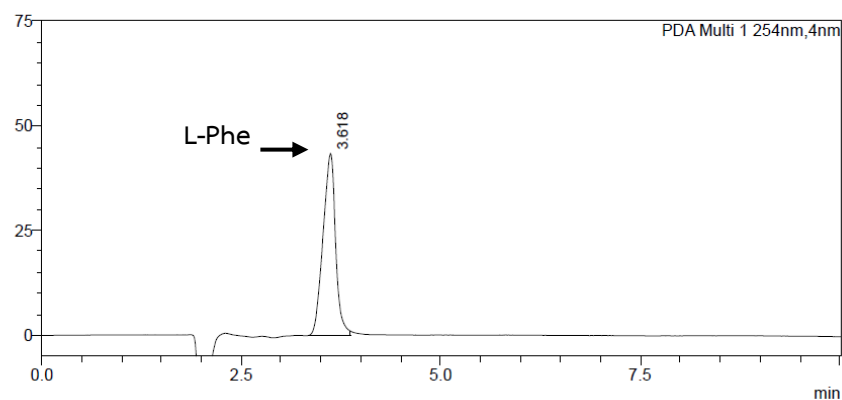
Chromatogram of L-phenylalanine

1. Standard of L-phenylalanine

a. L-Phe 0.2 g/L

<Chromatogram>

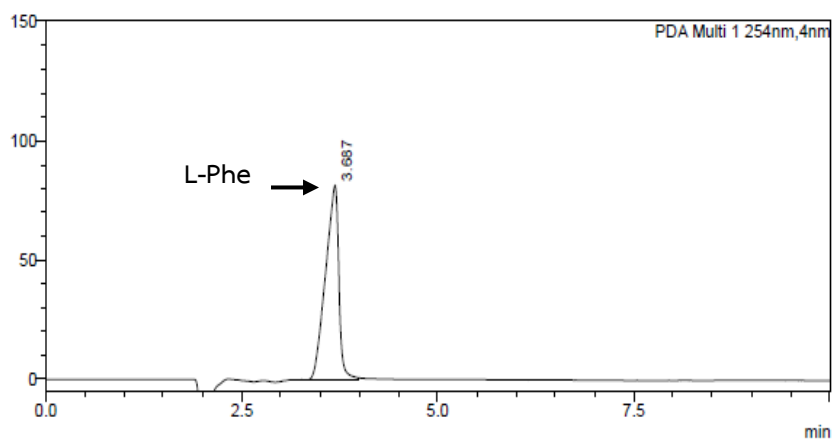
mAU



b. L-Phe 0.4 g/L

<Chromatogram>

mAU



HPLC technique using Chirex 3126 (D) - penicillamine column

Mobile phase : 2 mM copper sulfate : methanol ratio (75:25)

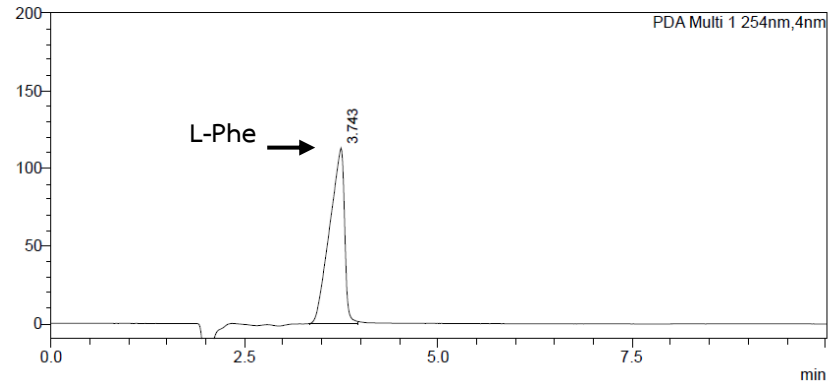
Flow rate : 0.7 mL/min

Peak detected : 254 nm

c. L-Phe 0.6 g/L

<Chromatogram>

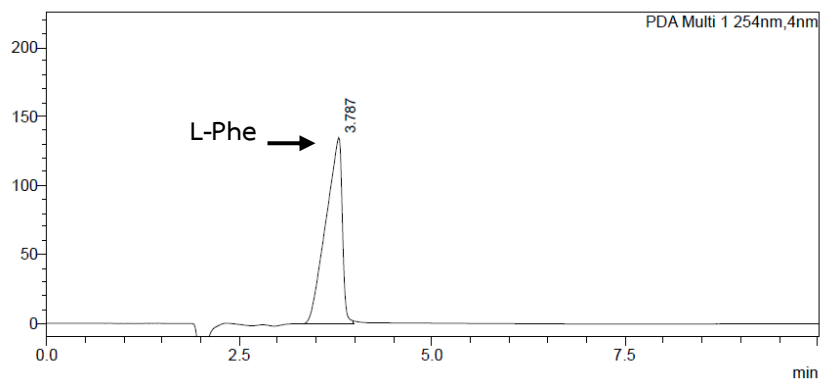
mAU



d. L-Phe 0.8 g/L

<Chromatogram>

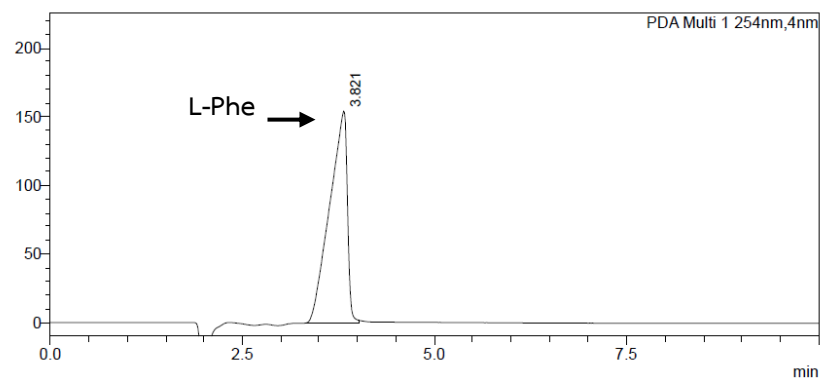
mAU



e. L-Phe 1.0 g/L

<Chromatogram>

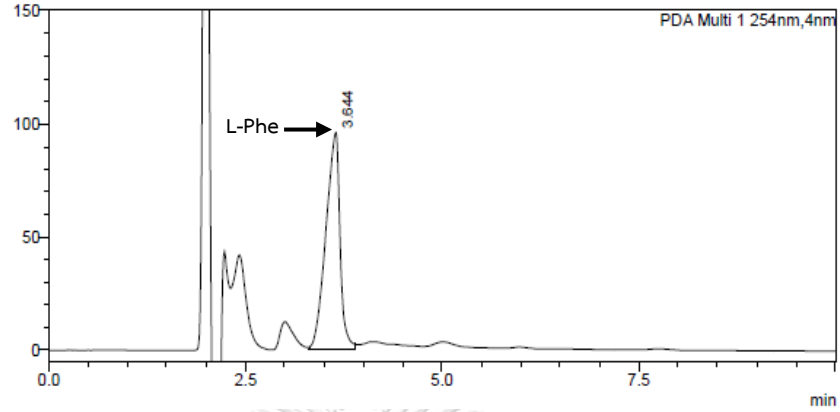
mAU



2. Sample

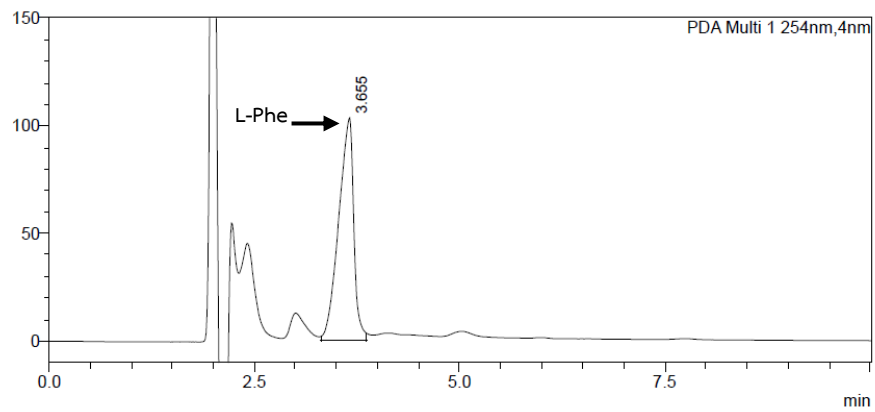
<Chromatogram>

mAU



<Chromatogram>

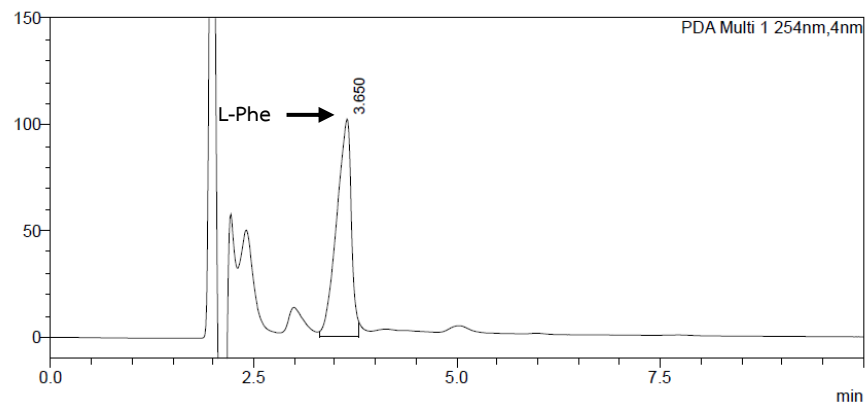
mAU



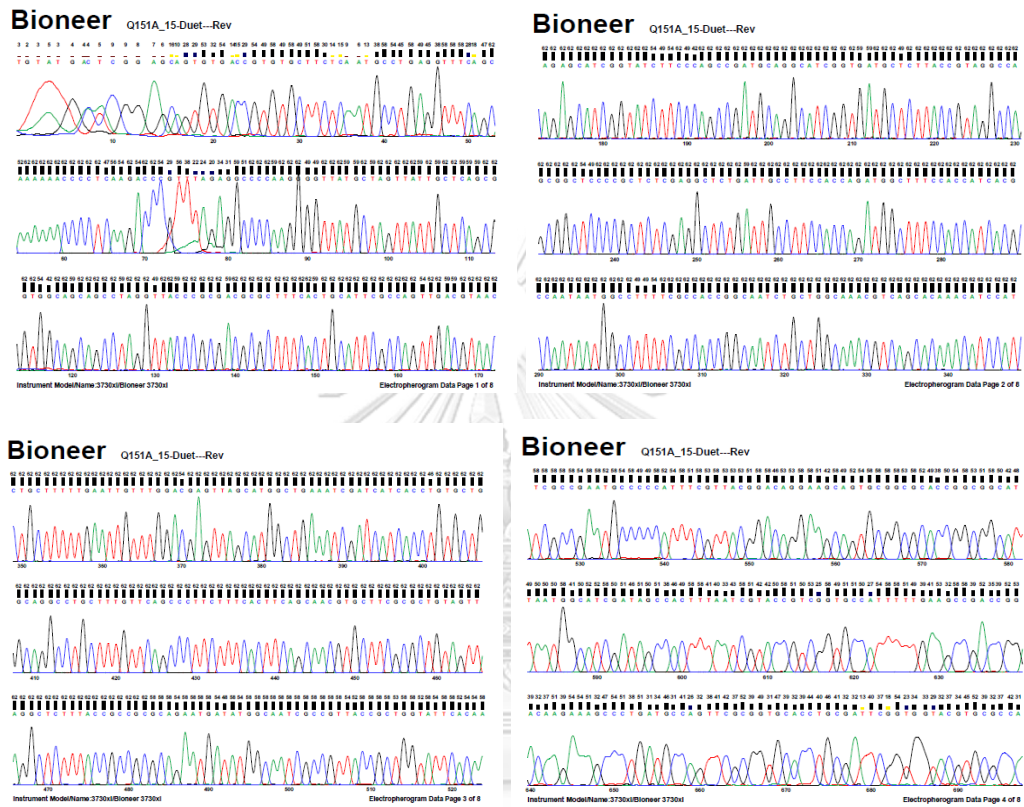
CHULALONGKORN UNIVERSITY

<Chromatogram>

mAU



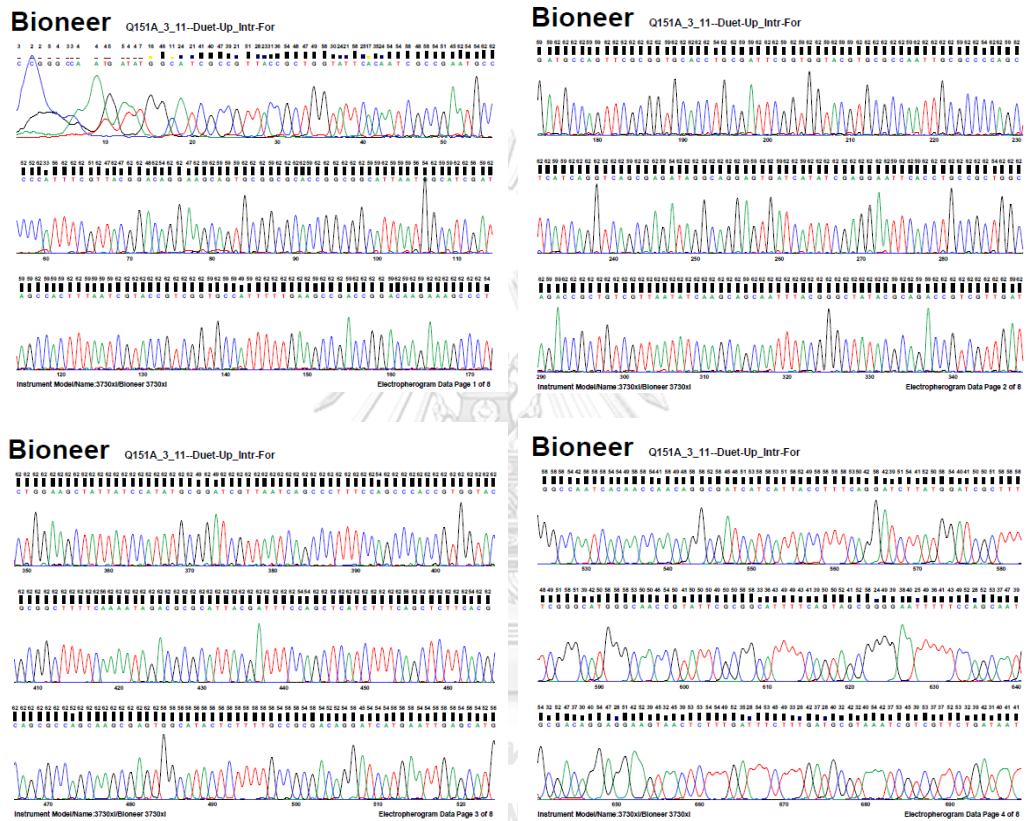
(B)



APPENDIX I

The sequencing chromatogram of *aroG*^{fbr} Q151A in pBLPTG*Q151A using primers F_DuetUP_aroG_Intr (A) and R_Duet (B)

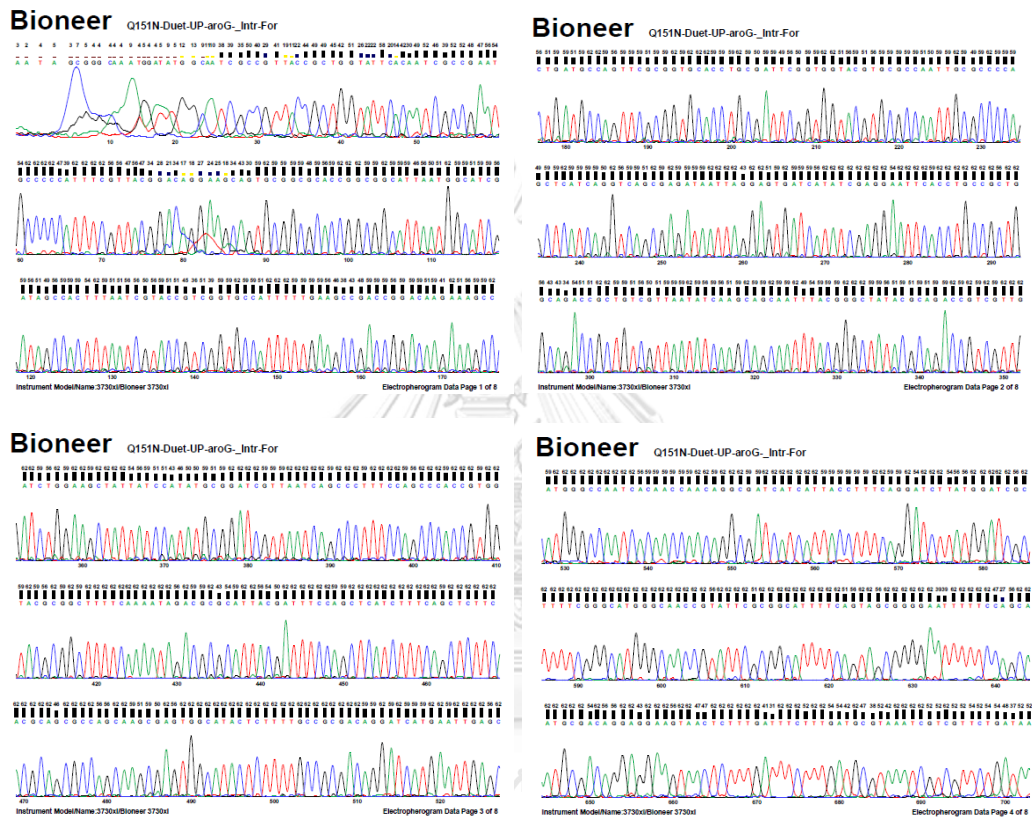
(A)



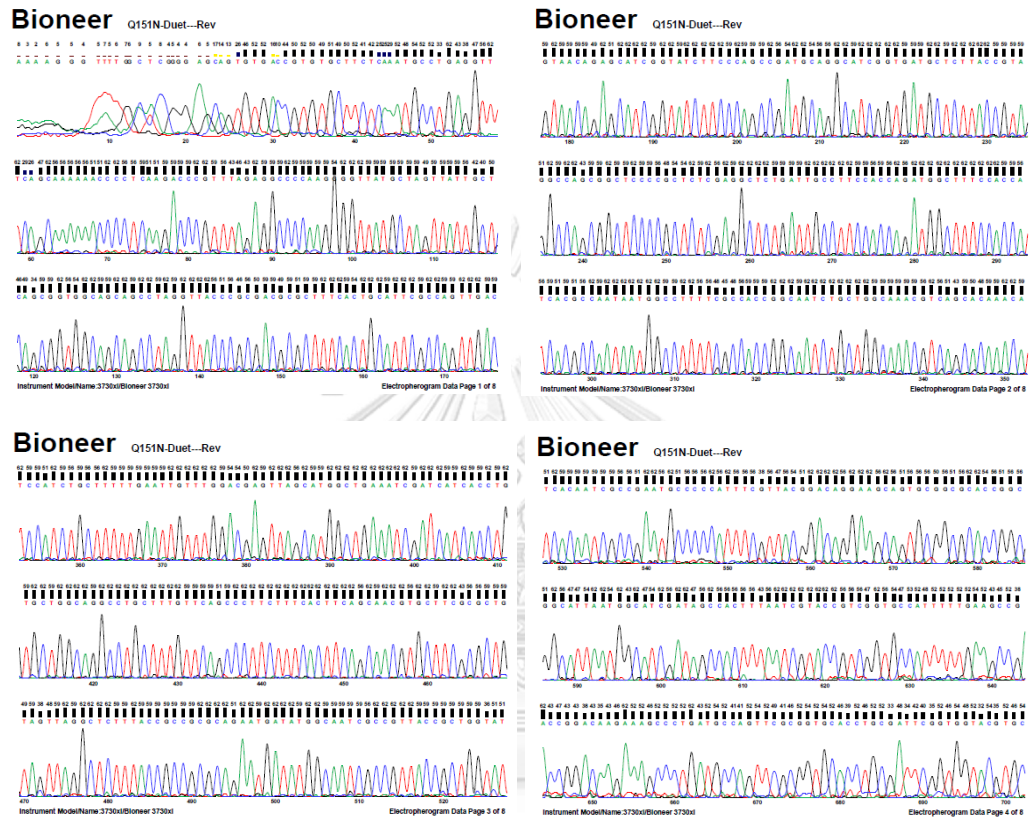
APPENDIX K

The sequencing chromatogram of *aroG*^{for} Q151N in pBLPTG*Q151N using primers F_DuetUP_aroG_Intr (A) and R_Duet (B)

(A)



(B)



VITA

NAME Maria Ulfah

DATE OF BIRTH 18 August 1982

PLACE OF BIRTH Bekasi, West Java, Indonesia

INSTITUTIONS ATTENDED State University of Jakarta

HOME ADDRESS Diana Court, R 501. Petchaburi road soi 6, Bangkok,
Thailand 10400

PUBLICATION L-Phenylalanine production in Escherichia coli harboring
feedback-resistant aroG.
The 30th Annual Meeting of the Thai Society for
Biotechnology and International Conference (TSB2018),
Bangkok, Thailand.

AWARD RECEIVED -